PROGRAM AND ABSTRACTS OF THE 29TH ANNUAL

GASEOUS ELECTRONICS CONFERENCE

19–22 OCTOBER 1976
CLEVELAND, OHIO

A TOPICAL CONFERENCE OF THE AMERICAN PHYSICAL SOCIETY
ASSISTED BY THE LAMP BUSINESS DIVISION OF THE GENERAL ELECTRIC COMPANY

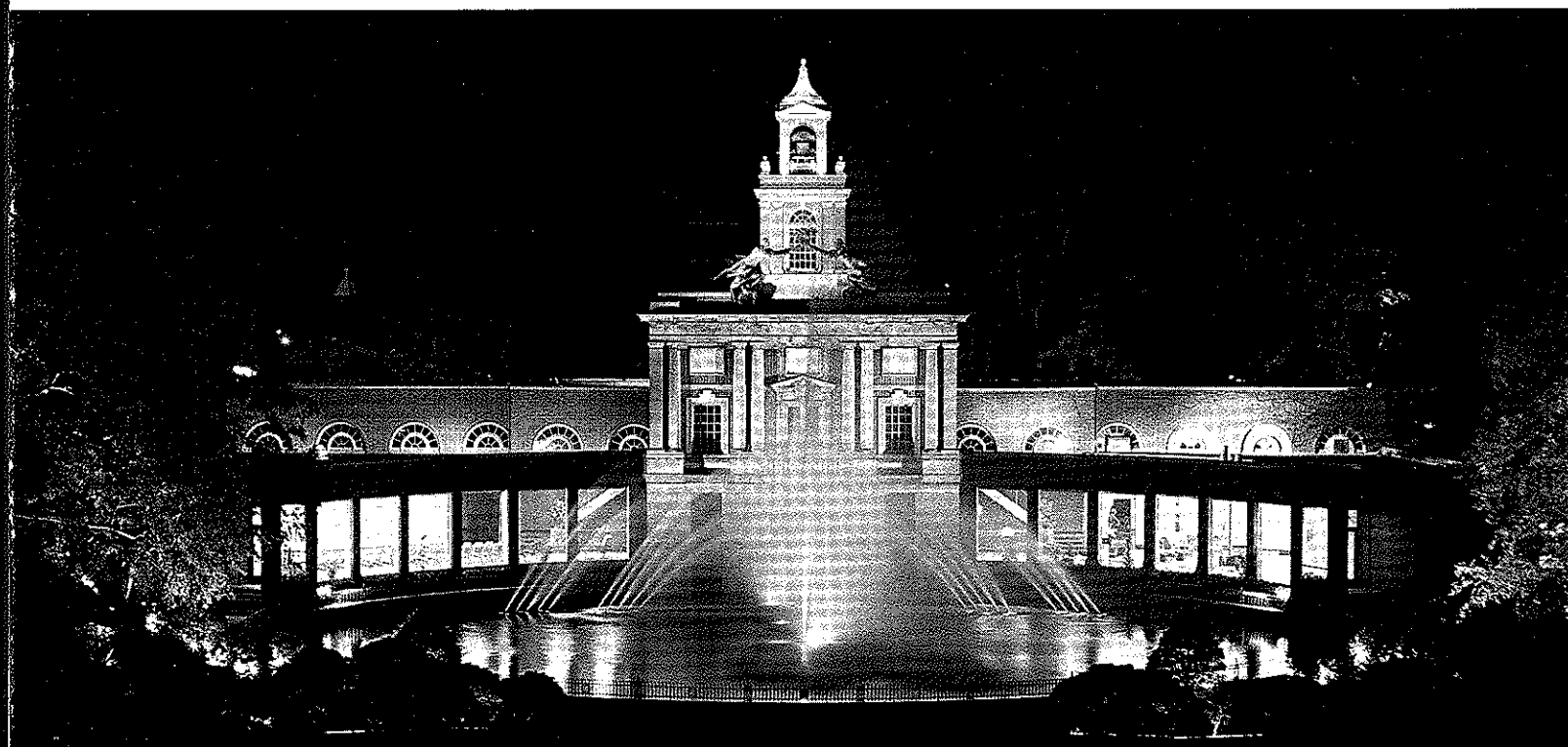

GENERAL ELECTRIC LIGHTING INSTITUTE • NELA PARK, CLEVELAND, OHIO

Twenty-Ninth Annual
Gaseous Electronics Conference
October 19-22, 1976
Cleveland, Ohio

29th GASEOUS ELECTRONICS CONFERENCE

PROGRAM
AND
ABSTRACTS

A Topical Conference of
The American Physical Society

Sponsored by

General Electric Co., Cleveland
American Physical Society
Division of Electron
And Atomic Physics

PROGRAM

TWENTY-NINTH ANNUAL

GASEOUS ELECTRONICS CONFERENCE

REGISTRATION AND MIXER (CASH BAR)

7:00 PM - 10:00 PM
MONDAY, OCTOBER 18, 1976
6th FLOOR ASSEMBLY AREA

SESSION A: UV AND VISIBLE LASERS I

9:00 AM - 10:30 AM, Tuesday, October 19
East Ballroom
Chairman: A.W. Johnson, Sandia

A1 E-BEAM CONTROLLED XeF LASER DISCHARGE (7 min.)
J.J. Jacob, J.A. Mangano, E.T. Salesky

A2 DISCHARGE CHARACTERISTICS OF KrF AND ArF EXCIMER LASER SYSTEMS IN A DOUBLE PULSED LARGE VOLUME DEVICE (7 min.)
R.C. Sze, T.R. Loree, C. Brau and S.D. Rockwood

A3 GAIN AND ABSORPTION OF KrF^* LASER DISCHARGE MEDIUM (7 min.)
A.M. Hawryluk

A4 ENERGY PATHWAYS STUDIES OF GASEOUS LASER CANDIDATES (7 min.)
C.H. Chen, J.P. Judish, M.G. Payne and G.S. Hurst

A5 SPECTRAL EMISSION AND KINETICS OF ELECTRON BEAM PUMPED ARGON-KRYPTON-FLUORINE MIXTURES (7 min.)
R.M. Hill, D.L. Huestis, D.C. Lorents, M.V. McCusker and H.H. Nakano

A6 PERFORMANCE OF SELF- AND EXTERNALLY-SUSTAINED KrF LASER DISCHARGES (7 min.)
L.E. Kline

A7 KINETIC MODELING OF ELECTRICAL LASERS: RESULTS FOR KrF (7 min.)
W.B. Lacina and R.S. Bradford, Jr.

SESSION BA: UV AND VISIBLE LASERS II

10:45 AM - 12:15 PM, Tuesday, October 19
East Ballroom
Chairman: L.A. Weaver, Westinghouse

BA1 EXCIMER EMISSION FROM OPTICALLY PUMPED XENON (7 min.)
W.M. Hughes and J.D. King

BA2 NEAR ATMOSPHERIC PRESSURE XENON EXCIMER LASER (7 min.)
C.E. Turner, Jr. and P.W. Hoff

BA3 ENERGY TRANSFER REACTIONS IN e-BEAM EXCITED XENON-DOPED ARGON (7 min.)
T.D. Bonifield, R.E. Gleason, J.W. Keto and G.K. Walters

BA4 ORGANIC VAPOR EXCITATION BY ELECTRON BEAM PUMPING OF RARE GAS-ORGANIC VAPOR MIXTURES (7 min.)
S.A. Edelstein, T.F. Gallagher, H.H. Nakano and D.C. Lorents

BA5 GAIN VERSUS WAVELENGTH NEAR 5577 Å IN ELECTRON-BEAM-EXCITED Kr/O_2 MIXTURES (7 min.)
J.R. Woodworth and J.K. Rice

BA6 RED BAND EMISSION IN Cs-RARE GAS DISCHARGES (7 min.)
B. Sayer, M. Ferray, J. Lozingot and J. Berlande

BA7+ DISCHARGE PROPERTIES OF THE $Ne-Cu^+$ ULTRAVIOLET LASER
F.J. De Hoog, G.J. Collins

BA8+ ULTRAVIOLET LASER ACTION IN Cu^+, Ag^+ AND Au^+
J.R. McNeil, G.J. Collins

BA9 MOLECULAR ION ELECTRONIC TRANSITION LASERS PUMPED BY THERMAL ENERGY CHARGE TRANSFER REACTIONS (7 min.)
J.B. Laudenslager, T.J. Pacala

+Combined presentation, total time alloted for both papers - 10 min.

SESSION BB: POSITIVE ION REACTIONS

10:45 AM - 12:15 PM, Tuesday, October 19
West Ballroom
Chairman: R.C. Dunbar, Case-Western Reserve University

BB1 THREE-BODY ASSOCIATION REACTIONS OF H^+ AND H_3^+ IONS IN HYDROGEN FROM 135 K TO 300 K (7 min.)
R. Johnsen, Chou-Mou Huang and M.A. Biondi

BB2 MEASUREMENT OF THE RATE COEFFICIENTS FOR THE BIMOLECULAR AND TERMOLECULAR CHARGE TRANSFER REACTIONS OF He_2^+ WITH Ne, Ar, N_2, CO, CO_2, and CH_4 (7 min.)
C.B. Collins, F.W. Lee, and R.A. Waller

BB3 MECHANISMS FOR $He^+/H2$ REACTIVE AND RADIATIVE PROCESSES (7 min.)
D.G. Hopper and A.C. Wahl

BB4 REACTIONS OF SIMPLE HYDROCARBON IONS WITH MOLECULES AT THERMAL ENERGIES (7 min.)
D. Smith and N.G. Adams

BB5 Xe^+-Ca CHARGE-TRANSFER CROSS-SECTION (7 min.)
K.B. Butterfield, D.C. Gerstenberger, T. Shay, G.J. Collins

BB6 MOLECULAR EXCITATION IN LOW ENERGY ION-MOLECULE COLLISIONS (7 min.)
G.H. Bearman, H.H. Harris, P.B. James and J.J. Leventhal

SESSION CA: NEUTRAL GAS LASERS AND NUCLEAR PUMPING

2:00 PM - 3:30 PM, Tuesday, October 19
East Ballroom
Chairman: B.E. Cherrington, University of Illinois

CA1 GAIN ON THE MERCURY 5461Å and 3650Å LINES IN THE AFTERGLOW OF A HIGH PRESSURE PULSED DISCHARGE (7 min.)
J.K. Crane, B.E. Cherrington, J.T. Verdeyen

CA2 ELECTRON-COLLISIONAL EXCITED STATE KINETICS IN ARGON AND MERCURY ELECTRICAL DISCHARGES (7 min.)
O. Judd

CA3 RESULTS OF A PARAMETRIC STUDY OF A FLOWING COPPER VAPOR LASER (7 min.)
B.G. Bricks, T.W. Karras, R.S. Anderson, C.E. Anderson

CA4 GAIN IN NEUTRAL GAS LASERS (7 min.)
P.J. Walsh

CA5 RECOMBINATION PUMPING OF ATOMIC NITROGEN AND CARBON LASERS (20 min.)
G.W. Cooper and J.T. Verdeyen

CA6+ DIRECT NUCLEAR PUMPING OF A ^{3}He-Ar LASER
N. W. Jalufka, R.J. DeYoung, F. Hohl

CA7+ COLLISIONAL PROCESSES IN THE ^{3}He-Ar NUCLEAR PUMPED LASER
P.A. Winters, N.W. Jalufka, R.J. DeYoung

CA8+ DIRECT NUCLEAR PUMPING OF ^{3}He-Kr AND ^{3}He-Xe
R.J. DeYoung, N.W. Jalufka, F. Hohl

CA9† STUDY OF A DIRECT NUCLEAR PUMPED, He-Hg LASER
M.A. Akerman, G.H. Miley

CA10† POPULATION PROCESSES FOR THE He-Hg DIRECT NUCLEAR PUMPED LASER
M.A. Akerman, W.E. Wells

+Combined presentation, total time alloted for three papers - 12 min.
† " " " " " two " - 10 min.

SESSION CB: NEGATIVE ION PROCESSES

2:00 PM - 3:00 PM, Tuesday, October 19
West Ballroom
Chairman: D. Smith, University of Birmingham, G.B.

CB1 FLOW-DRIFT TUBE STUDIES OF THE REACTIONS OF O_3^- AND CO_3^- WITH NO, NO_2, AND SO_2. (7 min.)
D.L. Albritton, I. Dotan, F.C. Fehsenfeld

CB2 MEASUREMENTS OF NEGATIVE ION CLUSTER FORMATION AND DISSOCIATIVE ATTACHMENT IN HCl AND HCl + N_2 MIXTURES (7 min.)
R.J. Corbin, N.J. Nygaard, W.R. Snow

CB3 ROTATIONAL "DIPOLE STATES" OF MOLECULAR NEGATIVE IONS (7 min.)
W.R. Garrett

CB4 THERMAL RYDBERG ATOM MOLECULE COLLISION: FORMATION OF MOLECULAR NEGATIVE IONS (7 min.)
W.C. Tam, P.M. Rackov, S.F. Wong, G.J. Schulz

CB5 PHOTODETACHMENT OF EXCITED NO_2^- (7 min.)
B.A. Huber, P.C. Cosby, J.T. Moseley, J.R. Peterson

CB6 CALCULATION OF PHOTODETACHMENT CROSS SECTION OF ATOMIC NEGATIVE IONS (7 min.)
R.M. Stehman and S.B. Woo

SESSION DA: IR LASERS

3:45 PM - 5:15 PM, Tuesday, October 19
East Ballroom
Chairman: W.T. Leland, LASL

DA1 DESCRIPTION AND ANALYSIS OF THE MODE-MEDIUM INTERACTION IN CW-CO_2 E-BEAM SUSTAINER LASERS (20 min.)
M.J. Yoder and D.R. Ahouse

DA2 PUMPING CHARACTERISTICS OF MULTI ATMOSPHERE CO_2 AMPLIFIERS (7 min.)
L.J. Denes, L.H. Taylor, L.E. Kline, R.J. Spreadbury, R.V. Babcock

DA3 CAUSES OF THERMAL INSTABILITY IN EXTERNALLY SUSTAINED MOLECULAR DISCHARGES (7 min.)
W.L. Nighan

DA4 DISTRIBUTION OF E/N AND N_e IN A CROSS-FLOW ELECTRIC DISCHARGE LASER. (7 min.)
J.W. Dunning, Jr., R.B. Lancashire, E.J. Manista

DA5 HIGH-POWER HIGH-PRESSURE PHOTO-IONIZATION STABILIZED GLOW DISCHARGE LASERS (7 min.)
V. Hasson, J. Brink, H.M. Von Bergmann

DA6 EXPERIMENTAL STUDIES OF ELECTRON ENERGY DISTRIBUTION FUNCTION IN CO_2 LASER PLASMAS (7 min.)
S. Ono and Sin-Li Chen

DA7 PHOTOIONIZATION AND ABSORPTION CROSS-SECTIONS OF SEEDING MATERIALS FOR PHOTO-PREIONIZED LASERS (7 min.)
D.F. Grosjean, P. Bletzinger

DA8 TIME-RESOLVED He-Xe AND Ar-Xe LASER CHARACTERISTICS (7 min.)
R.A. Olson, A. Garscadden

SESSION DB: HEAVY NEUTRALS

3:00 PM - 5:15 PM, Tuesday, October 19
West Ballroom
Chairman: L.D. Schearer, University of Missouri-Rolla

DB1 MEASUREMENT OF THE RATE COEFFICIENTS FOR THE BIMOLECULAR AND TERMOLECULAR CHANNELS FOR THE DESTRUCTION OF $He(2^3S)$ METASTABLES IN COLLISIONS WITH Ne, Ar, N_2, CO, CO_2, and CH_4 (7 min.)
C.B. Collins and F.W. Lee

DB2 COLLISIONAL BROADENING IN THE SPECTROSCOPIC MEASUREMENT OF HELIUM METASTABLE POPULATIONS AT HIGH PRESSURE (7 min.)
G.D. Meyers, D.P. Colton, R.A. Sierra

DB3 MEASUREMENT OF THE IONIZATION OF ARGON BY COLLISIONS WITH NEON METASTABLES (7 min.)
T. Rhymes

DB4+ ELECTRONIC ENERGY TRANSFERS IN Ar-Xe MIXTURES
P.K. Leichner, E.T. Hall, K.F. Palmer

DB5+ ELECTRONIC ENERGY TRANSFER REACTIONS IN Ar-Kr MIXTURES
M.D. Thieneman, P.K. Leichner

DB6+ ELECTRONIC ENERGY TRANSFERS IN Kr-Xe MIXTURES
J.D. Cook and P.K. Leichner

DB7 RADIATIVE DECAY AND QUENCHING OF $Na(3^2P)$ LEVELS AT HIGH Na DENSITIES (7 min.)
L. Lam, T. Fujimoto, A.C. Gallagher, A.V. Phelps

DB8 TIME-OF-FLIGHT DETERMINATION OF RADIATIVE DECAY RATES FOR HIGH RYDBERG STATES IN ATOMIC NITROGEN (7 min.)
C.A. Kocher and C.E. Fairchild

DB9 THE INFLUENCE OF MOLECULAR ROTATION ON VIBRATION-TRANSLATION ENERGY TRANSFER (20 min.)
R.L. McKenzie

DB10 TEMPERATURE DEPENDENCE OF THE LASER ENHANCED REACTION NO + $O_3(001)$ (7 min.)
R.J. Gordon, J. Moy, E. Bar-Ziv

DB11 VIBRATIONAL RELAXATION OF SF_6 (7 min.)
J.S. Cohen and A.E. Greene

DB12 HEATING OF D_2 GAS TARGETS BY INTENSE TRITON BEAMS (7 min.)
A.E. Greene and A.M. Lockett III

+Combined presentation, total time alloted for three papers - 10 min.

SESSION E: ISOTOPE SEPARATION WORKSHOP

7:30 PM, Tuesday, October 19
East Ballroom
Discussion Leader: S.D. Rockwood, LASL

E1 RYDBERG STATES OF ATOMIC URANIUM
R. Solarz

E2 ROLE OF VIBRATIONAL ENERGY IN MOLECULAR REACTIONS
J. Birely

E3 THEORETICAL ASPECTS OF REACTIONS BETWEEN EXCITED SPECIES
R. Porter

E4 LASER ALCHEMY
A. Hartford

SESSION FA: CO LASERS

8:30 AM - 10:30 AM, Wednesday, October 20
East Ballroom
Chairman: D.H. Douglas - Hamilton, Avco

FA1 PERFORMANCE OF A CW DOUBLE DISCHARGE IN CONTINUOUS SUPERSONIC FLOW (7 min.)
A.C. Stanton, R.K. Hanson and M. Mitchner

FA2 PERFORMANCE OF A CW PRE-EXCITED CO LASER (7 min.)
J.W. Daiber and H.M. Thompson

FA3 ELECTRICAL AND LASER DIAGNOSTICS OF A 60 kW SUPERSONIC CW CO ELECTRIC LASER (7 min.)
E.L. Klosterman and S.R. Byron

FA4 LARGE SCALE CW SUPERSONIC CARBON MONOXIDE LASER EXPERIMENTS (7 min.)
M.J. Yoder and D.R. Ahouse

FA5 STABILIZATION OF A SUPERSONIC FLOW GAS DISCHARGE BY AUXILIARY PIN DISCHARGES (7 min.)
M. Garcia, G. Bienkowski and J. Lawless

FA6 CW DISCHARGE STABILIZATION IN SUPERSONIC FLOWS USING AUXILIARY PIN DISCHARGES (7 min.)
J.A. Smith and G. Srinivasan

FA7 HIGH REPETITION RATE DISCHARGE PULSING OF A SUPERSONIC CO LASER (7 min.)
T.G. Jones and W.B. Shepherd

FA8 MEASUREMENT OF THE CATHODE FALL IN THE SUPERSONIC CO LASER (7 min.)
M.F. Weisbach

FA9 CRYOGENIC "POKER" CO ELECTRIC LASER (7 min.)
A.E. Hill and W.M. Moeny

FA10 LIMITS ON ENERGY DISPOSITION IN CO-Ar MIXTURES (7 min.)
W.H. Long, Jr. and A. Garscadden

FA11 THE EFFECTS OF OXYGEN IN THE CO MOLECULAR LASER (7 min.)
W. Lowell Morgan and E.R. Fisher

SESSION FB: ARCS I

9:00 AM - 10:30 AM, Wednesday, October 20
West Ballroom
Chairman: E.F. Wyner, GTE-Sylvania

FB1 EXISTENCE AND ROLE OF THE HIGH DENSITY VAPOR CLOSE TO THE ELECTRODE IN THE CATHODE SPOT (7 min.)
A. Leycuras

FB2 VACUUM ARC WITH KV ARC VOLTAGE (7 min.)
R. Dethlefsen and A.S. Gilmour, Jr.

FB3 AIR TRANSPORT PROPERTIES FROM MEASURED ARC PROPERTIES (20 min.)
R.S. Devoto, U. H. Bauder, J. Cailleteau and E. Shires

FB4 TIME-DEPENDENT MEASUREMENTS AND MODEL-CALCULATIONS OF HIGH PRESSURE Na-Xe DISCHARGES (7 min.)
J.A.J.M. van Vliet and B.R.P. Nederhand

FB5 MODELLING THE HIGH PRESSURE SODIUM DISCHARGE (7 min.)
J.H. Ingold

FB6 THERMAL AND ELECTRICAL CHARACTERISTICS OF A TWO-DIMENSIONAL TANH-CONDUCTIVITY ARC (7 min.)
P.S. Ayyaswamy, G.C. Das, I.M. Cohen and A.M. Whitman

FB7 CONTINUUM RADIATION FROM THE MERCURY ARC (7 min.)
R.J. Zollweg, R.W. Liebermann, R. Burnham

SESSION GA: EXCITATION AND IONIZATION

10:45 AM - 12:15 PM, Wednesday, October 20
East Ballroom
Chairman: D. Spence, Argonne National Lab.

GA1 ELECTRON EXCITATION OF THALLIUM $7^2S_{1/2}$ AND $6^2D_{3/2,5/2}$ LEVELS (7 min.)
S.T. Chen and A. Gallagher

GA2 ELECTRON IMPACT CROSS SECTION MEASUREMENT FROM THE HELIUM 2^3S LEVEL (7 min.)
M.L. Lake and A. Garscadden

GA3 LIFETIMES AND EXCITATION FUNCTIONS OF OPTICAL EMISSIONS (2300A-2900A) FROM N_2 EXCITED BY ELECTRON BOMBARDMENT (7 min.)
D.J. Burns and C.R. Hummer

GA4 ELECTRON IONIZATION OF ATOMIC CHLORINE (7 min.)
G.W. Howser, R.J. Corbin, K.J. Nygaard and W.R. Snow

GA5 ELECTRON IMPACT DOUBLE IONIZATION CROSS SECTIONS OF Cs^+ IONS (7 min.)
R.K. Feeney and W.E. Sayle, III

GA6 IONIZATION NEAR THESHOLD OF VIBRATIONALLY EXCITED N_2 BY ELECTRON IMPACT (7 min.)
J.A. Michejda and P.D. Burrow

GA7 LOW ENERGY PHOTOIONIZATION OF H_2 (7 min.)
J.R. Rumble and S.A. Hagstrom

GA8 PHOTOIONIZATION OF Cs EXCITED STATES (7 min.)
M.H. Nayfeh, J.P. Young and G.S. Hurst

GA9 THREE-PHOTON IONIZATION OF ATOMS BY STRONG PULSED LASER FIELDS (7 min.)
C.W. Choi and M.G. Payne

GA10 EVIDENCE FOR $^1\Delta_g$ SINGLET OXYGEN IN A HIGH PRESSURE ELECTRON-BEAM CONTROLLED DISCHARGE (7 min.)
D. Pigache, G. Fournier, D. Proust, M. Lecuiller

SESSION GB: ARCS II

10:45 AM - 12:15 PM, Wednesday, October 20
West Ballroom
Chairman: G. Ecker, Ruhr-Universität Bochum

GB1 THEORY AND EXPERIMENT FOR CIRCUIT BREAKER ARCS STABILIZED BY FORCED CONVECTION (20 min.)
H.C. Ludwig

GB2 TURBULENT AC ARCS (7 min.)
D.M. Benenson and P.A. Reiser

GB3 RADIAL SHOCK WAVES IN A CYLINDRICAL PULSED CESIUM DISCHARGE (7 min.)
H.L. Witting

GB4 ONSET OF HELICAL INSTABILITY OF CONFINED ARCS (7 min.)
R.J. Zollweg

GB5 EMISSION AND ABSORPTION MEASUREMENTS OF RF-HEATED ARGON-CONFINED URANIUM PLASMAS (7 min.)
W.C. Roman

GB6 COLLISIONAL PROCESS EFFECTS ON ELECTRON ENERGY DISTRIBUTION IN U-He PLASMAS (7 min.)
G.H. Miley and Chan K. Choi

GB7 SODIUM DIMER EMISSION OBSERVED IN ARC DISCHARGE AFTERGLOW (7 min.)
E.F. Wyner and J. Maya

SESSION HA: ION INTERACTIONS

2:00 PM - 3:30 PM, Wednesday, October 20
East Ballroom
Chairman: D.L. Albritton, NOAA/ERL

HA1 DETERMINATION OF ION-NEUTRAL INTERACTION POTENTIALS FROM MOBILITY MEASUREMENTS (20 min.)
L.A. Viehland, E.A. Mason and I.R. Gatland

HA2 MONTE CARLO STUDIES OF ION MOBILITIES (7 min.)
S.L. Lin and J.N. Bardsley

HA3 EFFECT OF ENDOTHERMIC REACTIONS ON THE ION VELOCITY DISTRIBUTION IN DRIFT TUBE EXPERIMENTS (7 min.)
J.H. Whealton, R.M. Stehman and S.B. Woo

HA4 NEGATIVE IONS IN CO_2 (7 min.)
T.D. Fansler, L.M. Colonna and R.N. Varney

HA5 COLLISIONAL DISSOCIATION OF CO_3^- (7 min.)
J.F. Paulson and P.J. Gale

HA6 FLOW-DRIFT TUBE AND VARIABLE TEMPERATURE FLOWING AFTERGLOW STUDIES OF THE REACTION $O_3^- + CO_2 \rightarrow CO_3^- + O_2$ (7 min.)
I. Dotan, D.L. Albritton, G.E. Streit, J.A. Davidson, F.C. Fehsenfeld

SESSION HB: DIAGNOSTICS AND DISCHARGES

2:00 PM - 3:30 PM, Wednesday, October 20
West Ballroom
Chairman: G.J. Kazek, General Electric

HB1 NEAR-RESONANT RAYLEIGH SCATTERING AS A TOOL FOR DETERMINING Na DENSITIES IN LOW- AND HIGH-PRESSURE DISCHARGES. (20 min.)
L. Vriens

HB2 FIR ABSORPTION DETERMINATION OF TRANSIENT ELECTRON DENSITIES IN HIGH PRESSURE IONIZER-SUSTAINER LASERS (7 min.)
L.A. Newman, M.R. Schubert, T.A. DeTemple

HB3 THE ELECTRON TEMPERATURE IN A MEDIUM PRESSURE D.C. DISCHARGE POSITIVE COLUMN PLASMA (7 min.)
Jen-Shih Chang, Sin-Li Chen

HB4 DETERMINATION OF ELECTRON DENSITIES BY TWO PHOTON DOPPLER FREE SPECTROSCOPY (7 min.)
R.A. Sierra, D.P. Colton, G.D. Myers

HB5 MEASUREMENTS OF ELECTRON-NEUTRAL FREE-FREE ABSORPTION IN A HIGH PRESSURE ELECTRON-BEAM SUSTAINED DISCHARGE (7 min.)
W.H. Christiansen and S. Alroy

HB6 CURRENT DENSITIES AND DISCHARGE RADIUS MEASURED BY SPECTROSCOPIC TECHNIQUE FOR CORONA DISCHARGE IN OXYGEN (7 min.)
F. Bastien, E. Marode

SESSION IA: DISSOCIATION

3:45 PM - 5:15 PM, Wednesday, October 20
East Ballroom
Chairman: B.A. Huber, SRI and Ruhr-Universität Bochum

IA1 PHOTODISSOCIATION SPECTRUM OF O_3^- (7 min.)
P.C. Cosby, J.H. Ling, J.T. Moseley, and J.R. Peterson

IA2 PHOTODISSOCIATION MEASUREMENTS OF NITRIC OXIDE ION CLUSTERS (7 min.)
J.A. Vanderhoff

IA3 THRESHOLD PHOTOFRAGMENT SPECTROSCOPY OF O_2^+ ($a^4\Pi_u \rightarrow f^4\Pi_g$) (7 min.)
J.T. Moseley, M. Tadjeddine, J. Durup, J.B. Ozenne, C. Pernot, and A. Tabche-Fouhaille

IA4 ANGULAR DISTRIBUTION AND ENERGY OF IONIC FRAGMENTS FROM THE PHOTODISSOCIATION OF GASEOUS METHYL CHLORIDE CATION (7 min.)
R.G. Orth and R.C. Dunbar

IA5+ TUNABLE DYE LASER PHOTODISSOCIATION OF O_3: KINETIC ENERGIES AND ANGULAR DISTRIBUTIONS OF O ATOM PHOTOFRAGMENTS
C.E. Fairchild, E.J. Stone, G.M. Lawrence

IA6+ KINETIC ENERGIES AND ANGULAR DISTRIBUTIONS OF OXYGEN ATOM PHOTOFRAGMENTS PRODUCED BY PHOTODISSOCIATION OF O_2 AND N_2O IN THE VACUUM ULTRAVIOLET
E.J. Stone, G.M. Lawrence and C.E. Fairchild

IA7 SELECTIVE PROCESSES IN BROMINE (7 min.)
K.B. McAfee Jr., R.M. Lum and V.E. Bondybey

IA8 DISSOCIATION OF CD_4, C_2D_4, AND CF_4 BY ELECTRON IMPACT (20 min.)
H.F. Winters

IA9 RATE COEFFICIENTS FOR DISSOCIATIVE EXCITATION OF H_2 BY LOW ENERGY ELECTRONS (7 min.)
C.H. Muller and A.V. Phelps

+Combined presentation, total time alloted for two papers - 10 min.

SESSION IB: DISCHARGES

3:45 PM - 5:15 PM, Wednesday, October 20
West Ballroom
Chairman: L. Vriens, Philips

IB1 E-I CHARACTERISTICS AND IONIZATION INSTABILITIES IN UNIFORM GLOW DISCHARGES (20 min.)
P.J. Chantry

IB2 NUMERICAL STUDY OF NEON DISCHARGE (7 min.)
A.A. Garamoon and I.A. Ismail

IB3 ANALYTICAL MODEL FOR LOW PRESSURE MERCURY+INERT GAS DISCHARGES (7 min.)
W.L. Lama, C.F. Gallo, T.J. Hammond, P.J. Walsh

IB4 INFLUENCE OF HELIUM ATOMS ON THE IONISATION AND RECOMBINATION PROCESSES IN Cs-He DISCHARGES (7 min.)
B. Sayer, G. Gousset, M. Ferray, J. Lozingot, J. Berlande

IB5 DEVELOPMENT OF CATHODE FALL IN PLANAR DISCHARGE IN HELIUM (7 min.)
H.C. Chen and A.V. Phelps

IB6 DEPENDENCE OF BREAKDOWN STRENGTHS OF GASEOUS DIELECTRICS ON ELECTRON ATTACHMENT CROSS SECTIONS AND INELASTIC SCATTERING (7 min.)
R.Y. Pai, L.G. Christophorou, D.R. James, M.O. Pace

IB7 IMPORTANCE OF 2-STEP EXCITATIONS IN THE POSITIVE COLUMN OF Ne-0.1% Ar MIXTURES (7 min.)
O. Sahni, W.P. Jones

IB8 SPECTRA OF VIBRATIONALLY HOT GASES IN ELECTRIC DISCHARGES BY CARS (7 min.)
J.W. Nibler, W.M. Shaub, A.B. Harvey

SESSION J: ION CLUSTERS WORKSHOP

7:30 PM, Wednesday, October 20
East Ballroom
Discussion Leader: J.R. Peterson, SRI

J1 BINDING ENERGIES - STABILITIES AND NATURE OF BONDING IN ION-MOLECULE CLUSTERS (25 min.)
P. Kebarle

J2 REACTIONS OF CLUSTER IONS (25 min.)
F.C. Fehsenfeld

J3 CLUSTER IONS IN THE IONOSPHERE (20 min.)
R.S. Narcisi

J4 PHOTODISSOCIATION OF CLUSTER IONS (20 min.)
J.T. Moseley

J5 RECOMBINATION OF CLUSTER IONS WITH ELECTRONS (15 min.)
M.A. Biondi, C.M. Huang, R. Johnsen

SESSION K: VACUUM ARCS PANEL DISCUSSION

9:00 AM - 12:00 AM, Thursday, October 21
East Ballroom
Discussion Leader: J.F. Waymouth, GTE-Sylvania

K1 CURRENT DENSITY AND EROSION MEASUREMENT AT THE ARC CATHODE SPOT (20 min.)
G.A. Farrall

K2 ION CURRENTS FROM THE CATHODE SPOT REGIONS OF VACUUM ARCS (20 min.)
C.W. Kimblin

K3 CELLULAR SUBSTRUCTURE IN ARC CATHODE SPOTS (20 min.)
L.P. Harris

K4 CATHODE SPOT THEORY, - A PHENOMENON OF MANY ASPECTS (20 min.)
G.H. Ecker

BUSINESS MEETING, EAST BALLROOM
12:00 PM - 12:30 PM, Thursday, October 21
CHAIRMAN: R.H. BULLIS, UNITED TECHNOLOGIES RESEARCH CTR.

SESSION L: SCHULZ MEMORIAL SESSION

2:00 PM - 5:15 PM, Thursday, October 21
East Ballroom
Chairman: M. Biondi, University of Pittsburgh

L1 SHAPE RESONANCES AND RESONANCES NEAR THESHOLDS
A. Herzenberg

L2 ELECTRON SCATTERING, PAST AND PROLOGUE
C.E. Kuyatt

L3 RESONANCES IN ELECTRON SCATTERING FROM HYDROCARBON MOLECULES
P.D. Burrow, J.A. Michejda, K.D. Jordan

L4 RESONANT SCATTERING OF MOLECULES BY LOW ENERGY ELECTRON IMPACT: VIBRATIONAL EXCITATION
S.F. Wong

L5 NEW APPLICATIONS OF SCHULZ'S TRAPPED ELECTRON METHOD
D. Spence

L6 ELECTRON SCATTERING FROM EXCITED ATOMS AND MOLECULES
M.J.W. Boness

SOCIAL HOUR AND BANQUET
THURSDAY, OCTOBER 21
BALLROOM OF THE BOND COURT HOTEL

6:30 PM: SOCIAL HOUR
7:30 PM: BANQUET

CHAIRMAN: R.H. BULLIS, UNITED TECHNOLOGIES RESEARCH CTR.

SPEAKER : J.H. JENSEN, GENERAL ELECTRIC CO.
MANAGER, LIGHTING EDUCATION

TOPIC : "THE MANY LIGHTS IN YOUR LIFE"

SESSION M: ELECTRON SCATTERING I

8:45 AM - 10:30 AM, Friday, October 22
East Ballroom
Chairman: A. Herzenberg, Yale

M1 IS STANDARD ELASTIC CROSS SECTION DATA NOW AVAILABLE FOR ELECTRON-HELIUM SCATTERING? (20 min.)
H.B. Milloy

M2 COLLISION CROSS SECTIONS FOR LOW ENERGY ELECTRONS WITH O_2 (20 min.)
A.V. Phelps and S.A. Lawton

M3 SCALING LAW FOR ELECTRON COLLISIONS WITH POLAR MOLECULES (20 min.)
F.T. Smith, D. Mukherjee, D. Huestis

M4 ELECTRON DIFFUSION IN SWARMS (20 min.)
J. Lucas

SESSION NA: ELECTRON SCATTERING II

10:45 AM - 12:15 PM, Friday, October 22
East Ballroom
Chairman: R.J. Van Brunt, JILA

NA1 ELECTRON DRIFT VELOCITIES IN SODIUM VAPOUR (7 min.)
Y. Nakamura, J. Lucas

NA2 THE EFFECT OF ENERGY INEQUILIBRIUM ON THE SWARM PARAMETER MEASUREMENT (7 min.)
N. Ikuta, S. Yuasa, Y. Shinohara

NA3 ELECTRON TRANSPORT IN ARGON (7 min.)
W.H. Long, Jr.

NA4 ABSOLUTE TOTAL ELECTRON-IMPACT CROSS-SECTIONS FROM A TIME-OF-FLIGHT TRANSMISSION TECHNIQUE (7 min.)
R.E. Kennerly, R.A. Bonham

NA5 GLAUBER CROSS SECTIONS FOR ELASTIC SCATTERING OF ELECTRONS BY METASTABLE (2^1S, 2^3S) HELIUM ATOMS (7 min.)
S.T. Chen, G.A. Khayrallah

NA6 POST COLLISION INTERACTION IN ELECTRON SCATTERING FROM XENON (7 min.)
N. Swanson, R.J. Celotta

NA7 FESHBACH RESONANCES IN CH_3X(X=Cl,Br,I). CLASSIFICATION OF RESONANCES AND PREDICTION OF RYDBERG STATES (7 min.)
D. Spence

SESSION NB: RECOMBINATION

10:45 AM - 12:15 AM, Friday, October 22
West Ballroom
Chairman: R. Johnsen, University of Pittsburgh

NB1 STUDY OF KINETICS OF n=2 STATES IN RECOMBINING HELIUM PLASMA JETS (7 min.)
C.C. Poon and F.A. Robben

NB2 CHARGE NEUTRALIZATION IN A HIGH PRESSURE HELIUM AFTERGLOW (7 min.)
D.P. Colton, G.D. Myers, R.A. Sierra

NB3 MERGED ELECTRON-ION BEAM STUDIES OF DISSOCIATIVE RECOMBINATION (7 min.)
B. Mitchell, J. Keyser and J.WM. McGowan

NB4 ELECTRON TEMPERATURE DEPENDENCE OF DISSOCIATIVE RECOMBINATION IN XENON (7 min.)
Y.J. Shiu, M.A. Biondi, D.P. Sipler

NB5 ELECTRON-ION RECOMBINATION RATES IN GAS MIXTURES (7 min.)
T.W. Meyer, J.D. Hines, P.D. Tannen

NB6 MUTUAL NEUTRALIZATION OF SIMPLE AND CLUSTERED POSITIVE AND NEGATIVE IONS (7 min.)
D. Smith, M.J. Church

NB7 IONIC RECOMBINATION AND CHEMICAL REACTIONS IN ELECTRON IRRADIATED AIR (7 min.)
M.N. Hirsh

NB8 USES AND BASIC CHARACTERISTICS OF A COAXIAL DISCHARGE DIFFUSION PLASMA COLUMN (7 min.)
M. Kamitsuma, S.L. Chen, J.S. Chang

SESSION A

9:00 AM - 10:30 AM, Tuesday, October 19

East Ballroom

UV AND VISIBLE LASERS I

Chairman: A. W. Johnson, Sandia

A1 E-Beam Controlled XeF Laser Discharge*

J. H. JACOB, J. A. MANGANO and E. T. SALESKY, Avco Everett Research Laboratory, Inc., Everett, MA.

We have investigated E-beam controlled discharge characteristics of the XeF laser discharge. The mixes typically contain 99.4% Ar, 0.4% Xe and 0.2% NF_3. A kinetic model has been developed that predicts the temporal variation of the discharge voltage, current and fluorescence. As in the case of the KrF laser discharge[1] we find that rare gas metastables play a dominant role in the discharge physics. Initially most of the discharge energy is coupled into the argon metastables. The mechanisms that lead to the formation of XeF* from Ar* will be discussed. Detailed comparisons between the predictions of the code and experimental results are presented.

[1] J. H. Jacob and J. A. Mangano, Appl. Phys. Lett. 28, 724 (1976).

*This research was supported in part by the Advanced Research Projects Agency of the Department of Defense, monitored by ONR, and in part by the U.S. Energy Research and Development Agency through Univ. of California Lawrence Livermore Laboratory.

A2 Discharge Characteristics of KrF and ArF Excimer Laser Systems in a Double Pulsed Large Volume Device.* R. C. SZE, T.R. LOREE, C. BRAU, & S. D. ROCKWOOD., University of California, Los Alamos, NM-- We have obtained 100 mJ near 2485 Å in KrF and 50 mJ near 1930 Å in ArF in a large volume double discharge with a flashboard prepulse. Optimum operating conditions and lasing characteristics are given. Experiments concerning the role of the flashboard prepulse in the operation of these lasers are discussed. All indications to date point to the prepulse formation of long-lived negative ion species which provide electrons that initiate the main discharge. Conductivity measurements and the rate of decay of the negative ions have been obtained; they correlate with the observed lasing energy behavior as a function of time delay between the prepulse and the discharge.

A3 Gain and Absorption of KrF^* Laser Discharge Medium. ANDREW M. HAWRYLUK, Avco-Everett Research Laboratory, Inc. Everett, MA. Gain/Absorption of the KrF^* laser discharge medium has been measured from below 2480 Å to 2670Å using a tunable flashlamp pumped dye laser and a doubling crystal. KrF^* excitation has been accomplished by using an E-beam controlled discharge apparatus.[1] These measurements were made to determine the total rare gas metastable photoabsorption length, self-absorption length by KrF^* and the small signal gain. Parameters that were varied include gas pressure, gas mix and electric field strength in the discharge. The ratio of gain to excited state absorption plus self-absorption will have an impact on the scalability and ultimate efficiency of the KrF^* laser. Preliminary results indicate that excited state absorption exists near the peak of the KrF^* fluorescence band (2491Å) which could explain the observed laser emission at 2485Å and 2495Å.

1. J.A. Mangano and J.H. Jacob, Appl. Phys. Lett 27, 495 (1975); J.H. Jacob and J.A. Mangano, Appl. Phys. Lett. 28, 724 (1976)

A4 Energy Pathways Studies of Gaseous Laser Candidates.* C.H. CHEN, J.P. JUDISH, M.G. PAYNE, and G.S. HURST, Oak Ridge Nat'l. Lab. --During the past year we have searched extensively for high power uv gas lasers. In our studies we excite gaseous mixtures with 2-MeV proton pulses having 15-ns width and with variable numbers of protons/pulse. The repetition rate for proton pulses can also be varied over a wide range. Time resolved vuv and uv-visible spectroscopy has been utilized to study the energy precursors, fluorescence efficiencies, energy transfer cross sections, dissociative recombination, and natural lifetimes of excited molecules. Detailed kinetic studies have been made for Ar-Cl_2, Ar-H_2O, Ar-N_2, He-N_2, etc. In Ar-Cl_2 mixtures, we have studied a broad continuum from 2200 to 3000 Å, and in Ar-H_2O we have measured intense emission from OH^* around 3080 Å. The energy precursor for both of the latter emissions is $Ar_2^*(1_u)$. Ar-Cl_2 and Ar-H_2O are considered to be possible E-beam pumped, uv laser systems. The precursors for the strongest emissions from Ar-N_2 and He-N_2 have also been determined.

*Research sponsored by the U.S. Energy Research and Development Adm. under contract with Union Carbide Corp.

A5 Spectral Emission and Kinetics of Electron Beam Pumped Argon-Krypton-Fluorine Mixtures. R. M. HILL, D. L. HUESTIS, D. C. LORENTS, M. V. McCUSKER, and H. H. NAKANO, SRI.--We have studied the intensity and temporal behavior of the emissions from e-beam pumped mixtures of Ar, Kr, and F_2. Both the total gas pressure and the fractional composition were varied. In addition to the known KrF^* band at 248 nm we have investigated the broad band near 410 nm. This band may come from an excited polyatomic krypton-fluorine molecule, possibly Kr_2F. At 3 atm total pressure (50 torr Kr, 1 torr F_2) the total number of photons from the 410 nm band is nearly 3 times that from the 248 nm band. For fixed Kr and F_2 pressures, the total number of photons from the 248 nm band decreases with increasing argon pressure. The number from the 410 nm band increases linearly with argon pressure, indicating a constant photon yield per excited rare gas atom. A kinetic model will be discussed, as will several of the rate constants determined in this study.

*Work supported by DARPA through MICOM.

A6 Performance of Self- and Externally-Sustained KrF Laser Discharges L.E. KLINE, Westinghouse Research Laboratories -- Voltage-current (V-I) characteristics and metastable production efficiencies, η_m, are calculated for the F_2:Kr:Ar = 1:20:979 mixture of Ref. 1. A self-sustained discharge has a negative V-I characteristic and η_m > 80% for a wide range of current densities. Two-step ionization[1] dominates electron production in the self-sustained discharge. When an external ionization source is used, the V-I characteristic is positive at low current densities where the source dominates electron production. The calculated V-I characteristic agrees with experiment.[1] With the source, η_m falls off rapidly as the current density decreases. As the current density increases η_m approaches the value obtained with a self-sustained discharge at the same current density and two-step ionization becomes important. When two-step ionization produces more electrons than the external source, the V-I characteristic becomes negative. This result is consistent with a suggestion[2] that the instability of Ref. 1 corresponds to a negative V-I characteristic.

1 J.D. Daugherty, J.A. Mangano, and J.H. Jacob, Appl. Phys. Lett. 28, 581 (1976).
2 G.L. Rogoff (private communication).

A7 Kinetic Modeling of Electrical Lasers: Results for KrF. W. B. LACINA and R. S. BRADFORD, Jr., Northrop, Hawthorne, Calif. -- In recent years, there has been much interest in analytical modeling of electrically excited gas lasers, and several new schemes for visible and uv emission are currently under investigation. A generalized computer code which synthesizes a coupled analysis containing molecular and electron kinetics, optical radiation fields, and an external driving circuit has been developed. This code automatically generates its own subroutines by translating symbolic reactions into computer-coded equations. This makes it possible to construct an analysis for the most complicated reaction scheme, containing an arbitrary number of processes and interacting species, with no effort. This analysis, which consists of a numerical solution of the Boltzmann transport equation (with superelastic collisions) self-consistently coupled to the master equation for the population densities of the electrons, ions, and neutrals, is then executed for specified values of experimental input parameters. Results of calculations for the e^--beam excited and electric discharge KrF laser will be presented and compared with experimental data. Volumetric discharge stability, discharge impedance, sensitivity to F_2 concentration, population densities, and laser performance are predicted.

SESSION BA

10:45 AM - 12:15 PM, Tuesday, October 19

East Ballroom

UV AND VISIBLE LASERS II

Chairman: L. A. Weaver, Westinghouse

BA1 Excimer Emission from Optically Pumped Xenon.*
WILLIAM M. HUGHES and JOE D. KING, Los Alamos Scientific Laboratory.--Fast pulse optical pumping has been used to study kinetic processes in high pressure xenon gas. Optical pumping was used to avoid the effects of electron collisions, ion-recombination and uncertainty in deposition usually encountered in electron beam excited experiments. In addition specific initial state preparation is possible by using either argon or krypton-excimer light to pump either the $^1P_1$ or $^3P_1$ atomic xenon levels respectively. The data were taken over a wide range of xenon pressure (10 to 3 x 10^4 Torr). Computer analysis of the data yielded information about fine structure relaxation, radiative lifetimes, mixing rates between molecular states, branching ratio and collisional quenching.

*Work supported by the Energy Research and Development Administration.

BA2 Near Atmospheric Pressure Xenon Excimer Laser .*
C. E. TURNER, JR., and P. W. HOFF†, Lawrence Livermore Laboratory.--Laser action at 1720 Å has been obtained at a pressure of 1.5 atm xenon with a 1 meter length of gain medium pumped by a 230 kV, few Amp/cm^2, 1 μsec electron beam. The dependence of the experimental laser characteristics on gas pressure and e-beam intensity will be presented. The observed laser threshold was in agreement with the prior prediction of a dynamic kinetics/laser model.[1] Theoretical-experimental comparisons and model predictions regarding laser efficiency optimization will be given.

*Work performed under the auspices of the United States Energy Research and Development Administration, contract number W-7405-Eng-48.
†Present address: U.S. ERDA, DMA, Wash., D.C. 20545

[1]C. W. Werner, E. V. George, P. W. Hoff, and C. K. Rhodes Appl. Phys. Lett. 25, 235 (1974) and UCRL-77412 Preprint, (1975), submitted to Phys. Rev.

BA3 Energy Transfer Reactions in e-Beam Excited Xenon-doped Argon.* T.D.Bonifield, R.E.Gleason, J.W.Keto+ and G.K.Walters, Rice University--The time dependence of the VUV emissions from xenon-doped argon is measured following pulsed excitation by a low intensity e-beam. The argon continuum at ∿1250A is observed to be quenched in electronic energy transfer collisions with xenon atoms, forming $Xe^*(^1P_1)$, with the rate constant $(4.39 \pm .05)\times10^{-10}$ cm^3/sec. The xenon continuum near 1470A is found to be due to collision induced radiation from $Xe(^3P_2)$ with the rate constant $(3.2 \pm .7)\times10^{-16}$ cm^3/sec, as well as radiation from high vibrational levels of $Xe_2^*(0_u^+)$ which is formed from $Xe^*(^3P_1)$ and $Xe(^1S_0)$ with the rate constant $(2.1 \pm .2)\times10^{-31}$ cm^6/sec with argon as the third body. Collisional deexcitation of $Xe^*(^3P_1)$ to $Xe^*(^3P_2)$ is observed with the rate constant $(1.5 \pm .3)\times10^{-14}$ cm^3/sec in agreement with Atzmon et al.[1] The xenon continuum at ∿1720A is formed from $Xe^*(^3P_2)$ and $Xe(^1S_0)$ with the rate constant $(2.15 \pm .25)\times10^{-32}$ cm^6/sec with argon as the third body, in agreement with Rice and Johnson.[2]

*Work supported by the ERDA Division of Physical Research
+Now at University of Texas, Austin, TX.
[1]R.Atzmon, et al. Chem. Phys. Lett. 29, 310 (1974).
[2]J.K.Rice and A.W.Johnson, J.Chem.Phys. 63, 5235 (1975).

BA4 Organic Vapor Excitation by Electron Beam Pumping of Rare Gas-Organic Vapor Mixtures. S. A. EDELSTEIN, T. F. GALLAGHER, H. H. NAKANO and D. C. LORENTS, SRI.--We have studied the emission from an e-beam pumped vapor phase mixture of the dye α-NPO and Ar (1.8 torr α-NPO, 3 atm Ar). The experiments were carried out in a heated cell with the α-NPO vapor pressure determined from the cell temperature. The mixture was excited by a 2 nsec, 5j pulse of electrons from a Febetron 706. We observed a broadband emission whose maximum was at 4100 Å with a width of 800 Å FWHM. The measurements and conditions of the experiment suggest that excitation occurs via a two-step process. The e-beam produces metastable argon atoms which collisionally transfer their energy to the α-NPO. By comparing the integrated emission intensity to the intensity observed from an Ar-N_2 mixture, we determined that the photon yield per excited Ar atom was .09 ± .04. The implication of the results on the possibility of making a laser pumped by energy transfer to an organic molecule from an e-beam excited mixture will be discussed.

BA5 Gain Versus Wavelength Near 5577 Å in Electron-Beam-Excited Kr/O_2 Mixtures.* JOSEPH R. WOODWORTH AND JAMES K. RICE, Sandia Labs.--An intense relativistic electron beam (1.8 MeV, 50 ns, 4 kJ) was used to transversely excite a 50-cm-long laser cell containing high pressure krypton (100 psi) and O_2 (10 Torr). The optical gain in the excited medium was determined by measuring the time decay of a 5-ns dye-laser pulse trapped in the laser cell by two highly-reflecting mirrors. The narrow-band (0.04 Å) dye-laser pulse was carefully wavelength tuned over the 5574 to 5583 Å region. The peak gain occurs at 5578.4 ±.2 Å, which is 1.1 Å on the red side of the atomic $O(2^1S-2^1D)$ transition. The half width of the gain curve is $\approx$ 1.5 Å, and the band is strongly shaded towards the blue. Measurements of gain versus time in the afterglow of the excitation pulse will also be presented.

---

*Work supported by Energy Research and Development Administration.

BA6 Red Band Emission In Cs-Rare Gas Discharges. B. SAYER, M. FERRAY, J. LOZINGOT & J. BERLANDE, CEN Saclay, France. -- Broad red bands, which have been previously observed in the absorption spectrum of neutral cesium mixed with xenon at high pressures (1), are also observed in the discharge emission spectrum of Cs mixed with each rare gas (He through Xe), even when P_{RG} is only a few Torr (2). It is shown that the band intensities are correlated with the atomic Cs line intensities originating from the $5D_{5/2}$ and $5D_{3/2}$ levels. This strongly suggests that these bands are emitted by Cs (5D) state atoms interacting with ground state Rg atoms. The study of a transient discharge in Cs-Xe mixtures further reveals that at least a part of these bands are emitted by bound Cs^* -Xe molecular states.

(1) W. Happer et al. Phys. Lett. 54A, 405 (1975)
(2) B. Sayer et al. J. Phys. B 9, L293 (1976)

BA7 Discharge Properties of the Ne-Cu^+ Ultraviolet Laser*, F. J. DE HOOG, G. J. COLLINS, Dept. Electrical Eng., C.S.U., Ft. Collins, CO 80523 - The Ne-Cu^+ laser system is capable of providing c.w. laser action in the 2500 Å region.[1] A major practical advantage of this laser is that the copper density is generated via discharge sputtering rather than with an external oven. We have measured the neutral copper density in a Ne-Cu^+ laser discharge as a function of current, neon pressure and tube geometry. For low currents the Cu density varies as i^n ($n \simeq 3.5$), but as the current approaches the threshold value for laser oscillation the copper density varies linearly with increasing current. Copper densities generated solely by discharge sputtering have been measured to exceed 10^{13} atoms/cc under laser conditions.

*Research supported by ERDA.

1. J. R. McNeil, et al., Appl. Phys. Lett. 28, 1976, 207.

BA8 Ultraviolet Laser Action in Cu^+, Ag^+ and Au^+, J. R. MCNEIL and G. J. COLLINS, Dept. Electrical Eng., C.S.U., Ft. Collins, CO 80523 - We have observed twenty four cw ultraviolet laser transitions which span the wavelength region from 224.3 to 383.0 nm. All laser transitions are judged to be excited by charge transfer collisions. The strongest laser transitions in Cu^+ are at 259.1 and 260.0 nm and we have obtained over 300 mW peak power from these transitions when operating on a pulsed basis. The strongest Ag^+ and Au^+ lines are at 318.1 and 282.2 nm respectively. In the case of the 318.1 nm transition of Ag^+ we have obtained 350 mW of single line output power. Measurements of output power versus discharge current, rare gas pressure and discharge tube geometry will be presented. The unique advantages of the hollow cathode discharge for exciting the Cu^+, Ag^+ and Au^+ lasers will be outlined.

*Research supported by ERDA.

BA9 Molecular Ion Electronic Transition Lasers Pumped by Thermal Energy Charge Transfer Reactions. J. B. LAUDENSLAGER and T. J. PACALA, Jet Propulsion Laboratory. --Lasing on the first negative band system of N_2^+ pumped by a thermal energy charge transfer from He_2^+ has been achieved by means of both electron beam[1] and electrical discharge excitation.[2] The mechanism for thermal energy charge transfer reactions will be discussed with respect to the formation of electronically excited molecular ions. The characteristics of a preionized transverse electric discharge pumped N_2^+ laser built at JPL will be discussed in light of this charge transfer mechanism.

[1]C. B. Collins, A. J. Cunningham, and M. Stockton, Appl. Phys. Lett. 25, 344 (1974).

[2]V. N. Ishchenko, V. N. Lisitsin, A. M. Razhev, and V. N. Starinskii, JETP Lett. 19, 233 (1974).

SESSION BB

10:45 AM - 12:15 PM, Tuesday, October 19

West Ballroom

POSITIVE ION REACTIONS

Chairman: R. C. Dunbar, Case-Western Reserve University

BB1 Three-Body Association Reactions of H^+ and H_3^+ Ions in Hydrogen from 135 K to 300 K.* RAINER JOHNSEN, CHOU-MOU HUANG and MANFRED A. BIONDI, Univ. of Pittsburgh. -- Rate coefficients for the reactions $H^+ + 2\ H_2 \rightleftharpoons H_3^+ + H_2$ (reaction 1) and $H_3^+ + 2\ H_2 \rightleftharpoons H_5^+ + H_2$ (reaction 2) have been determined at several temperatures in a drift tube-mass spectrometer apparatus. Reaction 1 is found to have forward rate coefficients of (3.0 ± 0.3) and (4.3 ± 0.4) x 10^{-29} cm^6/sec at a temperature of 300 K and at temperatures between 135 K and 160 K, respectively. Reaction 2 is found to have forward rate coefficients of (12 ± 2), (9.5 ± 3), (6.2 ± 2.0) and (4.6 ± 1.5) x 10^{-30} cm^6/sec at 156, 195, 203 and 210 K, respectively. Equilibrium constants for reaction 2 have been determined in the temperature range 176 K - 320 K. The temperature dependence of the equilibrium constant indicates a dissociation energy of (0.35 ± 0.03) eV for breakup of H_5^+ into H_3^+ and H_2.

*This research was supported, in part, by the National Aeronautics and Space Administration under Grant No. NGR39-011-137.

BB2 Measurement of the Rate Coefficients for the Bimolecular and Termolecular Charge Transfer Reactions of He_2^+ with Ne, Ar, N_2, CO, CO_2, and CH_4*. C.B. COLLINS, F.W. LEE, and R. A. WALLER, Univ. of Texas at Dallas-- This work reports the measurement in afterglows of e-beam discharges into high pressure gas mixtures of reaction rate coefficients for bimolecular charge transfer reactions of He_2^+, such as,

$$He_2^+ + N_2 \rightarrow \text{Products} \quad , \qquad (1)$$

and for the termolecular analogs, such as,

$$He_2^+ + He + N_2 \rightarrow \text{Products}. \qquad (2)$$

Values for the bimolecular component, (1), have been found to agree with the ESSA flowing afterglow results,[1] while termolecular components were found to range from 2×10^{-30} for Ne to 67×10^{-30} cm^6/sec for CO_2. The sizes of the latter rates suggest the general importance of three-body ion-molecule reactions in high pressure plasmas such as those found in e-beam lasers.

*Research supported by NSF Grant ENG 74-06262 and by ONR Contract No. N00014-76-C-0174.

1. D. K. Bohme, N.G. Adams, M. Mosesman, D.B. Dunkin, and E. E. Ferguson, J. Chem. Phys. 52, 5094 (1970).

BB3 Mechanisms for $He^+/H2$ Reactive and Radiative Processes.≠ D. G. HOPPER and A. C. WAHL, Argonne National Laboratory and E. G. JONES, B. M. HUGHES, and T. O. TIERNAN, Wright State University -- In the present paper we present experimental and theoretical studies which were conducted in our laboratories to further the characterization of the excited state potential energy surfaces of HeH_2^+. Beam-collision cell experimental studies yield distinct, strong thresholds for the formation of H^+, $H^*(n)$, n=2,3,4 at relative collision energies of 7.5, 9.1, 12.7, and 14.4 eV. Ab initio MCSCF calculations place the $2^2\Sigma^+$ and $3^2\Sigma^+$ HeH_2^{+*} potential surfaces within experimental error of the H^+ and $H^*(2)$ thresholds at the $X^2\Sigma^+$ geometry and indicate the other surfaces lie near the other thresholds. An adiabatic correlation diagram for the $(HeH_2)^+$ system is then constructed to facilitate a discussion of mechanisms we suggest for the several $He^+ + H_2$ reactive and radiative processes yielding H^+, H^*, HeH^+, and H_2^+. These mechanisms incorporate the thermal energy evidence from other workers and represent a reasonably complete model of the He^+/H_2 interaction for the relative collision energy range 0-20 eV.

≠ Work supported in part by AFOSR.

BB4 Reactions of Simple Hydrocarbon Ions with Molecules at Thermal Energies. D.SMITH and N.G.ADAMS, University of Birmingham, England-- The Selected Ion Flow Tube (SIFT) technique will be described, which is designed to study ion-neutral interactions at thermal energies[1]. This in essence involves the injection of a mass analysed beam of a single ionic species into a flowing neutral gas and the reactions are then studied using conventional flowing afterglow reactant gas injection and mass spectrometric sampling techniques. Data will be presented for a number of ion-molecule reactions including their rate coefficients and in some cases their product branching ratios[2]. In particular, reactions of the C^+, CH^+, CH_2^+, CH_3^+ and CH_4^+ with H_2, N_2, O_2, CO, CO_2, H_2O, CH_4 and NH_3 will be discussed. The possible significance of these reactions to chemical synthesis in interstellar clouds will be briefly indicated.

[1] N.G.Adams and D.Smith, Int.J.Mass Spectrom.Ion Phys. 21, 349 (1976)

[2] N.G.Adams and D.Smith, J.Phys.B: Atom.Molec.Phys. 2, 1439 (1976)

BB5 Xe^+-Ca Charge-Transfer Cross-Section*, K. B. BUTTERFIELD, D.C. GERSTENBERGER, T. SHAY and G. J. COLLINS, Dept. Electrical Eng., C.S.U., Ft. Collins CO 80523 - A xenon-calcium discharge has been proposed as a possible laser medium, employing a thermal energy charge transfer reaction of the form,

$$Xe^+ + Ca \rightarrow Xe + (Ca^+) + \Delta\varepsilon \quad \text{(Kinetic Energy)}$$
Reaction (a)

A pulsed afterglow technique has been used to measure the cross-section for the Reaction (a). Our measurements yield a cross-section σ (Xe^+ - Ca) = 2.2 x $10^{-16}cm^2$. A curve crossing theory for the Xe^+ - Ca charge transfer reaction is proposed. This theory has been successfully used to explain the measured individual cross section results for He^+ - Zn, He^+ - I, He^+ - Hg reactions. Xenon-calcium constitutes an important test of the curve crossing theory of charge-transfer.

*Research supported by NASA-Lewis.

BB6 Molecular Excitation in Low Energy Ion-Molecule Collisions.* G.H. BEARMAN, H.H. HARRIS, P.B. JAMES and J.J. LEVENTHAL, U. of MO-St. Louis.**--Emission from Rydberg states of NO molecules has been observed in H^+-NO collisions at relative energies as low as 10 eV. Agreement between the observed NO γ band spectrum and a model spectrum based on vertical electronic transitions indicates that a relatively long range interaction produces these excitations. Collisions between protons and N_2, CO and O_2 molecules produced no neutral molecule emissions in the range 190-800 nm; the apparently anomalous behavior of NO is interpreted in terms of molecular electronic structure.

*Submitted by J.J. LEVENTHAL
**Supported by US ERDA Contract E(11-1)-2718

SESSION CA

2:00 PM - 3:30 PM, Tuesday, October 19

East Ballroom

NEUTRAL GAS LASERS AND NUCLEAR PUMPING

Chairman: B. E. Cherrington, University of Illinois

CA1 Gain on the Mercury 5461Å and 3650Å Lines in the Afterglow of a High Pressure Pulsed Discharge.* J.K.CRANE, B.E. CHERRINGTON and J.T. VERDEYEN, Gaseous Electronics Laboratory, University of Illinois -- Gain has been observed on the 5461Å ($7^3S_1 - 6^3P_2$) and 3650Å ($6^3D_3 - 6^3P_2$) transitions in atomic Hg. The media consists of 50-150 torr and He and 20-50 torr of Hg excited by a 1 μs, pulsed, 0.5-4 a/cm^2 discharge. Gain as high as 10% has been measured with an OSRAM spectral lamp. Gain appears in the afterglow from 2-10 μsec after the termination of the discharge pulse. The upper state appears to be pumped by recombination, during which time the lower state is being depopulated by collisions with electrons or Helium atoms.

*Work supported by the Division of Laser Fusion of ERDA.

CA2 Electron-Collisional Excited State Kinetics in Argon and Mercury Electrical Discharges.* O. JUDD, Los Alamos Scientific Laboratory.--The effects of inelastic electron collisional processes on the efficiency for population of electronic states in atomic argon and mercury in an electrical discharge have been studied theoretically as a function of excited state population fraction. Electron impact excitation rates for the lowest lying electronic states and rates for ionization from these states have been determined through the use of the Boltzmann transport equation for the range $5 \times 10^{-17} \leq E/N \leq 10^{-15}$ Vcm^2. It was found that the efficiency for populating these states by electron impact, can be reduced significantly as the excited state population fraction X* is increased; in Ar this occurs for $X^* > 10^{-5}$. These effects impose fundamental limitations on the efficiency and power extraction that can be obtained from electrical discharge excited visible and uv lasers that depend on the populated electronic states in the noble gases for pumping the lasing species.

*Work supported by the Energy Research and Development Administration.

CA3 RESULTS OF A PARAMETRIC STUDY OF A FLOWING COPPER VAPOR LASER* -- B. G. Bricks, T. W. Karras, R. S. Anderson, and C. E. Anderson, General Electric Space Sciences Laboratory -- A parametric study has been conducted of a flowing, high-gain, copper vapor laser operating in a transverse discharge configuration[1]. Parameters (voltage, current density, copper density) ranges were extended to values not previously explored. Higher values of gain (>1000 dB/m), specific energy (up to 100 $\mu J/cm^3$), and pulse repetition rate (>20 kHz) were achieved as a result of these extensions. The very high inversion densities implied by these results can be related to the increased electron temperature and density in the discharge. The effects of the macroscopic variables on the microscopic processes and their effect on laser output will be discussed.

*Work supported in part by AFWL, Contract F29601-74-C-0048.

1. B. G. Bricks, T. W. Karras, T. E. Buczacki, L. W. Springer and R. S. Anderson, et al, IEEE J.Q.E. QE-11, 57 (May 1975).

CA4 Gain in Neutral Gas Lasers, PETER J. WALSH, Fairleigh Dickinson Univ. -- A general, yet simple, technique for analyzing gas discharges has been applied to neutral gas lasers. This analysis yields the gain per unit length,g, directly in terms of the external parameters which control the gas laser: gas density,N, tube diameter,d, and discharge current,I. The analysis yields the gain "saturation" with current in a form which generalizes the result of White and Gordon. It gives the empirical laws for optimum gain: $g_{opt} \propto d^{-1}$, $N_{opt} \propto d^{-1}$, $I_{opt} \propto d^{m}$, where m=1 when wall diffusion or collision broadening is important. Calculated gain at 3.39μ in He-Ne is compared with empirical data over a wide range of current and pressure in order to illustrate the technique.

CA5 Recombination Pumping of Atomic Nitrogen and Carbon Lasers.* GARY W. COOPER, and J.T. VERDEYEN, Gaseous Electronics Laboratory, University of Illinois -- It is well established that lasing of atomic nitrogen or carbon can be obtained during the afterglow of an electrical discharge in gas mixtures of either neon or helium containing low partial pressures of N_2 or CO. In addition, the neon-nitrogen laser has recently been pumped directly by nuclear radiation. Microwave quenching experiments have shown conclusively that these afterglow lasers are being pumped directly by a recombination process. These results are incompatible with the dissociative excitation transfer mechanism originally proposed for these lasers. Inasmuch as the lasering occurs between levels of the neutral atom which are above the energy of the ground state molecular ion, we can identify the recombining ion as N^+ (or C^+). Since this recombination process is highly compatible with the reactor-generated plasma, it is not unreasonable to infer that this process is also the pumping mechanism in the nuclear excited neon-nitrogen laser.

*Work supported by Division of Physical Research of ERDA.

CA6 Direct Nuclear Pumping of a ^{3}He-Ar Laser. N. W. JALUFKA, R. J. DeYOUNG*, and F. HOHL, NASA-Langley Research Center.--Direct nuclear pumping of a ^{3}He-Ar laser utilizing the volumetric $^3He(n,p)^3H$ reaction has been achieved.[1] The effect of the variation of the argon concentration has now been determined. The laser output at 1.79μ (Ar I) was measured as a function of argon concentration (in ^{3}He) between 0.1% and 10%. The output was found to have a rather flat maximum from 0.1% to 5% Ar concentration. For a given concentration the laser output increases with total pressure. Time-resolved measurements of the laser output and the thermal neutron flux show that laser output continues after the neutron flux drops below threshold, suggesting that mechanisms other than direct electron impact excitation play a major role in obtaining the population inversion.

* Vanderbilt Univ. Supported in part by Grant NSG 1232.

[1] Jalufka, N.W., DeYoung, R.J., Hohl, F., and Williams, M.D., Appl. Phys. Lett. 29, 188 (1976).

CA7 Collisional Processes in the ^{3}He-Ar Nuclear Pumped Laser. P. A. WINTERS, N. W. JALUFKA, and R. J. DeYOUNG*, NASA-Langley Research Center.--Calculations of rates for dominant collisional processes in the ^{3}He-Ar direct nuclear-pumped laser have been carried out. Processes which result in ionization, excitation, and recombination are emphasized in an effort to determine which mechanisms are most likely to result in a population inversion in Ar I. The calculations were performed using the electron energy distribution function derived by Hassan and Deese[1] for nuclear radiation induced plasmas. The various rates are discussed and compared with the experimental results from the ^{3}He-Ar nuclear-pumped laser[2]. The compatibility of the two results suggests an adequate model for the ^{3}He-Ar laser and applications to other ^{3}He noble gas models will be presented.

* Vanderbilt Univ. Work supported in part by NASA Grant NSG 1232.

1 Hassan, H.A., and Deese, Jerry E.: NASA CR-2712, 1976.
2 Jalufka, N.W., DeYoung, R.J., Hohl, F., and Williams, M.D.: Appl. Phys. Lett. 29, 188 (1976).

CA8 Direct Nuclear Pumping of ^{3}He-Kr and ^{3}He-Xe. R. J. DeYOUNG*, N. W. JALUFKA, and F. HOHL, NASA-Langley Research Center.--Recent results with nuclear pumping of ^{3}He-Ar[1] have led to the investigation of other ^{3}He noble gas mixtures as potential candidates for direct nuclear pumping. In particular, Kr and Xe have been investigated using a high-pressure electrically pulsed afterglow discharge. Lasing occurs at 2.52μ and 2.026μ in Kr and Xe, respectively, in the afterglow discharge. The characteristics of the afterglow appear to be similar to the nuclear-induced plasmas. Results will also be presented on direct nuclear pumping of ^{3}He-Kr and ^{3}He-Xe which help substantiate that the nuclear discharge can be modeled by a "steady-state afterglow." The major population inversion mechanisms will also be discussed.

* Vanderbilt Univ., work supported in part by NASA Grant NSG 1232.

1 Jalufka, N. W.; DeYoung, R. J.; Hohl, F.; and Williams, M. D., Appl. Phys. Lett. 29, 188 (1976).

CA9 Study of a Direct Nuclear Pumped, He-Hg Laser*, M.A. AKERMAN and G.H. MILEY, Univ. of Illinois and D. McARTHUR, Sandia Labs--Direct nuclear pumping (DNP) of the 6150 A° Hg II transition has been achieved in a He-Hg mixture using a ^{10}B-coated tube bombarded by thermal neutrons from the Sandia Fast Burst Reactor. Of the five DNP lasers reported to date, this is the first output in the optical range. Optimum laser pressures of 2.5 mTorr Hg, 600 Torr total as well as neutron flux threshold of $\sim 1 \times 10^{16}/cm^2 sec$ are consistent with previous gain measurements using the Illinois Triga Reactor.[1,2] Both results, earlier spectra measurements, and rate equation solutions, indicate the important mechanisms involved. Below ~300 Torr, charge-exchange collisions populate the upper state of Hg. At higher pressures, other processes compete with charge-exchange.

[1]G.H. Miley, *et al.*, "Recent Nuclear Pumped Laser Results," *Princeton Conf. on Partially Ionized Plasmas* (June 1976).

[2]M.A. Akerman, *et al.*, "Charge Exchange Phenomena in a Nuclear Radiation Produced He-Hg Plasma," *1976 IEEE Conf. on Plasma Science* (May 1976).

*This work supported by Div. of Physical Research, USERDA.

CA10 Population Processes for the He-Hg Direct Nuclear Pumped Laser (DNPL) M.A. AKERMAN, University of Illinois, Urbana, IL W.E. WELLS, Miami Univ., Oxford, OH

A paper by M. A. Akerman, et al, in the proceedings of this conference describes the discovery of a He-Hg DNPL. This laser operating on an ion transition in Hg (6150 Å, the first visible wavelength DNPL) was predicted by lower neutron flux experiments and theoretical modeling of the plasma. These studies indicate that the lower pressure electrical operation is dominated by the charge exchange reaction.

$$He^+ + Hg(1\ S_o) \rightarrow Hg^+ 7^2P_{3/2} + He(1\ S_o),$$

while the higher pressure DNPL operation requires the mixed metastable ionizing collisions

$$He(2^3s) + Hg(6^3P_o) \rightarrow Hg^+(7^2P_{3/2}) + He(1\ S_o) + e.$$

This second process requires a lower Hg concentration regime for optimum operation. The results of this laser plasma modeling will be presented for comparison with the data from the above referenced paper.

This work supported in part by the Division of Physical Research, ERDA.

SESSION CB

2:00 PM - 3:00 PM, Tuesday, October 19

West Ballroom

NEGATIVE ION PROCESSES

Chairman: D. Smith, Univ. of Birmingham, G.B.

CB1 Flow-Drift Tube Studies of the Reactions of O_3^- and CO_3^- With NO, NO_2, and SO_2.* D. L. ALBRITTON, I. DOTAN and F. C. FEHSENFELD, NOAA Aeronomy Laboratory, Boulder, CO 80302.---The relative kinetic energy dependence of the following reactions has been investigated in the range 0.04 - 2 eV:

$$O_3^- + NO \rightarrow NO_2^- + O_2 \qquad (1)$$

$$O_3^- + NO_2 \rightarrow \begin{matrix} NO_2^- + O_3 \\ NO_3^- + O_2 \end{matrix} \qquad (2)$$

$$O_3^- + SO_2 \rightarrow SO_3^- + O_2 \qquad (3)$$

$$CO_3^- + NO \rightarrow NO_2^- + CO_2 \qquad (4)$$

$$CO_3^- + SO_2 \rightarrow SO_3^- + CO_2. \qquad (5)$$

Reactions (1) and (4) are slow at 0.04 eV but increase rapidly at higher energies. The others are fast with little energy dependence, except for (5) which exhibits a deep minimum. The branching ratio of (2) is 0.5 at 0.04 eV, with NO_2^- favored at higher energies.

* Supported in part by DNA

CB2 Measurements of Negative Ion Cluster Formation and Dissociative Attachment in HCl and HCl + N_2 Mixtures. R.J. CORBIN, K.J. NYGAARD, and W.R. SNOW, University of Missouri-Rolla.* --We have been using a drift tube - quadrupole mass spectrometer apparatus to study the negative ions produced in pure HCl as well as in HCl and N_2 over a wide range of pressure and E/p -values. For average electron energies high enough to produce positive nitrogen ions, the most abundant negative ion detected is Cl^- formed by dissociative attachment of HCl. At lower electron swarm energies the primary negative ion, Cl^-, is converted to clusters of the type $Cl^- \cdot (HCl)_n$ (with n=1,2 observed so far). Near onset the clusters are predominant, and an estimate for the rate of formation of the first cluster (n=1) exceeds $10^{-26} cm^6/sec$. The results are of importance in explaining anomalously low negative ion drift velocities found in other experiments.
*Supported in part by AFOSR.

CB3 Rotational "Dipole States" of Molecular Negative Ions.* W. R. GARRETT, Oak Ridge National Laboratory, Oak Ridge, Tennessee 37830.--Some molecules are able to bind an extra electron to form a stable negative ion in which the valence orbital is very external in character, with low binding energy and large average radius. Strongly polar closed shell molecules fit in this category. In systems of this type, the electron binding energy is measurably influenced by rotational motion of the nuclei.[1] This breakdown in the Born-Oppenheimer approximation leads to rotational energy states of a negative ion which are uncharacteristic of the neutral molecules. The shift in energy of the rotational levels as a function of total angular momentum, J, is determined by the moment of inertia and the dipole moment of the polar molecule.

*Research sponsored by the Energy Research and Development Administration under contract with the Union Carbide Corporation.

[1]W. R. Garrett, Phys. Rev. A11, 509 (1975).

CB4 Thermal Rydberg Atom Molecule Collision: Formation of Molecular Negative Ions.* W. C. TAM, P. M. RACKOV, S. F. WONG and G. J. SCHULZ, Yale U -- Charge transfer reactions $A^{**} + BC \rightarrow A^{+} + BC^{-}$ between rare gas atoms A = He, Ar, Kr, Xe in high Rydberg states and BC = O_2 and NO have been studied. The high Rydbergs are generated by electron impact on rare gas atoms in a gas cell which also contains a small fraction of the molecular gas. A quadrupole mass spectrometer is used to monitor the molecular negative ions thus formed, as the electron energy traverses the I.P. of the atom. A signal of BC^{-}, linearly proportional to the partial pressure of BC in the mixture, is observed with an onset below the I.P. of the atom. The energy position of this onset can be related to the electron affinity of BC. The electron affinities of O_2 and NO derived are compared with previous experiments, in particular, the recent photodetachment studies. An estimate for the relative reaction rates for the reactions $A^{**} + BC \rightarrow A^{+} + BC^{-}$ is also given.

*This work supported by NSF.

CB5 Photodetachment of Excited NO_2^-.* B.A. HUBER, P.C. COSBY, J.T. MOSELEY, & J.R. PETERSON, SRI -- In an attempt to study the peroxy ($NO \cdot O^-$) isomer of NO_2^-, photo destruction cross sections were measured at photon energies (1.95-2.25 eV) below the photodetachment threshold for the ground state species. Using a drift tube-laser apparatus, no stable isomer of NO_2^- was observed in NO_2/O_2 and N_2/O_2 mixtures. Instead, the apparent photodestruction cross section decreased with the number of collisions between NO_2^- formation and its interaction with the laser. Cross sections of 4×10^{-19} to 6×10^{-19} cm^2 over this photon energy range for nascent NO_2^- are consistent with those reported[1] for the excited ion but decrease to zero at high pressures and long drift distances. Apparent relaxation rates of 10^{-13} and 10^{-10} cm^3/sec for collisions with O_2 and NO_2 suggest loss of vibrationally excited NO_2^- by collisional relaxation and charge transfer, respectively.

*Work supported by BRL through Army Research Office.

[1]E. Herbst, T. A. Patterson, and W. C. Lineberger, J. Chem. Phys. 61, 1300 (1974) and references therein.

CB6 Calculation of Photodetachment Cross Section of Atomic Negative Ions.* R. M. Stehman and S. B. Woo, Univ. of Del.--Using a bound state wave function proportional to $[\exp(-\gamma r)]/r$ for $r>R$, the relative photodetachment cross section, σ, of atomic negative ions as a function of energy and the differential cross section as a function of angle are calculated. The results agree with experimental results for electrons detached from either s or p orbitals. R is a radius characteristic of the neutral atom, derived from atomic structure tables. $\gamma = \sqrt{(2mE)}/h$, where E is the electron affinity. This method assumes a potential well having a range no greater than R, and its success results from the fact that contribution to σ from the wave function in the region $r<R$ is small for photon energies used in experiments. This allows σ to be determined without knowledge of the wave function inside the core, and minimizes the need to include phase shifts in the final continuum wave function. The calculation is therefore very simple. However the lack of information about the wave function for $r<R$ prevents calculation of the electron affinity, the absolute value of σ, and features of σ rising from final states which involve excited neutrals. The use of sum rules to provide absolute values of σ will be discussed.

* Work supported in part by NSF.

SESSION DA

3:45 PM - 5:15 PM, Tuesday, October 19

East Ballroom

IR LASERS

Chairman: W. T. Leland, LASL

DA1 Description and Analysis of the Mode-Medium Interaction in CW-CO_2 E-Beam Sustainer Lasers. M. J. YODER and D. R. AHOUSE, Avco-Everett Research Lab. Inc. 2385 Revere Beach Pkwy., Everett, MA -- The output flux of a flowing - gas CW CO_2 E-beam sustainer laser has been shown to exhibit large fluctuations (up to 100%) accompanied by severe optical medium distortions. Experimental results will be summarized as a function of gas pressure, electrical excitation rate and resonator configuration (both stable and unstable). A number of suggested causes of the output pulsations will be discussed, and relevant experimental data will be cited. An assessment of the current state of understanding of this phenomenon will be made.

DA2 Pumping Characteristics of Multi atmosphere CO_2 Amplifiers. L. J. DENES, L. H. TAYLOR, L. E. KLINE, R. J. SPREADBURY and R. V. BABCOCK. Westinghouse Research Labs.--Multi atmosphere CO_2 laser discharges are of particular interest as a means for obtaining temporally-undistorted-amplification of subnanosecond laser pulses. Limitations have occurred in the design of large laser systems due to parasitic oscillations and gain standoff considerations. Such processes are observed to have an inherent buildup time of $\sim$0.5 μsec in practical installations. Therefore, under conditions in which the amplifiers are pumped and the pulse extracted within 0.5 μsec, such limitations would be obviated. We have completed calculations which show that a self-sustained discharge can be pumped such that 95% of peak gain is achieved in about 0.5 μsec. These calculations were done for a CO_2:N_2:He = 1:1:6 mixture at 1800 Torr. The gain buildup time has also been studied as a function of pulse duration, input power, electric field-to-gas density ratio and for other mixture ratios. Discharge formation and circuit performance calculations indicate that the required 0.3 μsec (FWHM) current pulse can be achieved with a low inductance, single capacitor circuit.

DA3 Causes of Thermal Instability in Externally Sustained Molecular Discharges*. W. L. NIGHAN, United Technologies Research Center, - - The basic causes of thermal instability have been analyzed for conditions typical of high power cw electric lasers. It has been found that two distinctly different types of instability can occur, one driven by disturbances in electron-molecule vibrational excitation and a second caused by sudden collapse of the vibrational energy reservoir. The instability growth rate for the electron driven mode is exceptionally sensitive to specific details of electron production and loss processes, while the vibrational relaxation mode is sensitive to the degree of V-T nonequilibrium and the processes by which vibrational relaxation occurs. Specific details of those collision processes found to be most important will be emphasized.
*Work performed in part through the sponsorship of the Office of Naval Research, Contract No. N00014-72-C-0380, and by the U. S. Air Force, Contract No. F33615-76-C-2946.

DA4 Distribution of E/N and N_e in a Cross-flow Electric Discharge Laser. J. W. DUNNING, JR., R. B. LANCASHIRE, and E. J. MANISTA, NASA Lewis Research Center.--A study of the spatial distribution of the ratio of electric field to neutral density and electron density in a flowing gas, multiple pin-to-plate discharge will be discussed. Measurements were made in the high-power, closed-loop laser at the NASA Lewis Research Center. For the data presented, the laser was operated at a pressure of 140 torr (1:7:20; CO_2, N_2 He) with typically a 100m/sec velocity in the 5x5x200 cm. discharge volume. Measured E/N ratios ranged from 2.7×10^{-16} to 1.4×10^{-16} v cm^2 along the discharge while electron density ranged from 2.8×10^{10} to 1.2×10^{10} cm^{-3}.

DA5 High-power High-pressure Photo-ionization Stabilized Glow Discharge Lasers. V. HASSON*, J. BRINK, H.M. VON BERGMANN, Council for Scientific and Industrial Research, Pretoria, South Africa and K. BILLMAN, NASA-Ames Research Center.- The authors have recently developed a simple and versatile fast photo-ionization stabilized discharge scheme for exciting high-power high-pressure gas lasers. The stabilization scheme can operate over a wide range of overvoltages and current densities and is well suited to transverse and travelling wave excitation of a variety of established laser systems. We have used the technique to excite multimegawatt (U-V) nitrogen and (I.R) carbon dioxide lasers at pressures ranging from 0-5 and 0-7 bar respectively and shall discuss the important excitation and operating characteristics of these high-pressure systems. The principle is currently being adapted to the excitation of a variety of established high-pressure excimer and other U-V laser systems. The authors will provide an up-to-date summary and critical evaluation of this work.

* NRC Senior Resident Research Associate, NASA Ames.

DA6 Experimental Studies of Electron Energy Distribution Function in CO_2 Laser Plasmas. S. ONO and SIN-LI CHEN, Musashi Inst. of Tech., Tokyo, Japan. -- Electron energy distribution function in CO_2 laser plasmas has been studied by means of an electrostatic probe. Relations between the laser power and the gas flow velocity in connection with the plasma parameters, dissociation product CO and the vibrational temperature of $N_2C^3\pi_u$ state have been also examined. Experimental results show that:1) The electron energy distribution in plasmas is non-Maxwellian, depletion of electrons about 4-8 eV has been observed. 2) For gas mixtures of CO_2:N_2:He=1:1:8, laser power increases with increasing gas velocity, whereas for the case of CO_2:N_2:He=3:1:6, laser power does not increase with increasing gas velocity. 3) The behavior of the electron temperature, density and the dissociation product CO with varying gas velocity are almost the same for above two cases, but only the electron energy distribution function is quite different. In the case of CO_2:N_2:He=3:1:6, a considerable depletion of electrons near 4-8 eV has been observed by increasing gas velocity even when the plasma is not lasing. Discussions relating the experimental results and the laser excitation mechanism are also presented.

DA7 Photoionization and Absorption Crossections of Seeding Materials for Photo-Preionized Lasers,* D. F. Grosjean, Systems Research Laboratories, Dayton, Ohio and P. Bletzinger, Aero Propulsion Laboratory, WPAFB, Ohio. -- For the operation of UV-preionized lasers, seed gases increase the initial electron densities by a factor of 10^3 or more. To understand the details of the photoionization process we have used a double ionization chamber to measure photoionization and absorption cross sections of Tri-n-propylamine, Triethylamine, Trimethylamine and Dimethylaniline over the wavelength range of interest. The UV-source was calibrated against a NBS photodiode. We also report on quantitative measurements of emission spectra of spark sources similar to those used in molecular lasers in several gas mixtures. The importance of the measured cross sections and the spark emission spectra for the operation of CO_2 and CO lasers will be discussed.

* Supported by USAF Contract F33615-73-C-4130

DA8 Time-Resolved He-Xe and Ar-Xe Laser Characteristics.* R. A. Olson, Systems Research Laboratories, Inc., and A. Garscadden, Air Force Aero Propulsion Laboratory. -- Studies of high pressure He-Xe and Ar-Xe mixtures in a closed cycle high-repetition-rate TEA laser have revealed significant spectral and temporal differences in the laser pulses. With He-Xe mixtures, lasing occurs mainly on the Xe 7p-7s transitions whereas with Ar-Xe mixtures, only the 5d-6p transitions have been observed. The laser pulses typically last microseconds into the afterglow. The afterglow character of the lasing is accentuated in He-Xe, and under some conditions the laser pulse is delayed several microseconds with respect to the discharge current pulse. The increased laser output power and efficiency obtained with Ar-Xe as compared to He-Xe is consistent with recently published results.[1] An analysis of the temporal behavior of laser pulses in the afterglow provides a basis for discrimination among various possible pumping mechanisms.

* Supported by USAF Contract F33615-73-C-4130

[1] L. A. Newman and T. A. DeTemple, Appl. Phys. Lett. 27, 678 (1975)

SESSION DB

3:00 PM - 5:15 PM, Tuesday, October 19

West Ballroom

HEAVY NEUTRALS

Chairman: L. D. Schearer, University of Missouri-Rolla

DB1 Measurement of the Rate Coefficients for the Bimolecular and Termolecular Channels for the Destruction of $He(2^3S)$ Metastables in Collisions with Ne, Ar, N_2, CO, CO_2, and CH_4*. C.B. COLLINS and F.W. LEE, Univ. of Texas at Dallas--Measurements of the logarithmic destruction frequency of the population of $He(2^3S)$ metastable atoms obtained by optical absorption in afterglows of intense e-beam discharges into various gas mixtures have led to an appreciation of the importance of termolecular reaction channels. Such reactions of the type,

$$He(2^3S) + He + N_2 \rightarrow \text{Products},$$

have been studied for the cases of $He(2^3S)$ and Ne,Ar, N_2, CO, CO_2 and CH_4. In each case the termolecular channel has been found to dominate at pressures in the range of an atmosphere and corresponding rate coefficients have been found to vary from less than $1x10^{-30}$ for Ne to $8.3x10^{-30} cm^6/sec$ for CO_2.

*Research supported by NSF Grant ENG 74-06262 and by ONR Contract No. N00014-76-C-0174.

DB2 Collisional Broadening in the Spectroscopic Measurement of Helium Metastable Populations at High Pressure. G.D. MYERS, D.P. COLTON, and R.A. SIERRA, U. of Texas at Dallas -- Optical emission and absorption techniques have been used to extend the study of metastable chemistry in the helium afterflow to high pressure regimes (.5 to 5 Atms.). Both atomic and molecular species destruction rates have been extracted and are related to proposed processes. These include the metastable-metastable ionizing collisions, which are the primary source of late time energy in the afterglow. Destruction of metastable molecules by small admixtures of foreign gases (Ne, N_2, O_2) has also been investigated. Actual metastable populations have been calculated from the data with the aid of a computer model that recognizes the vital importance of collisional broadening at these pressures.

DB3 Measurement of the Ionization of Argon by Collisions with Neon Metastables.* T. RHYMES, Australian National Univ.-- The Cavalleri electron density sampling technique has been used to determine the rate of ionization of Ar by Ne in the $^3P_2$ metastable state. Measurements were performed at 295 K at pressures of 3,4,6,8, and 10kPa and for argon concentrations of 60 to 400 ppm. The results were analyzed including the effect of radiation trapping of the $^3P_1$ to $^1S_0$ resonance radiation. Results are compared with previous experiments utilizing thermal beams, merging beams. photoabsorption of a discharge afterglow, and microwave afterglow. Possible causes of the wide variation of the ionization cross section measured by different techniques are discussed.

*Submitted by: Stanley E. Babb, Jr.

DB4 Electronic Energy Transfers in Ar-Xe Mixtures.* P.K. Leichner, E.T. Hall, and K.F. Palmer, Univ. of Kentucky - - A 250-keV electron beam was used to study electronic energy transfers in mixtures of Ar (50-900 Torr) with small amounts of Xe (0.1 - 5 %). Two-body destruction rates of the $Ar(^1P_1)$ and $Ar(^3P_1)$ resonance states by Xe ground states atoms are 1.03×10^7 $sec^{-1}/Torr$ and 6.13×10^{-6} $sec^{-1}/Torr$, respectively. Quenching rates for the Ar_2^* molecular continuum radiators and collision coefficients for Xe excited atomic states in Ar-Xe mixtures will be presented. Such data are of importance in understanding the energy transfer mechanisms in the rare-gas-halide lasers. A kinetic model for collisional excitation transfer in Ar-Xe mixtures will be discussed.

*Work supported in part by USERDA through a subcontract from Oak Ridge National Laboratory.

DB5 Electronic Energy Transfer Reactions in Ar-Kr Mixtures.* M.D. Thieneman and P.K. Leichner, Univ. of Kentucky - - Time - resolved emission spectroscopy was employed to investigate excitation transfers in Ar-Kr mixtures. Total gas pressure ranged from 50 Torr to about 1.2 atm; Kr impurity concentration was varied from 0.1 to 3%. Excitation of the gases was provided by a 250-keV electron beam. Quenching rates of the $Ar(^1P_1)$ and $Ar(^3P_1)$ resonance states in two-body collisions with Kr ground state atoms are 3.47×10^4 sec^{-1}/Torr and 2.22×10^5 sec^{-1}/Torr, respectively. Energy transfer rates for Kr excited atomic states in Ar-Kr Mixtures will be presented, and a kinetic model for excitation transfers in the Ar-Kr system will be proposed.

*Work supported in part by USERDA through a subcontract from Oak Ridge National Laboratory.

DB6 Electronic Energy Transfers in Kr-Xe Mixtures.* J.D. Cook and P.K. Leichner, Univ. of Kentucky - - We have studied excitation transfers in Kr-Xe mixtures. The Kr host gas pressure was varied from 25 to 900 Torr with Xe impurity concentrations ranging from 0.1 to 5%. The gas mixtures were excited with 250-keV electrons. Destruction rates of $Kr(^1P_1)$ and $Kr(^3P_1)$ resonance atoms in two-body collisions with normal Xe atoms have been measured to be 1.21×10^5 sec^{-1}/Torr and 7.84×10^5 sec^{-1}/Torr. Rates for the formation and decay of Xe excited atomic and molecular species in Kr-Xe mixtures will be presented. A model for excitation transfers in Kr-Xe mixtures will be discussed.

*Work supported in part by USERDA through a subcontract from Oak Ridge National Laboratory.

DB7 Radiative Decay and Quenching of Na(3^2P) Levels at High Na Densities.*--L. LAM, T. FUJIMOTO, A.C. GALLAGHER, and A.V. PHELPS, JILA, U. of Colorado and NBS and M.M. HESSEL NBS/Boulder. Measurements have been made of decay constants for the resonance radiation emitted by Na atoms in the 3^2P states. A pulsed dye laser was used to excite the Na atoms at Na densities from 10^{13} to $3\times10^{16}cm^{-3}$. At Na densities below about $3\times10^{14}cm^{-3}$ the decay constants are in reasonable agreement with predictions of theory.[1] At higher sodium densities the excited atoms are destroyed primarily by excitation transfer collisions with sodium molecules with a rate coefficient of the order of $3\times10^{-9}cm^3/sec$. The observed dependence of the decay and of the band emission on molecular concentration is consistent with this model. Analysis of time constant and relative molecular intensity data in terms of collisional coupling among the excited atomic and molecular states is continuing.

*This work was supported in part by ERDA and by ARPA/ONR.

[1]T. Holstein, Phys. Rev. 83, 1159 (1951).

DB8 Time-of-flight determination of radiative decay rates for high Rydberg states in atomic nitrogen. C. A. KOCHER and C. E. FAIRCHILD,* Dept. Phys., Ore. St. Univ. -- A method is presented for atomic beam time-of-flight measurements of radiative decay rates in high Rydberg atoms. The method is applied to an experimental study of nitrogen atoms in which Rydberg states were produced in the dissociative excitation of N_2 by pulsed electron impact. State selection was achieved by passing the atomic beam through an electric field region, which selectively ionizes atoms in the highest lying Rydberg levels. From studies of the atomic beam transit-time distribution at electric fields up to 4.5 kV/cm, radiative decay rates Γ_n have been inferred for states having principal quantum numbers n in the range $19 \lesssim n \lesssim 35$. The data are consistent with Γ_n given by a power law of the form $\Gamma_n = (6.4\pm0.6) \times 10^4\ sec^{-1} \times (25/n)^{\alpha}$, and with an excitation cross section having the n-dependence $\sigma_n \propto 1/n^{\alpha+1}$, where $\alpha = 2.7 \pm 0.8$.

*JILA-LASP Visiting Fellow, Univ. of Colo., 1975-76.

DB9 The Influence of Molecular Rotation on Vibration-Translation Energy Transfer. ROBERT L. MCKENZIE, NASA-Ames Res. Cntr - The role of molecular rotations in the exchange of vibrational and translational energy is investigated for collisions between diatomic molecules and structureless atoms. A three-dimensional semiclassical description is applied with emphasis on the influence of rotational coupling on the net rate of vibrational energy transfer summed over all final rotational states. The results are compared with the predictions of an equivalent collinear collision model. The mechanisms of vibrational energy transfer including rotational transitions are shown to be separable into three classes with the molecules belonging to each class identified first by their ratio of fundamental vibrational and rotational frequencies, ω_e/B_e, and second by the proximity of their initial state to a near-resonant vibration-rotation transition with a small change in angular momentum. While the dynamics of molecules with ω_e/B_e ratios comparable to the range of angular momentum transitions having strong coupling are found to require a complete three-dimensional description, the rates of vibrational energy transfer in molecules with large ω_e/B_e ratios appear to be well approximated by a collinear collision model.

DB10 Temperature Dependence of the Laser Enhanced Reaction $NO + O_3(001)$.* R. J. GORDON, J. MOY and E. BAR-ZIV, U. of Illinois at Chicago Circle. The title reaction was studied over the temperature range 156-430 K, using a CO_2 TEA laser to excite ozone in a flow apparatus.[1] The ratio of the laser induced chemiluminescent signal to the thermal background was combined with laser absorption measurements to yield the ratio k_{2a}/k_{1a}, where k_{2a} is the rate coefficient of the enhanced reaction producing chemiluminescent NO_2*, and k_{1a} is the thermal rate coefficient. We found that the activation energy of the enhanced luminescent reaction is lowered by 1.3 ± 0.2 kcal/mole, or 43±7% of the vibrational energy supplied by the laser. The ratio of the preexponential factors for reactions (2a) and (1a) was approximately unity. From the decay rate of the laser induced signal we determined the sum $k_{2a}+k_{2b}+k_3^{NO}$, where k_{2b} is the rate coefficient of the laser enhanced reaction producing ground state NO_2, and k_3^{NO} is the vibrational relaxation rate of $O_3(001)$ by NO. Deviation from a single exponential decay enabled us to extract k_3^{NO} from this sum.

*Supported by the NSF.

[1]R. J. Gordon and M. C. Lin, J. Chem. Phys. 64, 1058 (1976).

DB11 Vibrational Relaxation of SF_6.* J.S. COHEN and A.E. GREENE, LASL. -- Kinetic modeling of laser-excited gas mixtures of SF_6 has been performed. It is assumed that no more than two or three photons can be absorbed by a given molecule. Vibrational transitions can occur by one of several mechanisms depending on the mass and structure of the collision partner: short-range repulsive potential, long-range coupling between similar molecules, partial energy transfer to the vibrational or rotational modes of the collision partner. Our calculations indicate that there are experimentally observed examples of each of these mechanisms. The theory for the short-range coupling, based on the distorted-wave approximation, is similar to that of Schwartz, Slawsky, and Herzfeld (SSH), Tanczos, and Stretton. The results are in generally good agreement with experiment. The steps in the deactivation of the excited SF_6 molecule are found to be quite different for collisions with light and heavy rare-gas atoms. Rotational excitation appears to be important in deactivation by N_2, but the rapid rate for H_2 appears to be mainly a result of its light mass. It is shown by an eigen-analysis that the decay time observed in time-resolved spectroscopic experiments may not always be representative of total relaxation of the system.
*Supported by the USERDA.

DB12 Heating of D_2 Gas Targets by Intense Triton Beams.* A.E. GREENE and A.M. LOCKETT III, Los Alamos Scientific Laboratory. -- A detailed study has been undertaken to determine the time required for energy in a D_2 target gas. Ionization, excitation (electronic, vibrational, and rotational) and dissociation of D_2 by both tritons and secondary electrons are considered. For tritons the effects of charge exchange and for electrons the effects of diffusion and recombination are also examined. In our computer analysis of the time evolution of the electron energy spectrum appropriately modified H_2 electron impact cross sections are used. In a 2×10^{19} molecules-cm^{-3} gas that starts at a very low (35°K) initial temperature all pathways, except vibrational and electronic excitation, lead to thermal energy on a sub μsec. time scale. More than 30% of the enrgy can hang up in vibrational excitations for several microseconds; the relaxation time being dependent upon the triton beam intensity.
*Work supported by USERDA.

SESSION E

7:30 PM, Tuesday, October 19

East Ballroom

WORKSHOP

ISOTOPE SEPARATION

Discussion Leader: S. D. Rockwood, LASL

E1 RYDBERG STATES OF ATOMIC URANIUM
R. Solarz, Lawrence Livermore Laboratory

E2 ROLE OF VIBRATIONAL ENERGY IN MOLECULAR REACTIONS
J. Birely, Los Alamos Scientific Laboratory

E3 THEORETICAL ASPECTS OF REACTIONS BETWEEN EXCITED SPECIES
R. Porter, SUNY - Stonybrook

E4 LASER ALCHEMY
A. Hartford, Allied Chemical Corporation

SESSION FA

8:30 AM - 10:30 AM, Wednesday, October 20

East Ballroom

CO LASERS

Chairman: D. H. Douglas-Hamilton, Avco

FA1 Performance of a cw Double Discharge in Continuous Supersonic Flow.* A. C. STANTON, R. K. HANSON, and M. MITCHNER, Stanford University. -- Experiments with a continuous double discharge[1] for excitation of supersonic flows are reported. The test facility is a supersonic channel (M=3.5 to 4.0) with a 50-cm^3 transverse discharge volume formed by flush-mounted plane electrodes (1.2-cm electrode gap). A completely cw glow discharge, stabilized by auxiliary pin discharges along the cathode, has been achieved in continuous N_2, CO/N_2, and CO/Ar flows. The power delivered to the auxiliary discharge is 20-30% of the main discharge power in low pressure tests (<15 torr). Increased pin currents are required to stabilize the discharge as the pressure is raised. Injection of gases into the electrode boundary layers has extended the limits of diffuse discharge operation. The best performance in CO mixtures has been at low pressures and for CO concentrations less than 10%. Estimated energy loadings on the order of 0.1 eV/CO molecule have been attained in mixtures with either N_2 or Ar diluent.

*Research supported by NASA-Ames Research Center and the National Science Foundation.

[1] J. H. Blom and R. K. Hanson, Appl. Phys. Lett. 26, 190 (1975).

FA2 Performance of a CW Pre-Excited CO Laser. J.W. DAIBER and H.M. THOMPSON, CALSPAN CORPORATION, BUFFALO, N.Y. -- The performance of a CO laser having electrical excitation by a continuously operating, self-sustained glow discharge in a high-pressure gas mixture followed by a supersonic expansion to the cavity region has been studied. A threshold for lasing was found which corresponded to 0.035 eV of input energy per CO molecule. Beyond this, nearly 15% of the additional energy was extracted by the resonator. The total laser power reached 940 W with a maximum electro-optical efficiency of 13.7% and a specific power of 17 kJ/lb. This efficiency was lower than predicted by numerical codes. Therefore, additional diagnostic measurements were carried out which demonstrated that energy was being lost by vibrational relaxation during the expansion. The spontaneously emitted first overtone spectrum of the CO was measured at the beginning and end of the expansion. From the band intensities the population of each vibrational level was found and, hence, the total energy stored in vibration was determined. The data indicated that an enhanced de-excitation accounting for 20% of the input power had occurred. This was collaborated by measurements of rotational temperature which gave values 15°K higher than anticipated for an isentropic expansion.

FA3 Electrical and Laser Diagnostics of a 60 kW Supersonic CW CO Electric Laser.* E.L. KLOSTERMAN and S.R. BYRON, Mathematical Sciences NW.**--CW energy loadings of up to 190 kJ/lb in laser mixtures of CO-N_2-He-Ar-H_2 have been achieved in an e-beam stabilized supersonic CW CO electric discharge laser. The energy loading was increased by 50% by using a multipin externally ballasted discharge electrode and resulted in twice the extracted laser power. Detailed measurements of the current density distribution for these electrodes showed that the ballasted electrode greatly decreased nonuniformities in current density. Electrostatic probe measurements made of the electric field distribution showed a relatively uniform field with minimal change in the boundary layer regions, indicating a significant increase in E/N in the boundary layer. The cathode fall was less than 200 V. Laser performance measurements showed significant improvement by adding small amounts of H_2, O_2, or N_2 to laser mixtures of CO-He-Ar. Small signal gain measurements made from J=7 to J=13 showed that the gas heating rate corresponds to 10% of the electric power input. Gains as high as 7.5%/cm were measured.
*Submitted by R.E. CENTER
**Supported by AFWL, Contract No. F29601-76-C-0013

FA4 Large Scale CW Supersonic Carbon Monoxide Laser Experiments. M.J. YODER and D.R. AHOUSE, Avco-Everett Research Laboratory, Inc., 2385 Revere Beach Pkwy. Everett, MA -- A large scale supersonic-flow electron-beam sustained laser has been used to achieve very high output power. A N_2-CO gas mixture was accelerated through a supersonic slot nozzle generating a Mach 4, 1/10 atmosphere pressure, 71°K flow in a 4 x 20 x 100 cm laser cavity. Electrical discharge times of up to 6 ms were used to achieve quasi-CW operation (22 cavity flow times). Electrical efficiencies of 20-21% were attained using an unstable resonator. One of the major findings of this study was the strong dependence of power loading and extraction efficiency on discharge pulse length. For electrical discharges of 1-2 cavity flow times much larger values of power loading and efficiency could be achieved. This was because the primary limit to gas power loading was arcing which occurred through the cathode fall layer to the anode well downstream of the main discharge. This comples flow/discharge interaction required several flow times to be established.

FA5 Stabilization of a Supersonic Flow Gas Discharge by Auxiliary Pin Discharges.* M. GARCIA, G. BIENKOWSKI, and J. LAWLESS, Princeton U.--In a number of CO and CO_2 discharge lasers, electron impact excitation of molecular vibrational states must be achieved in a high speed gas stream. Simultaneous tailoring of electron energy and stable glow discharge operation requires external ionization sources such as e-beams or u-v radiation. Blom and Hanson[1] demonstrated that a double-discharge arrangement without external ionization can be stably operated in some regimes where self-sustained operation is not possible. In order to attempt to understand the mechanism for this phenomenon and extend its range of operation, a larger device has been constructed and its characteristics with N_2 investigated. Initial data has: 1) established the strong dependence of performance and stability characteristics on the auxiliary pin current and 2) the most common mode of instability. Detailed diagnostics of the plasma properties are in progress. Present data is not inconsistent with a quasi-neutral model including ambi-polar diffusion, convection, and volume ionization.
*This research supported by U. S. Air Force Office of Scientific Research Contract No. F44620-73-C-0059.
[1]J. H. Blom and R. H. Hanson, Appl. Phys. Lett. 26 190 (1975).

FA6 cw Discharge Stabilization in Supersonic Flows Using Auxiliary Pin Discharges. J.A. SMITH* and G. SRINIVASAN†, NASA Ames Res. Ctr. -- Tests have been conducted to study the applicability of a discharge stabilization scheme, initially described by Blom and Hanson[1], in conditions appropriate for high energy CO lasers. A Ludwieg tube impulse flow facility and a ballasted capacitor bank provided essentially steady flow and 'd.c.' discharge conditions for times longer than ten electrode length-flow transit times. Electrodes (6.5 x 15 cm^2 with a 2.5 cm nominal gap) were mounted on opposite walls of a Mach 3 test cavity. Insulated pins embedded in the cathode were used to create an auxiliary discharge along the cathode. Steady, arc free, volume discharges were produced in pure N_2 when pin currents were comparable to sustainer currents. No combination of gas composition, discharge currents, or pressures was found to provide arc free operation in CO mixtures consistently. Most significant is the lack of observed plasma E/N changes in response to auxiliary discharge current changes under conditions where volume discharges existed.
*Present Address: Gas Dynamics Lab, Princeton Univ.
†National Research Council Postdoctoral Research Assoc.
[1]J. H. Blom and R. K. Hanson, Appl. Phys. Lett., 26, p. 190 (1975)

FA7 High Repetition Rate Discharge Pulsing of a Supersonic CO Laser.* T.G. Jones and W.B. Shepherd, Boeing Aerospace Co. -- Measurements of the performance of a large scale (2.5 liter) supersonic CO electric discharge laser has been made for repetitively pulsed and quasi-cw operating conditions. The maximum pulse length and repetition rate that is feasible, from an optical quality standpoint, was determined from interferometric and movie shadowgraph data of the wave system generated by the electric discharge. Laser measurements indicate that repetitively pulsed operation of the device is possible in a 10/80/10 CO/Ar/He mixture for 35 μsec pulses and a pulse repetition rate of 2.5 kHz. The arc limit for ten pulses under these conditions is approximately the same as that for a single pulse for the same initial conditions. The maximum measured electrical efficiency was 28 percent.

*Work in part supported by AFWL Contract No. F29601-76-C-0092.

FA8 Measurement of the Cathode Fall in the Supersonic CO Laser.* M.F. Weisbach, Boeing Aerospace Co. -- The cathode fall of an electron-beam sustained glow discharge in high density, supersonically flowing CO laser gas mixtures has been inferred by measuring the voltage-current characteristics of the discharge as a function of electrode spacing (supersonic channel height). Values for the cathode fall between 50 and 400 volts have been observed, depending on the gas mixture and discharge current density.

*Work in part supported by AFWL Contract No. F29601-73-A-0038-0002

FA9 Cryogenic "Poker" CO Electric Laser.* A.E. HILL and W.M. MOENY, Air Force Weapons Laboratory -- An experimental study of Poker[1]- controlled electric discharges and associated laser characteristics has been carried out in $CO/N_2/He$ mixtures and CO/He mixtures at temperatures ranging continuously from 300°K to 76°K. Discharge characteristics at 76°K are similar to room temperature discharges, with high electric fields ($E/N = 1.8X10^{-16}$ $v\text{-}cm^2$) achievable stably with 150-200μsec discharges at densities of 0.066 - 0.1 amagat. The effect of temperature, density, and Poker characteristics on discharge and laser characteristics are discussed.

*Submitted by P. D. TANNEN

[1]"Poker" is a controlled avalanche ionization technique for producing CW gas laser plasmas. Alan E. Hill, "Continuous Uniform Excitation of Medium-Pressure CO_2 Laser Plasmas by Means of Controlled Avalanche Ionization", Appl. Phys. Let., Vol. 22, No. 12, pp. 670-673 (1973)

FA10 Limits on Energy Deposition in CO-Ar Mixtures, W. H. Long, Jr. and A. Garscadden, AF Aero Propulsion Laboratory, WPAFB, Ohio. -- An analysis has been made of the limits on electrical excitation of carbon monoxide-argon mixtures as a function of the mixture ratio and the applied E/N. At low concentrations of CO, the mixtures exhibit negative differential conductivity (NDC) which can lead to ionization growth and arcing. At a CO concentration of 10% the NDC limit transitions to a thermal instability limit, where the energy driving the instability is the excess over that required to populate the CO vibrational manifold. The NDC instability results from the electron density and E/N fluctuations being in phase. Thus, ionization growth occurs, because an increased local electron density, E/N, and vibrational temperature all tend to raise the internal ionization rate while the recombination rate is falling. The thermal instability is fed by V-T heating and direct heating by electron impact. The direct heating and ionization rate both increase dramatically as the vibrational temperature rises above 2000°K. CO-He mixtures do not exhibit NDC but give lower e-beam ionization efficiencies than CO-Ar. Improvements should be possible by choosing triple mixtures CO-Ar-He and by programming of $(E/N)(t)$.

FA11 The Effects of Oxygen in the CO Molecular Laser* by W. LOWELL MORGAN+ and EDWARD R. FISHER, Research Institute for Engineering Sciences, Wayne State Univ., Detroit, Michigan 48202. -- Trace additions of several gases are known to significantly effect CO laser power and efficiency. Since small concentrations of additives are generally involved, these additives are recognized to predominantly influence the characteristics of the laser plasma. Oxygen has been an additive receiving substantial attention in past measurements. Our studies have been able to develop a consistent interpretation for all the observed oxygen effects both from our laboratories and elsewhere. Oxygen in small concentrations will be shown to improve laser efficiency and power through its effect on the electron-ion recombination process. At higher oxygen additions, laser output is degraded due to vibration-translation relaxation by oxygen atoms. In addition, carbon formation and removal, plasma heating and cooling effects, heterogeneous loss processes and the influence of polymer ions will be discussed through model calculations.

*Supported by DARPA through ONR-Boston.

+Present address, JILA, Boulder, Colorado 80302

SESSION FB

9:00 AM - 10:30 AM, Wednesday, October 20

West Ballroom

ARCS I

Chairman: E. F. Wyner, GTE-Sylvania

FB1 Existence and Role of the High Density Vapor Close to the Electrode in the Cathode Spot. A. LEYCURAS, L.P.O.C., Paris, France.-- Analysis of quantitative results on rates of evaporation of the cathode in vacuum arcs in the cathode spot regime shows the existence of high density vapor of the electrode material close to this electrode. Therefore the electrode emits not in vacuum (as it is generally supposed in attempts to explain the very high current densities in the cathode spots), but into its dense dielectric vapor. Under such conditions the effective work function is not ϕ_o but $\phi_o - \Delta E$ where ΔE is the polarization energy of an electron in excess in the vapor. Δ E depends on the vapor density. We establish two relations between the current density and the vapor density: the first one from thermodynamical and geometrical considerations, the second one from the Richardson - Dushman equation including ΔE. Elimination of the current density leads to an equation in which enter only thermophysical parameters and evaporation rate. Evaporation rates calculated in this way are in good agreement with measured ones.

FB2 Vacuum Arc with KV Arc Voltage, ROLF DETHLEFSEN, I-T-E/Gould, Greenburg, Pa. -- Experiments are reported on vacuum arcs in a coaxial geometry which generate several kV of arc voltage for arc currents ranging from 0.2 to 10kA. The high impedance mode is associated with oscillations which can be amplified by the application of magnetic fields and parallel capacitance.

FB3 Air Transport Properties From Measured Arc Properties. R. S. DEVOTO, Lawrence Livermore Laboratory*, U. H. BAUDER, Technische Universität München, J. CAILLETEAU and E. SHIRES.--A wall-stabilized arc of 5 mm diameter has been operated in air at 1 atm pressure. Measurements were made of the total current (12-100A), the electric field strength, the total emitted radiation and the temperature profiles. The latter were inferred from the total emission of the atomic lines NI4935 and OI4368, as well as the emission from a portion of the N_2(0-0) first negative system at 3914. These data have been analyzed to yield the electrical conductivity, the total emission coefficient and the thermal conductivity. Comparisons will be made with theory.

*Work performed under the auspices of the U.S. Energy Research and Development Administration under contract No. W-7405-Eng-48.

FB4 Time-dependent measurements and model-calculations of high pressure Na-Xe discharges, J.A.J.M. van Vliet and B.R.P. Nederhand, Lighting Division, N.V. Philips Gloeilampenfabrieken, Eindhoven, The Netherlands

Time-dependent plasma temperatures of high pressure sodium discharges have been measured spectroscopically and calculated from the energy balance equation, assuming LTE, for a.c. 50 Hz resistance stabilized operation. The measurements and calculations have been carried out for differing sodium pressures (p_{Na}==40-120 torr), xenon pressures (p_{Xe}=80-1600 torr) and arc tube diameters (Ø=4.0-11.2 mm). The results for an arc tube with Ø=0.76 cm, length 6.4 cm, p_{Na}=60 torr, p_{Xe}=80 torr, applied voltage 350 volts and a power input of about 30 Wcm^{-1} show the following. The plasma temperature at the axis varies from 4500K at current maximum to a minimum value below 2200K just before reignition. The calculations show that the thermal inertia of the discharge may be increased by the use of higher Xenon pressures, lower sodium vapour pressures and larger arc tube diameters. This then increases the minimum temperature value before reignition such that the reignition peak in the arc voltage, after current zero, is considerably reduced. This has been confirmed by experiment.

FB5 Modelling the High Pressure Sodium Discharge
J. H. INGOLD, General Electric Co., Cleveland, OH.
Previous theoretical models of the high pressure sodium discharge did not include the flow of reaction energy due to ionization of the sodium in the hot core and subsequent recombination in the cooler outer mantle of the discharge. This process is taken into account in the present paper, and is shown theoretically to have a significant effect on the operating characteristics of the discharge. The theoretical model is based on local thermodynamic equilibrium (LTE), and standard expressions for the radiation flux and the reaction energy flux are used in the numerical calculations. The main effect of the flux of reaction energy is to lower the center temperature of the discharge and to flatten the temperature profile.

FB6 Thermal and Electrical Characteristics of a Two-Dimensional Tanh-Conductivity Arc.* P. S. AYYASWAMY, G. C. DAS, I. M. COHEN, and A. M. WHITMAN, Department of Mechanical Engineering and Applied Mechanics, University of Pennsylvania, Philadelphia, Pa. 19174.--The two-dimensional, variable-property arc has been studied through the use of the tanh conductivity model. Results that describe the thermal and electric arc characteristics for various values of the heat fluxes, electrode temperatures, and aspect ratios are given. The numerical evaluation is carried out by the use of a Galerkin technique. The results exhibit several novel and interesting features depending on the arc parameters. For large aspect ratios (ratio of the interelectrode distance to that between the bounding walls) and small electrode temperatures, the current--electric field characteristics tend towards those of a slender arc. At a given aspect ratio, however, with large enough electrode temperatures, the distinct minimum noticed in the slender arc characteristic does not occur. Also, for a given aspect ratio and large enough differences in electrode potential, the electric field--current characteristic is nearly linear and is independent of the electrode temperature. The qualitative nature of the thermal characteristics are similar to those of a constant-property arc although significant differences in quantitative results exist.

*Work supported by EPRI.

FB7 Continuum Radiation from the Mercury Arc.
R. J. ZOLLWEG, R. W. LIEBERMANN, Westinghouse Research Labs and R. BURNHAM, NBS.--Independent, quantitative measurements of continuum radiation from mercury arcs have been made at our separate laboratories and the Abel-inverted emission coefficients analyzed together. Continuum at selected wavelengths (free of atomic lines) between 0.4 and 1.3 μm were included at mercury pressures of 0.1, 1.0 and 2.8 atmospheres. Equilibrium vapor compositions were calculated for the measured radial temperature profiles. The temperature dependence of the continuum emission was used to separate it into components from e-Hg^+ recombination, electron-neutral Hg bremsstrahlung and molecular radiation. Electron-neutral bremsstrahlung is particularly strong because of the large electron scattering cross section of mercury and low fractional ionization making quantitative comparison with theory possible. Our results for this interaction are in good agreement with recent theoretical calculations of S. Geltman at 1.0 μm but ∿3 times the theoretical value at 0.5 μm.

SESSION GA

10:45 AM - 12:15 PM, Wednesday, October 20

East Ballroom

EXCITATION AND IONIZATION

Chairman: D. Spence, Argonne National Laboratory

GA1 Electron Excitation of Thallium $7^2S_{1/2}$ and $6^2D_{3/2,5/2}$ Levels.* S. T. CHEN and A. GALLAGHER,† JILA, Univ. of Colo. and NBS. -- We have measured the relative optical excitation functions of the 3776 Å ($7^2S_{1/2} \rightarrow 6^2P_{1/2}$) and 2768 Å ($6^2D_{3/2} \rightarrow 6^2P_{1/2}$) resonance lines, and the polarization function of the 2768 Å line, using crossed beams of electrons and thallium atoms, for electron energies from thresholds to 1500 eV. By normalizing to Bethe theory in the high-energy limit the $7^2S_{1/2}$ and $6^2D_{3/2}$ resonance level-excitation cross sections are obtained. We have also obtained a normalized $6^2D_{5/2}$ level excitation cross section from measurements of the 3519 Å and 3529 Å lines. The $7^2S_{1/2}$ level excitation function rises very rapidly immediately above threshold, while the $6^2D_{3/2}$ level rises much more slowly. The 2768 Å polarization function shows strong resonance at a few eV above the threshold. The $6^2D_{5/2}$ level excitation function peaks at lower energy as expected for dipole-forbidden transition, but shows a small $E^{-1} \log_{10} E$ behavior at high-energy limit. The peak cross sections are measured to be 2.37 πa_0^2, 1.67 πa_0^2, and 0.46 πa_0^2 at 6.5 eV, 23 eV and 7 eV for the $7^2S_{1/2}$, $6^2D_{3/2}$, and $6^2D_{5/2}$ levels, respectively.

*Supported by the NSF contract No. MPS72-05169.

†Staff Member, Laboratory Astrophysics Division, NBS.

GA2 Electron Impact Cross Section Measurement From The Helium 2^3S Level.* M. L. Lake, Universal Energy Systems, Dayton, Ohio and A. Garscadden, Air Force Aero Propulsion Laboratory, WPAFB, Ohio. Measurements on the cross sections from the helium 2^3S state have now been extended to the 3^3S, 3^3P, 3^3D, 4^3S and 4^3D states using dual electron beams crossed with an atomic beam. One electron beam is used to excite the metastable state, while the second electron beam is swept in energy. Cross sections are inferred from the decay radiation from n^3l states obtained below the threshold for the direct cross section process. Results indicate that the 3^3D level has the largest cross section (apparent $Q_{2^3S \rightarrow 3^3D} = 7 \times 10^{-16}$ cm^2 at 20 eV) which compares favorably with Flannery's calculations (level $Q_{2^3S \rightarrow 3^3D} = 3.5 \times 10^{-16}$ cm^2 at 20 eV by the Eikonal method).

* Supported by USAF Contract F33615-75C-1082.

GA3 Lifetimes and Excitation Functions of Optical Emissions (2300Å-2900Å) from N_2 Excited by Electron Bombardment. DONAL J. BURNS and CHARLES R. HUMMER, Univ. of Nebraska. -- Using both D.C. and pulsed electron beams the excitation and subsequent decay of the $D^3\Sigma_u^+$, $E^3\Sigma_g^+$, $x^1\Sigma_g^-$ and $y^1\Pi_g$ states of N_2 have been investigated. Excitation functions for the (0,2) 2445Å, (0,3) 2548Å and (0,4) 2658Å $D^3\Sigma_u^+ - B^3\Pi_g$ emissions will be presented. Weak emissions from the fifth positive $x^1\Sigma_g^- - a'^1\Sigma_u^-$ system have been observed and the excitation function of (1,7) 2581Å has been measured. A preliminary measurement of the lifetime of the $x^1\Sigma_g^-$ state is 24.1 ± 3 ns. Weak emissions from Kaplan's second system have also been found and excitation of (1,7) 2722Å $y^1\Pi_g - w^1\Delta_u$ measured in detail. First measurements indicate a lifetime of 15.5 ± 2 ns for the $y^1\Pi_g$ state.

GA4 Electron Ionization of Atomic Chlorine. G.W. HOWSER, R.J. CORBIN, K.J. NYGAARD, and W.R. SNOW, University of Missouri-Rolla*--A quadrupole mass spectrometer has been used to measure the relative ionization cross section for atomic chlorine by electron impact. A beam of chlorine atoms was produced by an electrically heated mullite oven. The beam was mechanically modulated and synchronous ac detection was used to provide discrimination against ions formed in the background gas. Preliminary measurements of the e + Cl cross section (normalized e + Ar at 75eV) from threshold to 100eV will be presented.

*Supported in part by AFOSR

GA5 Electron Impact Double Ionization Cross Sections of Cs^+ Ions.* R. K. FEENEY and W. E. SAYLE, II, Georgia Institute of Technology.--Absolute cross sections for the electron impact double ionization of Cs^+ ions have been measured as a function of incident electron energy from below threshold to approximately 1000 eV. The measurements were accomplished with a crossed beam facility operating in the pulsed beam mode. The electron source utilized an oxide cathode and operated with typical currents of 1 mA. A thermionic-type ion source produced a collimated ion beam of approximately 100 nA. After undergoing collisions with the electron beam, the ion beam charge state components were separated in a two-stage parallel plate electrostatic analyzer. Two stages of analysis were used to improve the signal-to-noise ratio. The two beam current distributions were determined by means of a movable slit scanner. Numerous consistency checks were performed to evaluate possible sources of error.

*Work partially supported by USERDA.

GA6 Ionization Near Threshold of Vibrationally Excited N_2 by Electron Impact.* J. A. MICHEJDA and P. D. BURROW,** Yale U.--The relative cross sections for ionization of the three lowest vibrational levels of the ground electronic state of N_2 have been studied near their respective thresholds. Preliminary analysis of the data indicates that the cross sections are the same within a factor of two. This result is in sharp contrast to the predictions of a direct ionization mechanism and verifies the importance of autoionization of Rydberg states near the ionization threshold. A model is proposed to explain the general behavior of the cross sections. The vibrationally excited N_2 molecules were produced in a microwave discharge. The vibrational population at the location of the electron beam was determined by two independent techniques employing low energy electrons, namely, the trapped electron method and electron transmission spectroscopy.

*This work was supported by the National Science Foundation.
**Present address: Behlen Laboratory of Physics, University of Nebraska, Lincoln, Nebraska 68588

(GA7 WITHDRAWN)

GA8 Photoionization of Cs Excited States.*
M. H. NAYFEH,** J. P. YOUNG, and G. S. HURST, Oak Ridge National Laboratory.--We have studied the resonant two-photon ionization process of cesium ground state $6s_{1/2}$ with $7p_{1/2}$ or $7p_{3/2}$ as the intermediate state. A vapor pressure of two microns is attained in a cell at room temperature, and the ionization is collected by a parallel plate capacitor. When the intermediate resonant transitions are saturated, the results yield absolute single-photon ionization cross sections of the intermediate states. In order to compare with calculations, we are studying the cross sections as a function of energy above the ionization threshold.

*Research sponsored by the U.S. Energy Research and Development Adm. under contract with Union Carbide Corp.

**Postdoctoral research appointment through the Univ. of Kentucky and supported by Los Alamos Scientific Lab.

GA9 Three-Photon Ionization of Atoms by Strong Pulsed Laser Fields.* C. W. CHOI† and M. G. PAYNE, Oak Ridge Nat'l. Lab. -- We consider three-photon ionization due to two simultaneous laser pulses tuned such that $\hbar(\omega_1 + \omega_2)$ lies very near a two-photon transition. If $2\hbar\delta = \hbar(\omega_1 + \omega_2) - \Delta E$, where ΔE is the exact resonance energy for the two-photon resonance, we find for strong laser fields and for $|\delta|\tau > 10$ (τ = full width at half maximum of the smooth laser pulses) accurate analytical solutions for the ionization probability and for the upper state population. The line shape for ionization is very asymmetrical, rising sharply at $\delta = 0$ and having a slowly decreasing wing on the ac Stark shift side. A strongly inverted upper state population persists for a large fraction of the pulse.

*Research sponsored by the U.S. Energy Research and Development Adm. under contract with Union Carbide Corp.

†Oak Ridge Graduate Fellow from the Univ. of Kentucky under appointment from Oak Ridge Associated Universities. (This work is part of a thesis in partial fulfillment of the degree Doctor of Philosophy.)

GA10 Evidence For $^1\Delta_g$ Singlet Oxygen in a High Pressure Electron-Beam Controlled Discharge* -- D. PIGACHE, G. FOURNIER, D. PROUST, Office National d'Etudes et de Recherches Aerospatiales 92320 Chatillon, France and M. LECUILLER, Ecole Superieure d'Electricite, Plateau du Moulon, Gif-Sur-Yvette, France -- The radiations from $^1\Delta_g$ single and double transition are observed at 1,27 μm and 0,63 μm respectively; $^1\Sigma_g^+$ radiation is also observed at 0,76 μm. Typical discharge conditions are: pressure 200 mbar of pure oxygen, discharge current density 9 mA/cm^2, electric field/gas density 3×10^{-16} Vcm^2. $^1\Delta_g$ and ozone concentrations are estimated to be of the order of 5 per cent.

*Submitted by J. Taillet

SESSION GB

10:45 AM - 12:15 PM, Wednesday, October 20

West Ballroom

ARCS II

Chairman: G. Ecker, Ruhr-Universitat Bochum

GB1 Theory and Experiment for Circuit Breaker Arcs Stabilized by Forced Convection. H.C. LUDWIG, Westinghouse Research Laboratories.--The understanding of electric arcs and plasmas is of primary importance in circuit breakers and switches, particularly for SF_6 gas. A broad study of the dynamic properties of arcs has been underway for a number of years. Using a forced convective flow stabilized arc model, a coupled radiation-absorption, diffusion, axial convection energy transfer mechanism (RADAC) has been shown to be effective in SF_6 circuit breakers, controlling a circuit interruptive capacity. Decoupling of the energy transfer mechanism by over-loading of a given device leads to clogging of the SF_6 mass flow caused by a sensitive expansion of the arc conducting core above a certain current, which fills the throat of gas flow channel. The analysis of the subject theory is supported by two experiments, one carried on in-house and one by an independent external research group. The confirmation of the theoretical arc model as given provides a basic criterion for the design of all circuit breakers employing channeled forced convective gas flow, by recognition of the subject energy transfer mechanism and the determined critical nature of its conservation.

GB2 Turbulent AC Arcs,* D.M. BENENSON and P.A. REISER, State University of New York at Buffalo -- Experiments have been conducted to obtain qualitative information on the radial distributions of temperature at various times, τ, in the current cycle of turbulent AC arcs. The tests were carried out upon a 60Hz, 70 Arms, atmospheric argon column in a 1cm diameter channel, ~15cm long, with mass flow rates from ~0.1 g/s (laminar to 8 g/s (turbulent). Data aquisition time, at any τ, was ~5μs (for a 10 mm object). Estimates of the temperature distribution, at each τ, were obtained through an averaging of multiple scans (~1200) of the arc image past the entrance slits of a calibrated filter-photomultiplier arrangement. Over a portion of the current cycle - generally away from current zero - and particularly at the lower flow rates, the apparent appearance of turbulence in the multiple scans was found to be primarily due to gross motion of the arc column. In turbulent flows, the current zero centerline temperatures were <8,000K (about 1,000K lower than in laminar flows), approximately independent of mass flow rate. Maximum temperatures were ~10,000K.

*Research supported by National Science Foundation Grant ENG-74 15272 and by the General Electric Foundation.

GB3 Radial Shock Waves in a Cylindrical Pulsed Cesium Discharge. Harald L. Witting, General Electric Corporate Research & Development, Schenectady, NY--An experimental investigation was made of pulsed cesium discharges, operated in sapphire arc tubes of 8 mm bore and 70 mm arc length, at cesium pressures between 10 and 60 torr. Current pulses of 250A and 1 microsec. duration were applied, reaching a peak input power of 250 kW.

Time-resolved measurements of the radiation output showed an initial peak due to the current pulse, followed by several peaks in the afterglow at 10 microsec. intervals. Further experiments with high-speed framing and streak photography revealed that the later peaks are due to a radial shock wave that is reflected by the tube walls and that periodically concentrates the plasma near the tube axis.

GB4 Onset of Helical Instability of Confined Arcs. R.J. ZOLLWEG, Westinghouse Research Labs. -- Helical instability has been observed in ac and dc arcs confined by cylindrical walls in the atomic gases Ar, Xe and Hg at various pressures. This instability occurs when self-magnetic field forces exceed "wall-stabilizing" and inertial forces. Quantitative agreement between theory and experiment has been found for the onset of instability in the molecular gases H_2 and N_2[1]. We find the onset of instability for atomic gases to occur at significantly lower values of the critical ratio of material parameters $Mk_{cr} = (\rho h)\ \mu G/\eta$ with the expected dependence on arc channel to wall diameter ratio. The arc channel diameters of mercury arcs have been altered considerably by convection and small concentrations of additives with only minor changes in Mk_{cr}. The smaller thermal conduction stabilization force appears to be primarily responsible for the smaller value of Mk_{cr} for these heavier atomic gas arcs.

1. K.A. Ernst, J. Kopainsky, and J. Mentel, Z. Physik 265, 253 (1973)

GB5 Emission and Absorption Measurements of RF-Heated Argon-Confined Uranium Plasmas*. WARD C. ROMAN, United Technologies Research Center -- Experimental results and associated diagnostics are described in which pure UF_6 was injected (axial probe) into an argon-confined, steady-state, rf-heated plasma within a water-cooled fused-silica peripheral wall test chamber. RF energy was supplied by a 1.2 MW, rf induction heater operating at 5.4 MHz. Argon flow rates up to $\approx$ 3 g/s were used in establishing the radial-inflow vortex. Recent tests were conducted at chamber pressures up to 12 atm, UF_6 mass flow rates up to 0.2 g/s, and test times up to 41.5 minutes. To determine the radial temperature distribution within the plasma and, subsequently, for estimating the amount and distribution of the uranium vapor confined within the plasma, plasma emission and absorption (cw tunable dye laser at 591.54 nm) measurement techniques were included. X-ray absorption measurements were used to supplement the optical measurements. Results indicated centerline uranium atom densities of approximately 10^{16} atoms/cc.

*Work sponsored by NASA Langley Research Center, Contract NAS1-13291, Mod. 2.

GB6 Collisional Process Effects on Electron Energy Distribution in U-He Plasmas.* GEORGE H. MILEY, and CHAN K. CHOI, Univ. of Illinois--The electron energy distribution determines the intensity and energy spectrum of radiation from uranium plasmas which have applications, for example, in gaseous core reactors, to isotope separation, chemical processing, and nuclear pumped lasers. A model has been developed for U-Noble gas mixtures which extends earlier techniques[1,2] for pure U-plasmas. Temperatures from 2000°K to 5000°K and a total pressure of 1 atm are considered with the various mixture ratios. Collision processes for deceleration of primary electrons include Coulombic drag, excitation, and ionization encounters. The amplitude of the electron distribution function decreases with temperature. At 5000°K, it is relatively insensitive to composition due to the dominance of electrons from ionized uranium. However, at lower temperatures, the amplitude increases significantly (2x) as He is added (80%), while the shape is only perturbed at higher energies.

*Supported by US NASA NSG-1063

[1] C. Bathke and G. H. Miley, Trans. Am. Nucl Soc., 19, 64 (1974). [2] M. Makowski, C. Choi, and G. Miley, 3rd IEEE Int. Conf. on Plasma Sci., Austin, TX (1976).

GB7 Sodium Dimer Emission Observed in Arc Discharge Afterglow. E. F. WYNER and J. MAYA, GTE Sylvania, Danvers, Massachusetts. - The afterglow radiation of a high pressure sodium arc discharge has been measured and found to be dominated by molecular Na emission, emanating from the($A^1\Sigma - X^1\Sigma$) transition with a peak intensity at 805.0 ± 4nm. At 1500K the spectral shape of the A - X band agrees closely with calculations.[1] Emission spectra have been recorded for gas temperatures of 1500-1350K and Na pressures of 250 - 50 torr.

Peak intensity Na_2 ($A^1\Sigma - X^1\Sigma$) measurements as a function of gas and cold spot temperatures showed that early afterglow (less than $\backsim$ 6 sec.) has Na_2 pressure dependence whereas late afterglow (up to $\backsim$ 14 sec.) has $(Na)^2$ dependence. This suggests the importance of Na-Na associative processes in the late afterglow.

[1] L. Lam, A. C. Gallagher and M. M. Hessel (Unpublished)

SESSION HA

2:00 PM - 3:30 PM, Wednesday, October 20

East Ballroom

ION INTERACTIONS

Chairman: D. L. Albritton, NOAA/ERL

HA1 Determination of Ion-Neutral Interaction Potentials from Mobility Measurements.* L. A. VIEHLAND, E. A. MASON, and I. R. GATLAND, Brown University and Georgia Institute of Technology -- Recent developments in the kinetic theory of ion mobility at arbitrary electric field strengths make possible a quantitative connection between the ion-neutral interaction and the variation of mobility with E/N. Using mobility data, we directly test recent theoretical calculations of the potentials for alkali ions in rare gases, and show that the data contain further information. We also show how mobility data can be directly inverted to yield interaction potentials without assuming a mathematical form for the potential, and test the method on both simulated and real data.

*Supported in part by the U.S. Army Research Office and the National Science Foundation.

HA2 Monte Carlo Studies of Ion Mobilities.* S. L. LIN and J. N. BARDSLEY, Univ. of Pittsburgh. -- The mobility of K^+ ions in Ar has been studied by Monte Carlo simulation. Potentials have been derived to fit either of two independent measurements of the mobility as a function of E/N.[1,2] For each potential the well depth is close to 0.105 eV and the equilibrium separation is between 3.1 and 3.2A. However either set of data could be fit by a potential with smaller well depth and larger equilibrium separation. The influence of resonance charge transfer on mobilities has been explored through calculations on He^+ ions in He and Ne^+ ions in Ne, and preliminary studies of the effect of inelastic collisions of molecular ions have been completed.

*Research supported by ONR/ARPA (N000-1476-C0098).

[1]M. T. Elford, Aust. J. Phys. 24, 705 (1971).
[2]D. R. James, E. Graham, G. M. Thomson, I. R. Gatland and E. W. McDaniel, J. Chem. Phys. 58, 3652 (1973).

HA3 Effect of Endothermic Reactions on the Ion Velocity Distribution in Drift Tube Experiments.* J.H. Whealton, JILA, R.M. Stehman and S.B. Woo, Univ. of Del. --The effect of endothermic reactions on ion velocity distribution, f, in drift tubes is considered. The BGK approach is used to solve the Boltzmann equation in a model calculation. Results show that selective depletion of f occurs over the range of velocities $v \gtrsim v^*$, where v^* is the threshold speed corresponding to the activation energy of the reaction in the center of mass frame. The fractional depletion of integrated f over this velocity range is of the order of and less than $\delta=(n_R \cdot \bar{\sigma}_I)/(n_B \cdot \bar{\sigma}_E)$. n_R, n_B, $\bar{\sigma}_I$, and $\bar{\sigma}_E$ are respectively neutral number density of reactant gas, buffer gas, weighted cross section of ion-molecule reaction and elastic collisions. This points to a dependence of the measured rate constants as a function of δ even when $(n_R \cdot \bar{\sigma}_I)$ is kept constant. Fortunately, numerical studies show that correction to rate constants of endothermic reactions due to depletion is generally smaller than declared experimental uncertainties.However, an experiment can be designed to measure the δ dependence and consequently test the magnitude of the depletion computed by this investigation.
*Work supported in part by NASA

HA4 Negative Ions in CO_2. T. D. FANSLER, L. M. COLONNA-ROMANO, and R. N. VARNEY,* Ballistic Research Lab.--Negative ions in CO_2 have been studied with a drift-tube mass-spectrometer over the range $45<E/N<400$ Td at 320°K. Attachment of (gated) electrons in the drift region introduces features into the arrival-time spectra of the ions that enhance considerably the resolving power for evaluation of rate coefficients. Reaction rates have been obtained for attachment of O^- to CO_2 (forming CO_3^-), collisional dissociation of CO_3^- yielding O^-, and collisional detachment of electrons from O^-. The attachment rate coefficient of O^- approaches $(5\pm0.5) \times 10^{-28}$ $cm^6 s^{-1}$ at low E/N and declines slowly with increasing E/N. The CO_3^- dissociation rate coefficient falls below 10^{-14} $cm^3 s^{-1}$ for $E/N<300$ Td and rises to $\simeq 1 \times 10^{-11}$ $cm^3 s^{-1}$ at 400 Td. The rate coefficient for electron detachment from O^- is $< 10^{-14}$ $cm^3 s^{-1}$ at $E/N<180$ Td and rises to 9×10^{-12} $cm^3 s^{-1}$ at 400 Td.

*NRC Senior Research Associate

HA5 Collisional Dissociation of CO_3^{-*}. JOHN F. PAULSON, Air Force Geophysics Lab. and P. JANE GALE, Yale Univ.-- Using a double mass spectrometer system, we have measured cross sections for dissociation of CO_3^- in collisions with He, Kr, N_2, and O_2 in the range of reactant ion laboratory energies from about 0.5 eV to 100 eV. In all cases, the cross sections for production of O^- are non-zero at relative energies below the energy at which ground state CO_3^- is expected to dissociate. The cross sections increase only slowly with increasing energy and do not exhibit defind thresholds. They increase monotonically, reaching values of 5 to $20 \times 10^{-16} cm^2$ in the stated energy range. These results are consistent with the presence of vibrationally excited CO_3^- in the beam and with inefficient transfer of translational energy into the internal modes required for dissociation. In the case of CO_3^- colliding with O_2, we also observe production of O_3^- in an apparently endoergic reaction whose cross section reaches a maximum of $0.7 \times 10^{-16} cm^2$ at a relative energy of about 5 eV.

*Supported in part by the Defense Nuclear Agency.

HA6 Flow-Drift Tube and Variable Temperature Flowing Afterglow Studies of the Reaction $O_3^- + CO_2 \rightarrow CO_3^- + O_2$.* I. DOTAN, D. L. ALBRITTON, G. E. STREIT, J. A. DAVIDSON, and F. C. FEHSENFELD, NOAA Aeronomy Laboratory, Boulder, CO 80302.---The reaction

$$O_3^- + CO_2 \underset{r}{\overset{f}{\rightleftarrows}} CO_3^- + O_2$$

has been studied as a function of relative kinetic energy in the range 0.04 - 1.5 eV and as a function of temperature in the range 300-600K. The rate constant in the forward direction is found to be large, $k_f > 10\text{-}10$ cm^3/sec, clearly establishing this as the exothermic direction. The reverse direction could not be observed experimentally, thereby placing low upper limits on k_r. Applying the principle of microscopic reversability, these measurements imply that the $CO_2 + O^-$ bond dissociation energy of CO_3^- is substantially larger than the $O_2 + O^-$ bond energy of O_3^-. Breakup studies of CO_3^- relative to O_3^- support this. The implications of these observations on the electron affinity of O_3 will be discussed.

* Supported in part by DNA

SESSION HB

2:00 PM - 3:30 PM, Wenesday, October 20

West Ballroom

DIAGNOSTICS AND DISCHARGES

Chairman: G. J. Kazek, General Electric

HB1 Near-resonant Rayleigh scattering as a tool for determining Na densities in low- and high-pressure discharges. L. VRIENS, Philips Research Labs, Eindhoven, Netherlands.--Near-wing Rayleigh scattering from Na atoms has been studied in a Na-Ne low-pressure discharge and in a high-pressure metal-halide arc. For the Na-Ne discharge with a Ne filling pressure of 4.5 Torr and Na densities from 10^{12} up to 3×10^{14} cm^{-3}, Rayleigh scattering is measured using a single-mode dye laser. At 10-30 GHz detuning from resonance, the scattering signals are large enough to determine accurate local Na densities. The non-isotropic polarization of the Rayleigh scattering is used for discrimination versus the collision-induced fluorescence, which is isotropic due to collisional frequency redistribution and radiation trapping. In the metal-halide arc, the total pressure is a few atm. The narrow peaked Rayleigh scattering, when detuned beyond 4 Å from resonance, is spectrally well resolved from the broad-banded collision-induced fluorescence. The measured Na densities at the axis are of the order of 10^{14} - 10^{15} cm^{-3}. The technique of near-resonant scattering is applicable also to other metal vapors in discharges and neutral gases.

HB2 FIR Absorption Determination of Transient Electron Densities in High Pressure Ionizer-Sustainer Lasers.* L. A. Newman, M. R. Schubert and T. A. DeTemple, Univ. of Ill.--We report on electron density measurements in high pressure electron beam initiated discharges inferred from absorption measurements using a single transverse mode CW optically pumped FIR laser system operating at 170 μm and 118 μm. Discharges in He, He-SF_6, N_2, N_2-SF_6, Ar and Ar-Xe were investigated via transmission and V-I measurements with resulting thicknesses of 10^{16} electrons/cm^2, a spatial resolution of 2 cm over a path length of 60 cm and a time resolution of 40 nsec. The electron density determined from transmission and current agreed to better than 50% limited only by uncertainties in the specific spatial distribution of the electron density. The increased IR and UV laser output previously observed when small amounts of SF_6 were added to N_2, were found to be attributed to a slight increase in electron density due to discharge narrowing and to an increase in E/N during the time duration of the laser pulses.

HB3 The Electron Temperature in a Medium Pressure D.C. Discharge Positive Column Plasma, Jen-Shih Chang, York University,Canada, Sin-Li Chen, Musashi Institute of Technology,Japan -- The electron temperature T_e, in a medium pressure positive column with the presence of the volume recombination has been studied for both magneto- and nonmagneto-plasma. The plasma parameters are measured by electrostatic probes,micro-wave techniques and a sampling probe. The experimental results show that: (1) T_e determined from a sampling probe coincides with the recent theory of Chang[1] within 10 %. This strongly supports the theory that the discharge current dependence observed in previous experiments is a result of changes in the nondimensional volume recombination coefficient $\beta=\rho N_o R_d^2/D_a$,where ρ and D_a are volume recombination and ambipolar diffusion coefficient,N_o is plasma density at center,and R_d is tube radius;(2)For a magneto-positive column plasma,T_e determined from a magnetically shielded sampling probe coincides with the theory of Chang within 10 % when we introduce the magnetic field effect in the positive column in terms of the diffusion coefficient $D_\perp = D/(1+\omega^2\tau^2)$,where ω is cyclotron angular frequency,and τ is mean collision time.

1) J.S. Chang (1976)J.Phys.D:Appl.Phys.(August)

(HB4 WITHDRAWN)

HB5 Measurements of Electron-Neutral Free-Free Absorption in a High Pressure Electron-Beam Sustained Discharge,* W.H. Christiansen and S. Alroy, U. of Washington. - The nonsaturable continuum absorption due to electron-neutral inverse bremstrahlung can in some instances limit the performance of short pulse very high pressure infrared lasers. Using lasers at 0.63μ, 2.8μ, and 10.6μ this absorption has been observed for the first time in several homonuclear test gases under an applied electric field. Electron densities of up to $10^{14}/cm^3$ charge at pressures up to 15 atm. These conditions give rise to large absorption signals (in excess of 50% at 10.6μ. Absorption measurements have been compared with calculations based on known theories taking into account the electron distribution function under the influence of an electric field. To make this comparison, the electron density was infered from the sustainer current. Good agreement is found between the measurements and calculations for the experiments were the sustainer current is smooth with time. Poorer agreement exists wherever the current fluctuates rapidly indicating a rapid charge in electron density in the sustainer.

*Supported by Office of Naval Research

HB6 Current densities and discharge radius measured by spectroscopic technique for corona discharge in oxygen F. BASTIEN, E. MARODE
Labo. Physique Decharges E.S.E. Plateau du Moulon 91190 GIF SUR YVETTE FRANCE

The point to plane discharge in oxygen at some hundred torr is studied adding traces of hydrogen and measuring the H_α and H_β broadened profile. To interprate the measured profiles which has been presented two years ago, it was necessary to obtain theoritical profiles taking into account the space charge field. Results of that type of calculations is presented. H will be shown that under space charge conditions the line broadening measures the current density rather than the electron density. Comparing calculated and measured profiles the current density évolution within the filamentary corona discharge is determined and the radial characteristic dimension of the discharge is deduced. From this radius some properties of the filament and the the streamer head of the discharge is infered.

SESSION IA

3:45 PM - 5:15 PM, Wednesday, October 20

East Ballroom

DISSOCIATION

Chairman: B. A. Huber, SRI and Ruhr-Universität Bochum

IA1 Photodissociation Spectrum of O_3^-.* P.C. COSBY, J.H. LING, J.T. MOSELEY, and J.R. PETERSON, SRI--The total photodestruction cross section of ground state O_3^- has been measured at photon energies of 1.92-2.46 eV using a drift tube mass spectrometer and tunable dye laser. Over these energies, the cross section varies from 3×10^{-20} to 8×10^{-18} cm^2. Above 2.1 eV, the predominent destruction process is found to be photodissociation into O^- and O_2. The cross section exhibits considerable structure as a function of photon energy which is indicative of vibrational progressions in the photoabsorption to a predissociating O_3^- electronic state. Preliminary analysis of this structure using spectra of both vibrationally excited and collisionally relaxed O_3^- yields fundamental frequencies of 800 and 280 cm^{-1} for the predissociating state and 850 and 400 cm^{-1} for the ground $^2B_1$ state. Further, the origin of the predissociating state is found approximately 2.16 eV above the $^2B_1$ state. The implications of these data regarding the dissociation energy of O_3^- and the electron affinity of O_3 will be discussed.

*Work supported by BRL through Army Research Office.

IA2 Photodissociation Measurements of Nitric Oxide Ion Clusters. J.A. VANDERHOFF, Ballistic Research Lab. A drift tube mass spectrometer combined with an ion laser photon source has been used to measure the photodissociation cross section of NO^+ (NO) as a function of photon wavelength. The cross section appears to smoothly decrease from 2×10^{-17} cm^2 at 676 nm to about 3×10^{-19} cm^2 at 413 nm.

Photodissociation cross section measurements were obtained for NO^+ (H_2O) at 647 nm. It was determined that the cross section was small (less than 10^{-19} cm^2) or zero for this photon wavelength.

IA3 Threshold Photofragment Spectroscopy of O_2^+ ($a\,^4\Pi_u \rightarrow f\,^4\Pi_g$). J.T. MOSELEY,* M. TADJEDDINE, J. DURUP, J.-B. OZENNE, C. PERNOT, and A. TABCHÉ-FOUHAILLÉ, Université de Paris-Sud, Orsay, France.--A new technique of laser photofragment spectroscopy is introduced and applied to a study of transitions from the v=4 level of the $a\,^4\Pi_u$ state of O_2^+ to rotationally predissociated levels of the newly discovered[1] $f\,^4\Pi_g$ state near the dissociation limit. Since the observed transitions are between discrete levels, the resolution is determined by the linewidth of the laser. A resolution of 0.5 meV is obtained, compared with around 50 meV in normal photofragment spectroscopy,[1] and much higher resolution is possible. Specific (Ω,J) levels of the a state are identified.

*Permanent address: Molecular Physics Center, Stanford Research Institute, Menlo Park, Calif. 94025.

[1]A. Tabché-Fouhaillé, et al., "Laser Photofragment Spectroscopy of O_2^+," Chemical Physics (in press).

IA4 Angular Distribution and Energy of Ionic Fragments from the Photodissociation of Gaseous Methyl Chloride Cation.* R. G. ORTH and R. C. DUNBAR, Case West. Res. U.**--The spatial asymmetry in the trapping efficiency of a Penning ion trap[1] was utilized to obtain the angular distribution and average kinetic energy of the ionic fragments produced from the photodissociation of methyl chloride cation at various wavelengths. The photofragment CH_3^+ was found to have an average kinetic energy of 0.5 eV. The value for the anisotropy parameter which describes the angular distribution of the photofragments is approximately 2.0. The average kinetic energy of the methyl cation fragment yields information as to the partitioning of the available energy into the translational and internal modes. The anisotropy parameter gives an indication of the direction of the transition dipole moment.

*Submitted by R. C. DUNBAR

[1]M. Bloom and I. Riggin, Can. J. Phys., 52, 436 (1974).

IA5 Tunable Dye Laser Photodissociation of O_3: Kinetic Energies and Angular Distributions of O Atom Photofragments. C. E. FAIRCHILD,* Dept. Phys., Ore. St. Univ., E. J. STONE and G. M. LAWRENCE, LASP, U of Colo. -- A gas phase chemi-ionization process is used to detect O atoms produced by laser photodissociation of O_3. Photofragments kinetic energies are determined using an atomic beam time-of-flight technique, and their angular distributions are determined by rotating the plane of polarization of the laser light. At a wavelength of 600 nm the dissociation products are $O(^3P) + O_2(X^3\Sigma_g^-)$, with a broad distribution of energy partitioning between released kinetic energy and internal vibrational and rotational energy of the O_2 photofragment. In the wavelength range 270-305 nm two groups of dissociation products are observed: $O(^1D) + O_2[a^1\Delta_g(v\simeq 0\text{-}3)]$ and $O(^3P) + O_2[X^3\Sigma_g^- (v\simeq 0\text{-}10)]$. For the first group the wavelength threshold is 310 nm; thus it has been possible to determine approximately the wavelength dependence of the energy partitioning for this dissociation process. At a wavelength of 277 nm the second group of dissociation products comprise roughly 10-20% of the total product yield. Relative cross sections for $O(^1D)$ and $O(^3P)$ are determined for the process $Sm + O \rightarrow SmO^+ + e^-$.
*JILA-LASP Visiting Fellow, Univ. of Colo., 1975-76.

IA6 Kinetic energies and angular distributions of oxygen atom photofragments produced by photodissociation of O_2 and N_2O in the vacuum ultraviolet. E. J. STONE, G. M. LAWRENCE, LASP, U of Colo. and C. E. FAIRCHILD,* Dept. Phys. Ore. St. U. -- A gas phase chemi-ionization process is used to detect O atoms produced by photodissociation of O_2 and N_2O. For the photon energies used here the accessible O atom states are within the ground ^3P levels and the metastable ^1D and ^1S levels. Kinetic energies of the O atom photofragments are determined using an atomic beam time-of-flight technique, and the O atom angular distributions are determined by varying the angle between the direction of the photon beam and the atomic beam flight path. Dissociative transitions within the Schumman-Runge continuum of O_2 and the principal vacuum ultraviolet absorption continuum of N_2O yield results in agreement with previous predictions. For the dissociation of O_2 at wavelengths of 120 and 124 nm, the principal dissociation products are $O(^3P) + O(^1D)$; and, at these wavelengths, the O atom angular distribution is consistent with previous conclusions that predissociation is important. An angular asymmetry parameter having a value of (-0.61 ± 0.05) is obtained for predissociation in O_2 at the 10.0 and 10.3 eV absorption features.
*JILA-LASP Visiting Fellow, Univ. of Colo. 1975-1976.

IA7 Selective Processes in Bromine, K. B. MC AFEE, JR., R. M. LUM AND V. E. BONDYBEY, Bell Laboratories, 600 Mountain Ave., Murray Hill, N. J. 07974 - Measurements of selective processes in bromine have been carried out under molecular beam conditions and in the gas kinetic regime. Three processes are observed in pure bromine, two of which are selective under single-mode argon ion laser excitation. Predissociation occurs strongly in all three isotopic species and separate lifetime determinations have shown that predissociation rates dominate resonance fluorescence for the case of energy levels near the dissociation limit which are excited. The rates of nonselective direct dissociation are also measured and vary in magnitude from three to about ten times the selective predissociation rates. Under gas kinetic conditions a very rapid isotopic exchange occurs upon collision within the reaction chamber. Because of the location of the absorption frequency of the isotopically similar molecular species near the center of the argon ion laser emission spectrum, isotopic exchange collisions produce enhanced mixed isotope product molecules. Experiments in bromine-olefin mixtures have also been carried out to study reactions of electronically excited bromine molecules which have been selectively produced.

IA8 Dissociation of CD_4, C_2D_4, and CF_4 by Electron Impact. H. F. WINTERS, IBM Research Laboratory.--Total dissociation cross sections (the analogue of total ionization cross sections) have been measured for CH_4, CD_4, C_2D_6, C_2H_6, and CF_4. Maximum values of $4X10^{-16}cm^2$, $5X10^{-16}cm^2$, and $7.6X10^{-16}cm^2$ are obtained for CD_4, CF_4, and C_2D_6, respectively. There is no significant isotope effect, i.e., the deuterated and protonated molecules yield the same results within experimental error. Dissociation of CH_4 into ionic and neutral fragments has about equal probability for energies between 50 eV and 100 eV. At lower energies most of the fragments are uncharged ground state or long-lived excited state molecules. Both CD_4 and C_2D_6 exhibit a linear cross section at near threshold energies. Comparison of data from electron energy loss experiments with data obtained in our laboratory indicates that the lowest excited states of C_2D_6 are stable while those of CD_4 dissociate.

IA9 Rate Coefficients for Dissociative Excitation of H_2 by Low Energy Electrons.*--C.H. MULLER and A.V. PHELPS. JILA, U. of Colorado and NBS. Measurements have been made of the rate coefficients for the production of H atoms from H_2 by low energy electrons. The dissociation[1] occurs in a well-characterized discharge in He containing 0.2 to 1% H_2. The transient density of H was measured using the absorption[2] of Lyman α. The ratio of the rate of loss of atomic hydrogen to the discharge current was used to calculate the rate coefficient. Measured rate coefficients for 1% H_2 varied from 9×10^{-19} cm^2 at $E/N=7\times10^{-17}$ V-cm^2 to 2×10^{-18} cm^2 at $E/N=9\times10^{-17}$ V-cm^2. These rate coefficients are in good agreement with values calculated using cross sections previously found[3] to give agreement with rate coefficient measurements in pure H_2.

*This work was supported in part by the National Science Foundation and by the U.S. Energy Research and Development Administration.

[1]C.H. Muller and A.V. Phelps, Bull. Am. Phys. Soc. 21, 174 (1976).

[2]The authors thank V. Kaufman and G.G. Luther of NBS/Gaithersburg for assistance in measuring Lyα profiles.

[3]A.C. Engelhardt and A.V. Phelps, Phys. Rev. 131, 2115 (1963).

SESSION IB

3:45 PM - 5:15 PM, Wednesday, October 20

West Ballroom

DISCHARGES

Chairman: L. Vriens, Philips

IB1 E-I Characteristics and Ionization Instabilities in Uniform Glow Discharges. P. J. CHANTRY, Westinghouse Research Laboratories.-- When effects such as gas heating which lead to non-uniformities in the background gas are excluded, there remains a class of ionization instabilities, examples of which have been discussed by various authors[1]. In some instances a correspondence between the region of the instability and a negative region of the discharge E-I characteristic has been noted. In the present work the generality of this correspondence is explored. With the assumption that the electron current dominates simple criteria are derived for (i) stability against local perturbations in electron density n_e and electric field E, and (ii) a positive E-I discharge characteristic. These are compared to give a criterion for their equivalence. Application of these criteria to discharges having various electron production and loss processes is facilitated by expressing the dependence of the processes on n_e and E/N as power law approximations. With interesting exceptions criteria (i) and (ii) are found to be equivalent under most discharge conditions, provided the electron drift velocity increases with E/N.

1. See W. P. Allis, Physica 82C, 43 (1976) and references therein.

IB2 Numerical Study of Neon Discharge. A. A. GARAMOON and I. A. ISMAIL, Riyadh University, Saudi Arabia. -- A numerical solution of Boltzmann's equation using two imposed limiting equations that act as boundary conditions has been carried out for a neon discharge. In that equation, the diffusion of electrons and the partition of the remaining energy in the ratio of $1:\Delta$, between the ionizing electron and the one produced by ionization, is taken into consideration. Contradicting Thomas's conclusion, the distribution function has been found to be sensitive to the value of Δ. The distribution function, mean energy, mobility, diffusion, and ionization coefficient have been computed for different cases.

From the comparison of the computed results of the primary ionization coefficients, α/p_o, with experiment, it has been found that the best solution is for $\Delta = 0.5$ and for 30% reduced excitation cross-section of Maier-Leibnitz.

IB3 Analytical Model for Low Pressure Mercury+Inert Gas Discharges. W. L. LAMA, C. F. GALLO, T. J. HAMMOND, Xerox Corp., and P. J. WALSH, Fairleigh-Dickinson Univ. - A general but simple technique for analyzing gas discharges has been developed and successfully applied to a model of Hg+Ar discharges. This model includes electron excitation, electron de-excitation, self-absorbed Hg 2537Å radiation, gas heating, and two-stage mercury ionization through a saturated metastable level. The analysis yields the following analytic expression for the Hg 2537Å radiant intensity (I)

$$I = (C_1 R N_e \sqrt{N_o}) / (1 + C_2 N_e \tau)$$

where all C's are calculated constants, R is the tube radius, N_e is the electron density, N_o is the mercury ground state density, and τ is the Hg 2537Å self-absorbed lifetime which increases with N_o and R. This analysis also yields an expression for the axial electric field (E)

$$E^2 = (C_3 \sqrt{N_o}/R) / (1 + C_2 N_e \tau) + B$$

where the first term is related to Hg 2537A radiant energy while B denotes other energy loss terms which are either small and/or comparatively weak functions of the pertinent parameters. These expressions yield good quantitative agreement with the parametric dependence of our data on mercury pressure, current and tube radius, without the introduction of arbitrary constants.

IB4 Influence of Helium Atoms on the Ionisation and Recombination Processes in Cs-He Discharges. B. SAYER, G. GOUSSET, M. FERRAY, J. LOZINGOT & J. BERLANDE, CEN Saclay, France. -- The electron density and temperature, and also the population of some excited states are measured in a stationary glow discharge in cesium vapor mixed with helium (p_{He}= 60 Torr). By comparing with pure Cs discharge results, we find that, for $n_e < 10^{12}$ cm^{-3}, the presence of helium atoms in their ground state, induces a large increase in T_e, and the population of highly excited Cs states is in Boltzmann equilibrium at the gas temperature over an energy range of several kT_g. Yet, in an afterglow (p_{He} = 60 Torr, $n_e = 10^{12} cm^{-3}$) the $(Cs^+ + e + e)$ mechanism is shown to be the preponderant recombination process. An upper limit for the $(Cs^+ + e + He)$ recombination coefficient is deduced ($5.10^{-29} cm^6 s^{-1}$ at $T_e = T_g = 625°K$), which is much smaller than the values measured for $(He_2^+ + e + He)$.

IB5 Development of Cathode Fall in Planar Discharge in Helium.* H.-C. CHEN and A.V. PHELPS. JILA, U. of Colorado and NBS.--The time development of the cathode fall region of a planar discharge in helium has been calculated[1] using electron and positive ion rate equations, Poisson's equation, and experimental transport and rate coefficients. Secondary electrons are produced by photons or ions at the cathode. The initial ionization simulates a double discharge laser with a gap length of up to 3 cm at a gas density of $3\times10^{19}cm^{-3}$. After a period of reduced electric field near the peak initial ionization, the field near the cathode increases as electrons are swept toward the anode. This field causes an ionization wave to move toward the cathode to form the cathode glow. The sequence of field and charge distributions in the cathode region is essentially independent of gap length with the time scale decreasing as the gap length increases and the overvoltage decreases.
*This work was supported in part by the Advanced Research Projects Agency via the Office of Naval Research, Contract N00014-76-C-0123.
[1]See also L.E. Kline, J. Appl. Phys. 45, 2046 (1974) and 46, 1567 (1975); C.B. Mills, ibid., 45, 2112 (1974).

IB6 Dependence of Breakdown Strengths of Gaseous Dielectrics on Electron Attachment Cross Sections and Inelastic Scattering.* R.Y. PAI, L.G. CHRISTOPHOROU,** D.R. JAMES & M.O. PACE,** Oak Ridge National Laboratory. The electron attachment cross sections and breakdown strengths (BS) of SF_6m c-C_4F_8, iso-C_4F_8 and C_4F_6 were measured. The BS of the perfluorocarbons were higher than SF_6 (by $\sim$35%, $\sim$63% and $>$100% for c-C_4F_8, iso-C_4F_8 and C_4F_6 respectively); this is attributed to their higher attachment cross sections in the energy range 0.4 to $\sim$1 eV. Similar results were obtained for the mixtures c-C_4F_8/CCl_4, C_6F_6/c-C_4F_8 and C_6F_6/SF_6. The BS increase as c-C_4F_8 < iso-C_4F_8 < C_4F_6 indicating the importance of the double bond in iso-C_4F_8 and the triple bond in C_4F_6 in controlling breakdown. Scattering cross sections at epithermal energies increase with the number of molecular[1] double bonds. Multicomponent gaseous insultators with optimum overall electron attaching and electron thermalizing properties are under intense study.
*Research sponsored by ERDA under contract with Union Carbide Corporation.
**Also University of Tennessee, Knoxville, TN
[1]L.G. Christophorou et al., Chem. Phys. Lett. 22, 41 (1973)

IB7 Importance of 2-Step Excitations in the Positive Column of Ne-0.1% Ar Mixtures. O. SAHNI, and W. P. JONES, IBM Research, New York. -- The relative influence of multistep excitations in neon discharges has been investigated by measuring the optical intensity of strong neon lines as a function of electron density for both pure neon and neon-0.1% Ar mixtures over a pressure range from 5 to 50 Torr. Electrostatic probes were used to measure the electric field and to monitor simultaneously the electron temperature. These experiments were necessitated by the difficulty in estimating theoretically the rate processes in efficient Penning mixtures due to the lack of accurate cross section data for electron excitations, which compete with the very effective Penning deactivation of the metastable atoms. The dominance of the 2-step excitations involving neon metastable is ambiguously demonstrated under certain discharge conditions for the positive column of Ne-0.1% Ar mixtures. The corresponding results in pure neon indicate resonant trapping of photons by the metastable atoms. The currently available estimates of single-step electron excitation rates permit order of magnitude calculations of the reaction rate for the 2-step excitation from the 3s to the 3p states of neon.

IB8 Spectra of Vibrationally Hot Gases in Electric Discharges by CARS, J.W. NIBLER*, W.M. SHAUB** and A.B. HARVEY, Naval Research Lab. Code 6110, Washington, D.C. 20375 -- Coherent Anti-Stokes Raman Spectroscopy (CARS) is a new nonlinear spectroscopic tool using two laser sources, one fixed in frequency, the other tunable. When the frequency difference between the two laser beams is scanned over a vibrational (Raman) resonance in the medium, CARS emission emerges as a coherent, laser-like beam in the anti-Stokes region at very high efficiencies compared with normal Raman spectroscopy. Hence, there is little or no interference from strong background luminescence from the glow region of electric discharges. Using this method we have probed a small volume element (<0.1 mm^3) of an electric discharges through gases such as N_2 (10 torr) and D_2 (50 torr). In N_2 vibrational states up to V=8 have been observed. Computer calculations have been used to determine population distributions among the vibrational levels. In D_2 a vibrational temperature within the discharge is estimated to be about 1050°K while the rotational/translational temperature is near ambient (400°K).
Present address: *Dept. of Chem., Oregon State U., Corvallis, OR 97331; **Dept. of Chem., Geo. Mason U., Fairfax, VA 22030

SESSION J

7:30 PM, Wednesday, October 20

East Ballroom

WORKSHOP

ION CLUSTERS

Discussion Leader: J. R. Peterson, SRI

J1 Binding Energies - Stabilities and Nature of Bonding in Ion-molecule clusters. P. KEBARLE, Chem. Dept. Univ. of Alberta, Edmonton, Canada. - A brief simple survey and classification of bonding types and resulting bond energies in ion-molecule clusters will be given on basis of experimental and theoretical studies.

J2 Reactions of Cluster Ions.* F. C. FEHSENFELD, NOAA Aeronomy Laboratory, Boulder CO 80302.--Ions produced in low temperature, high pressure gases rapidly associate with neutrals to form cluster ions. Although the ions and the neutrals are weakly bound, with bond dissociation energies typically less than one electron volt, the production of these cluster ions can profoundly alter the ion chemistry, giving rise to new reaction sequences and terminating others. The nature of the association bond and the systematic effects of clustering on ion reactivities will be described. In this connection different isomeric states of the same ion can be formed having considerably different reactivities. The implications of this will be discussed.

* Supported in part by DNA

J3 Cluster Ions in the Ionosphere.* R.S. NARCISI, Air Force Geophysics Lab.--The positive and negative ion clusters measured in the ionospheric D-region (50-90 km) and the current status of D-region theory are reviewed. Over three dozen positive ion species and about two dozen negative ion species have been measured by rocket-borne mass spectrometers. The D-region positive ion composition is dominated by water cluster ions, $H^+(H_2O)_n$, n = 1-8. Presently, only the nighttime, highly disturbed D-region created by solar proton ionization can be theoretically modelled with some accuracy. For other conditions, including the quiescent state and its variations, the theory is inadequate. Negative ions are found in greatest concentrations below 92 km and are composed mainly of large clusters tentatively identified as $NO_3^-(H_2O)_n$, n = 0-8. Ionospheric negative ion chemistry is, in major part, unexplained. The upper mass limit and the relative abundances of the cluster ions are uncertain due to fragmentation processes which occur during measurement.

*Submitted by J.R. PETERSON

J4 Photodissociation of Cluster Ions. J.T. MOSELEY, Molecular Physics Center, SRI.--Photodissociation cross sections have been recently measured for a number of ions commonly considered to be "cluster" ions. The ions studied include the hydrates of O_2^-, CO_3^-, HCO_3^-, O_2^+ and NO^+, the dimer ions Ar_2^+, Kr_2^+ and Xe_2^+, and the weakly bound complexes $O_2 \cdot O_2^-$, $O_2 \cdot O_2^+$, $N_2 \cdot N_2^+$ and $NO \cdot NO^+$. From the wavelength dependence of the photodissociation cross sections and identification of fragment ions, information is obtained on the strength and nature of the relatively weak bonds in these ions. The bonds appear to be only rarely purely electrostatic; in general chemical bonds appear to exist, with the ions photodissociating via repulsive states. In negative ions, dissociation may be accompanied by detachment. For the unhydrated CO_3^- ion, a bound, predissociated excited state is observed. Some of these photodissociations are likely to be important in the ionosphere and other ionized gases.

J5 Recombination of Cluster Ions with Electrons.*
MANFRED A. BIONDI, CHOU-MOU HUANG and RAINER JOHNSEN, Univ. of Pittsburgh. -- Cluster ions consisting of a core ion and attached polar molecule(s) exhibit very large rates for the capture of slow electrons. Studies of the $H_3O^+ \cdot (H_2O)_n$ and $NH_4^+ \cdot (NH_3)_n$ series ions[1,2] yield recombination coefficients α in the range 10^{-6} to 10^{-5} cm^3/sec at thermal energies for n = 1 to 6. The ions $NH_4^+ \cdot (NH_3)_{1,2}$ and $H_3O^+ \cdot (H_2O)_3$ are found to exhibit much weaker dependences of α on T_e over the range 300 - 3000K than the approximate $T_e^{-\frac{1}{2}}$ variation found for dissociative recombination of simple diatomic ions with electrons. A new recombination mechanism, cluster-detachment recombination, is discussed as a possible explanation of the observations.

*Research supported, in part, by ARO-DNA (DAAG29-76-G-0019) and NASA (NGR39-011-137).

[1]M. T. Leu, M. A. Biondi and R. Johnsen, Phys. Rev. A7, 292 (1973).
[2]C. M. Huang, M. A. Biondi and R. Johnsen, Phys. Rev. A14, (Sept. 1976).

SESSION K

9:00 AM - 12:00 AM, Thursday, October 21

East Ballroom

PANEL DISCUSSION

VACUUM ARCS

Discussion Leader: J. F. Waymouth, GTE-Sylvania

K1 Current Density and Erosion Measurement at the Arc Cathode Spot. G.A. Farrall, General Electric Co.--The determination of current density in the emission zones of vacuum arcs and the measurement of cathode metal loss by cathode spot erosion have commanded the attention of experimentalists for decades because a knowledge of these quantities is vital in determining the energy balance at arc cathode spots and would therefore lead to a more fundamental understanding of vacuum arcs. Further, the techniques for measuring these quantities have appeared to be relatively simple. Measurements of current densities by independent investigators, however, have given widely varying results, differing typically by four orders of magnitude under ostensibly similar conditions. In recent years Rakhovskii has applied sophisticated opto-electronic techniques to the problem and has obtained results which favor the low range of current density. Measurements of erosion rates for given cathode metals similarly vary over a wide range. Eckhardt and Daalder have recently provided new experimental data and new interpretations for erosion measurements. This paper will constitute a critical review of the techniques and results of current density and erosion measurements.

K2 Ion Currents from the Cathode Spot Regions of Vacuum Arcs, C. W. KIMBLIN, Westinghouse Research Laboratories--During the past ten years there have been extensive experimental investigations of the ion currents associated with the cathode spots of vacuum arcs. Measurements have included determination of the ion current magnitude for about twenty cathode materials, the energies of the ions, their degree of ionization, and the spatial distribution of the ion flux. It has been established that ion currents with values of 7 to 10% of the arc current are associated with the cathode regions of both refractory and non-refractory materials, and comparison with the measured erosion rate shows the cathode regions to be associated with a high fractional ionization. It has also been established that ions moving away from the cathode plane have energies, in electronvolts, which significantly exceed the interelectrode voltage. The ions move essentially without collision from the neighborhood of the cathode, and the spatial distribution of these ions is the subject of continuing investigation. The author will discuss the experimental techniques which have been used to investigate the vacuum arc ions, present the experimental data, and show the relevance of these data to cathode spot phenomena.

K3 Cellular Substructure in Arc Cathode Spots. L.P. HARRIS, General Electric Co.--Recent numerical calculations of cathode spot parameters have yielded dimensions and currents substantially smaller than most estimates derived from spot counts for the largest units of cathode spots over which surface temperature, electric field, current density, etc., are approximately uniform. For clean copper cathodes, the calculations yield 8.7 Amp current and 3 micrometers diameter, while typical experimental estimates might be 100 Amp current and 200 micrometers diameter. These discrepancies have been interpreted as evidence for a possible cellular substructure in cathode spots on many metals similar to that found by Kesaev for mercury cathodes. A study of electron micrographs of arc cathodes of several metals arced in air or in vacuum under widely varying conditions has revealed the weidespread occurrence of cell structures of characteristic appearance and diameters of 0.1-10.0 micrometers. These cells may provide the fundamental units from which the commonly observed cathode spots are formed.

K4 Cathode Spot Theory, - a Phenomenon of Many Aspects. G.H. ECKER, Ruhr-Universität Bochum, Germany. --- Cathode spot theory is a subject as old as difficult. Recently, a number of new ideas have been forwarded, - some not so new, some really new. In a survey of the present status we aim to order the theoretical models. Then we will try to select what seems reliably known from the theoretical treatments and what may be considered reasonable estimates. Finally we also classify those areas of the theoretical understanding which are still uncertain. This will lead to conclusions with respect to the comparison of experiment and theory and it may give indications for useful future activities.

SESSION L

2:00 PM - 5:15 PM, Thursday, October 21

East Ballroom

SCHULZ MEMORIAL SESSION

Chairman: M. Biondi, University of Pittsburgh

L1 Shape Resonances and Resonances near Thresholds.
A. HERZENBERG, Yale University

Three threads through G.J.S.' career will be followed to their most recent developments:

(1) An electron with an energy somewhere below 10 eV can often enter a vacant orbital in a molecule, giving rise to a shape resonance. The electron becomes temporarily trapped within a barrier from the centrifugal potential, for a time which depends on the strength of the barrier. Recent examples of the different possible regimes will be described.

(2) The narrow resonance discovered by G.J.S. at 19.3 eV in e-He scattering is a prototype of many in which two electrons cruise around a positive ion in a bound state of large radius. This state occurs typically $\sim$ 0.5 eV below an excitation threshold in the neutral. The bound state also influences electron scattering above the threshold.

(3) Some dipolar molecules can bind an extra electron in the attractive potential hole at their positive end. The effect of this state on scattering at positive energies will be discussed.

L2 Electron Scattering, Past and Prologue. C. E. KUYATT, National Bureau of Standards.--The decade of the sixties saw the development of high resolution electron spectrometers and the discovery of electron scattering resonances. A key event was the discovery of the 19.3 eV resonance in helium by George Schulz in 1963. Succeeding work in the laboratories of Schulz and others showed that resonance effects are both important and pervasive in low energy electron scattering. A brief look at earlier work attempts to shed some light on why resonance effects went undiscovered for so long. A similar examination of early attempts to observe spin polarization in low energy electron scattering, using the hindsight made possible by results of the last few years, indicates that significant opportunities were neglected. These opportunities may be as fruitful as those ushered in by the discovery of resonances.

L3 Resonances in Electron Scattering From Hydrocarbon Molecules. P. D. BURROW,* J. A. MICHEJDA and K. D. JORDAN, Yale U. --The electron transmission technique of Sanche and Schulz[1] is used to study the temporary negative ion states of selected hydrocarbons. In contrast to small molecules such as N_2 and CO_2, in which the scattering below 5 eV is dominated by a single shape resonance due to a state of the negative ion[2], unsaturated hydrocarbons may possess many such resonances. Furthermore, by varying the separation and orientation of the functional groups in the molecules, the characteristics of the resonances, that is, their energies and lifetimes, may be altered. In certain sufficiently large molecules, the scattering cross section is essentially resonant over a continuous range of energy from 0-5 eV. These features will be illustrated by results from ethylene (C_2H_4) to stilbene ($C_{14}H_{12}$).

*Present address, Dept. of Physics, University of Nebraska, Lincoln, Nebraska

[1]L. Sanche and G.J. Schulz, Phys. Rev. A 5,1672 (1972).
[2]G.J. Schulz, Rev. Mod. Phys. 45,423 (1973).

L4 Resonant Scattering of Molecules by Low Energy Electron Impact: Vibrational Excitation.* S. F. Wong, Yale University -- Recent experimental studies on resonant vibrational excitation of molecules[1] by the crossed-beam method are discussed. In diatomic molecules, we present results on the rotational and vibrational excitation in N_2, in the energy range (1-4 eV) dominated by the $^2\Pi g$ shape resonance. Theory is in good agreement with the experimental observations. The role of large electric-dipole moment on vibrational excitation (dipole-dominated resonance) relating to experimental results in CO (near the 6 eV $a^3\Pi$ state) and H_2O (near the vibrational threshold) is discussed. In polyatomic molecules, we show results on the resonant vibrational excitation in benzene, a prototype hydrocarbon molecule. Several new and unexpected features in the energy loss spectra and in the energy and angular dependance of the vibrational cross sections are presented and discussed.

[1]For a review, see Schulz, G.J. Rev. Mod. Phys. 45, 423, 1973. See also Schulz, G. J.,1976,"High Power Gas Lasers", edited by G. Bekefi, Wiley and Sons. Chapter 2.

*This work supported by NSF, ONR and AROD.

L5
New Applications of Schulz's Trapped Electron Method.*
D. Spence, ARGONNE NATIONAL LABORATORY, Argonne, Ill.--Almost twenty years after its invention by Schulz,[1] the trapped-electron technique is undergoing a major renaissance. Originally conceived as a technique for measuring total inelastic cross sections within a few eV of threshold, a capability only recently realized,[2] the trapped electron method has lately thrown new light on a plethora of electron collision phenomena. Some recent application of the trapped electron method to be discussed include measurement of secondary electron energy distributions, total inelastic cross section measurements to about 10 eV above threshold and near threshold electron spectroscopy. The latter measurements include studies of threshold electron impact ionization laws, doubly excited states, and the recently discovered phenomena of "post-collision interaction."

*Work performed under the auspices of the U.S. ERDA.

[1]G. J. Schulz, Phys. Rev. 112, 150 (1958).
[2]H. H. Brongersma, F. W. E. Knoop, and C. Backx, Chem. Phys. Lett. 13, 16 (1972).

L6 Electron Scattering from Excited Atoms and Molecules. M. J. W. BONESS, AVCO Everett Research Laboratory, Everett, Ma. - - Progress in the field of high power gas laser technology has emphasized the important practical role which electron interactions with excited atomic and molecular species play in the physics of gas discharges. Knowledge of these processes is essential for modeling the collision processes which determine the lasing kinetics, for understanding the electrical behavior of the discharge and ultimately for deriving the scaling relationships which are fundamental to predicting laser performance. These developments have underlined the relatively modest amount of data available and have stimulated an interest in performing further accurate measurements and calculations of the relevant cross sections and rate constants. The manner and extent to which certain of these processes may affect the operation and performance of several important electric discharge lasers such as copper vapor, carbon monoxide and the rare-gas halide systems will be discussed. Experiments to measure the cross sections for collisions between electrons and metastable atoms currently in progress will be described and progress in the field of electron collisions with excited species will be reviewed.

SESSION M

8:45 AM - 10:30 AM, Friday, October 22

East Ballroom

ELECTRON SCATTERING I

Chairman: A. Herzenberg, Yale

M1 Is Standard Elastic Cross Section Data Now Available for Electron-Helium Scattering? H.B. MILLOY, Ion Diffusion Unit, Australian National University -- The e^--He momentum transfer cross section of Crompton, Elford and Robertson has been extended to 12 eV by analysing recent drift velocity data in the range up to E/N = 7.0 Td. It is estimated that the cross section is now known to within ± 2% in the range $\varepsilon \leq 3$ eV, ± 3% in the range $3 < \varepsilon(\text{eV}) \leq 7$ and ± 5% in the range $7 < \varepsilon(\text{eV}) \leq 12$. The derived cross section differs at energies > 4 eV by < 2% from many of the recent *ab initio* calculations and is in good agreement with the beam data of Andrick and Bitsch. At $\varepsilon < 4$ eV there are significant disagreements between our cross section and the *ab initio* calculations.

The accuracy of the theory used in the analyses of swarm data for inert gases has been critically examined by comparing simulated and predicted values of the transport coefficients. It is shown that although the theory is not generally valid for elastic scattering there are not significant errors incurred in the analysis of electron motion in helium, neon and argon.

M2 Collision Cross Sections for Low Energy Electrons with O_2. A.V. PHELPS and S.A. LAWTON, JILA, NBS and U. of Colorado.--Collision cross sections for low energy electrons with O_2 are derived from a) beam measurements of total scattering, vibrational and electronic excitation,[1] dissociative attachment, and ionization cross sections and of three-body attachment coefficients and b) swarm measurements of drift velocity and of diffusion, attachment, excitation, and ionization coefficients. At mean energies below 0.14 eV energy loss is by rotational excitation. Between 0.14 and 1 eV swarm data shows that beam measured vibrational excitation cross sections are much too small or that the energy is lost by rotational excitation. At energies above 1.5 eV measured[2] excitation rate coefficients for the $O_2(b^1\Sigma_g^+)$ state are much larger than predicted from the $b^1\Sigma_g^+$ cross sections. Collision induced cascading from 6 eV and $B^3\Sigma_u^-$ state is proposed.

*Supported in part by Advanced Research Projects Agency and Office of Naval Research, Contract N00014-76-C-0123.

[1]F. Linder and H. Schmidt, Z. Naturforsch. 26a, 1617 (1971); R.I. Hall and S. Trajmar, J. Phys. B 8, L293 (1975).
[2]S.A. Lawton and A.V. Phelps, Bull. Am. Phys. Soc. 21, 160 (1976).

M3 Scaling Law for Electron Collisions with Polar Molecules. FELIX T. SMITH, DEBASISH MUKHERJEE, and DAVID HUESTIS, SRI.--The mobility, diffusion, energy loss, and thermalization rate of electrons, and the excitation of infrared radiation, in a medium containing polar molecules are often dominated by electron-dipole collisions. We have derived scaling laws and general cross section formulas from the S-matrix in the SPS (semiclassical perturbation scattering) approximation, for any change Δj in rotational state j. They depend on the dipole moment D, moment of inertia I, and energy E through the dimensionless parameters $\beta = mDe/\hbar^2$ and $g = \hbar^2(2j+1)/2IE$, where $j = \frac{1}{2}(j_1+j_2) = j_1 + \frac{1}{2}\Delta j$. The scaling is accomplished through the reduced collision strengths $n|\Delta j|(\beta^2,g,j) = \sigma_{\Delta j}(j_1,E,\beta,g)\cdot(\pi\hbar^2/2mE)\cdot(2j_1+1/2j+1) = (4/3)\beta^2 \ell n\, g\cdot\delta_{1,|\Delta j|} + f_{|\Delta j|}(\beta^2) + h_{|\Delta j|}(\beta^2,g,j)$, where h includes corrections that exceed 1% only for small j ($j \leqslant 5$) or unusually large g ($g \geqslant 0.01$). For $\Delta j = \pm 1$, the result agrees with Born approximation for small β and g, and provides important corrections elsewhere. The scaling functions $f_{|\Delta j|}(\beta^2)$ are presented, and the agreement with experiments and other calculations is shown.

M4 Electron Diffusion in Swarms. J. LUCAS, Liverpool University -- Electron swarm motion has been experimentally and theoretically studied for a number of years. A special effort has been made to determine the ratio of electron diffusion coefficient to mobility ($D/_{\mu}$) at high E/N in the range 10 to 1000 Td. Special experimental techniques have been developed in order to allow for the presence of ionisation and secondary electrons. Both radial and longudinal diffusion have been calculated and measured in a large number of atomic and molecular gases.

SESSION NA

10:45 AM - 12:15 AM, Friday, October 22

East Ballroom

ELECTRON SCATTERING II

Chairman: R. J. Van Brunt, JILA

NA1 Electron Drift Velocities in Sodium Vapour, Y. NAKAMURA, J. LUCAS, Liverpool University, Liverpool England. -- A new technique has been developed for combining the heat pipe with a drift tube in order to measure electron drift velocities in vapours. Using this technique electron velocities have been measured for the first time in sodium for the range

$$2.6 < \frac{E}{N} < 61 \quad \text{Td.}$$

The heat pipe has a diameter of 29 mm and operates with a stainless steel wick. The drift tybe has a drift distance of 2 cm. The operating vapour pressure is from 2 to 36 torr with nitrogen as the buffer gas.

NA2 The Effect of Energy Inequilibrium on the Swarm Parameter Measurement.* N. IKUTA, S. YUASA, Y. SHINOHARA Technical College, Tokushima University, Tokushima, Japan. Precise measurements of electron diffusion current density distribution by a Townsend-like method were carried out using a revised apparatus which has 15 annular collectors and an auxiliary drift space. Measured current density distributions gave much information on the behavior of drift and diffusion of electrons in gases. Theoretically reasonable distributions supposing energy equilibrium in full space were realized only when the voltages applied to the main and auxiliary drift space were high enough. The voltages needed to reach energy equilibrium for electrons at a given E/p seem to be several times larger than the energy values in eV at which the gas species have large inelastic collision cross sections as were shown by the results of Monte Carlo simulations.[1] The effect of energy inequilibrium manifested itself vigorously in argon, and it was also observed even in molecular nitrogen over a range of E/p where the energy equilibrium is considered easily obtainable.

* Submitted by M. A. Biondi

1 Y. Sakai, H.Tagashira, S.Sakamoto; J. Phys. B, Atom. Molec. Phys. vol.5, 1010, (1972)

NA3 Electron Transport in Argon, W. H. LONG JR., AF Aeropropulsion Laboratory, WPAFB, Ohio. ---- The electron continuity equation can be derived from the Boltzmann equation as an expansion in spatial derivatives of the number density. The higher-order coefficients of this expansion, which account for the spatial variation of the electron energy distribution, have been calculated for argon. The dispersive terms are shown to significantly affect the interpretation of drift and diffusion data in electron swarm experiments. The adjustment to the drift velocity is proportional to D_{z3}/hD_L , where D_{z3} is the dispersion coefficient, h is the shutter spacing and D_L is the longitudinal diffusion coefficient. When this correction term is applied to the measured electron drift velocities in argon, a momentum transfer cross section can be inferred which predicts the D_T/μ data within experimental error. At values of E/N below 0.01 Td, fourth order terms begin to affect the diffusion measurements, making data analysis more difficult. However, the electron continuity equation is still adequate to describe the observations at all values of E/N and N, if enough terms are retained in the expansion.

NA4 Absolute Total Electron-Impact Cross-Sections from a Time-of-Flight Transmission Technique. R. E. KENNERLY and R. A. BONHAM, Indiana U. --A new transmission method of total cross-section (TCS) measurement employing time-of-flight (TOF) monochromatization of an initially sub-nanosecond multichromatic electron pulse in free flight through the gas to be studied has been developed. The pulse source is secondary emission from a solid surface. The TCS of the gas from about 0.5 eV to several hundred eV is determined at all energies simultaneously using one gas pressure. A timing uncertainty of 250 picoseconds has been achieved, allowing energy resolution of from 20 to 50 meV in the energy range below about 10 eV. It will be shown that this TOF approach is simpler and more accurate than previously reported methods. Absolute TCS for several gases will be reported and compared with results obtained by other methods.

NA5 Glauber cross sections for elastic scattering of electrons by metastable (2^1S, 2^3S) helium atoms.* S. T. CHEN and G. A. KHAYRALLAH, JILA, Univ. of Colo. and NBS. -- The recently proposed analytic methods by Thomas and Chan, which reduce the Glauber amplitude for charged-particle -- neutral-atom collisions to a one-dimensional integral representation involving the modified Lommel function, are used to evaluate the cross sections for the elastic scattering of electrons by metastable (2^1S, 2^3S) helium atoms. The Glauber differential and total cross sections are calculated for the energies from 10-500 eV. The results are compared with some other theoretical calculations. It is found that within the present energy range the Glauber total cross sections agree with the first Born cross sections calculated using the quite complicated unrestricted Hartree-Fock wave-functions. At very low energies, the Glauber results do not reproduce resonant structure, it is not in complete disagreement with the far more complicated many-channel calculations that disagree with each other by as much as a factor of 10.

*Supported by NSF contract No. MPS72-05169.

NA6 Post Collision Interaction in Electron Scattering from Xenon. N. SWANSON and R. J. CELOTTA, National Bureau of Standards, Washington, D.C. 20234.--A progressive shift in the energy of electrons ejected from the 7p' J=1 and J=0 autoionizing levels in Xe at 12.28 and 12.35 eV, respectively, has been observed when the incident electron energy was decreased from 4 eV to 30 meV above the excitation threshold of these states. The magnitude of these shifts was $\approx$ 20 meV for the 7p' J=1 level, and $\approx$ 60 meV for the 7p' J=0 level. These small energy shifts required a resolution of 20-25 meV in the energy analyzer section of the electron spectrometer to locate the peak positions accurately. A plot of the energy shift vs $(E_1)^{-1/2}$, where E_1 is the excess energy above threshold, gives a good fit to the data.[1]

[1]R. B. Barker and H. W. Berry, Phys. Rev. 151, 14 (1966).

NA7 Feshbach Resonances in CH_3X(X=Cl,Br,I). Classification of Resonances and Prediction of Rydberg States.*

D. SPENCE, Argonne National Laboratory, Argonne, Ill.--

Using an electron transmission spectrometer we locate Feshbach resonances in the alkyl halides. Combination of data from the acid halides and aklyl halides indicate that for structurally related molecules the energies of Feshbach resonances $E_{n\ell\ell''}(m)$ are related to the appropriate ionization potentials I(m) by the relationship. $E_{n\ell\ell'}(m) = A_{n\ell\ell'}I(m) + B_{n\ell\ell'}$ where $E_{n\ell\ell'}(m)$ is the nth resonance with excited electrons of angular momenta ℓ and ℓ' in species m, and $A_{n\ell\ell'}$ and $B_{n\ell\ell'}$ are constants independent of molecular species. This relationship enables easy identification or prediction of resonance energies in chemically related compounds. We show how low rydberg state energies may be obtained from Feshbach resonance spectra.

*Work performed under the auspices of the U.S. Energy Research and Development Administration.

SESSION NB

10:45 AM - 12:15 PM, Friday, October 22

West Ballroom

RECOMBINATION

Chairman: R. Johnsen, University of Pittsburgh

NB1 Study of Kinetics of n=2 States in Recombining Helium Plasma Jets.* C. C. POON† and F. A. ROBBEN, U. of California, Berkeley.--The principal kinetic processes between the four n=2 states in helium plasma jets were identified from the densities of excited states, which were determined spectroscopically from intensity and absorption measurements. These processes were the de-excitation of the 2^1P, 2^3P and 2^1S state by superelastic collisions to the nearest n=2 state of lower ionization energy. The rate coefficients at 0.12 eV of the three processes He (2^1P) + e^- → He (2^3P) + e^- → He (2^1S) + e^- were found to be 2.3, 3.3 and 2.7, respectively, in units of 10^{-7} cm^3 s^{-1}. Detailed study of the electron energy balance indicated that these three processes were unimportant in electron heating.

*Work supported by the National Science Foundation (Grant ENG75-02033).

†Present Address: Institute for Aerospace Studies, U. of Toronto, Downsview, Ontario, Canada M3H 5T6.

NB2 Charge Neutralization in a High Pressure Helium Afterglow. D.P. COLTON, G.D. MYERS, and R.A. SIERRA, U. of Texas at Dallas -- Molecular spectral emissions from pulsed e-beam excited helium afterglows at room temperature have been studied at pressures ranging between 1 and 5 atms. Comprehensive reaction rate equations were proposed to account for the observed behavior of the emissions studied. The adequacy of the model was shown by comparison of the results obtained experimentally to those generated by the model. One result showed that the emissions were controlled mainly by the collisonal-radiative recombination of the He_2^+ ions. The origin of the He_2^+ ions was found to vary with time where late in the afterglow the contribution from metastable-metastable ionizing collisons was confirmed. Additionally, strong evidence for a three-body, pressure-squared dependent collisional destruction of He_2^* radiating levels was found. Also found were the inverse transition probabilities of four of the molecular emission bands studied.

NB3 Merged Electron-Ion Beam Studies of Dissociative Recombination.* B. MITCHELL, J. KEYSER and J.WM. McGOWAN, Physics Dept. and Centre for Chemical Physics, Univ. of Western Ontario.--A Merged Electron Beam apparatus has been developed which allows us to study dissociative recombination cross-sections through the energy range from <0.01 eV to >4 eV with a resolution ~0.04 eV. Preliminary studies have already been reported for $e\text{-}H_3^+$ and $e\text{-}H_2^+$ collisions where fast neutrals have been measured as a function of the electron center of mass energy. In this report we discuss more recent measurements of these systems. We show even more clearly the role that the Rydberg States of the molecules play in the recombination process. It is possible in our data to identify competition of recombination with autoionization, and negative-positive ion pair production. As we have demonstrated in the case of H_2^+ the state of vibrational excitation of the parent ion has a marked effect upon the cross-section and the structure that one measures in the cross-section curve. Our results will be discussed in comparison with recent theoretical calculations.

*Supported by the National Research Council of Canada.

NB4 Electron Temperature Dependence of Dissociative Recombination in Xenon.* YUEH-JAW SHIU, MANFRED A. BIONDI, and DWIGHT P. SIPLER, Univ. of Pittsburgh. -- A three-mode microwave afterglow apparatus has been used in conjunction with a high-speed grating spectrometer to study the variation with electron temperature of the recombination coefficient $\alpha(Xe_2^+)$ and of the Xe^* excited states produced by dissociative recombination over the range 300 K $\leq T_e \leq$ 8000 K. At low electron temperatures 300-700 K, $\alpha(Xe_2^+)$ varies approximately as $T_e^{-1/3}$, with a smooth transition to a $\sim T_e^{-2/3}$ variation at higher electron temperatures, 1300-7400 K. At $T_e=T_+=T_n=300$ K, $\alpha(Xe_2^+) = (2.3 \pm 0.2) \times 10^{-6}$ cm^3/sec, in qualitative agreement with several earlier studies at room temperature. The principal Xe^* excited states produced by recombination at thermal (300 K) energy belong to the 6p group lying $\gtrsim$ 2.2 eV below the $Xe^+(^2P_{3/2})$ ground state. With microwave heating to $T_e \sim$ 8000 K higher states such as 5f, 6f, 7d, 8s and 9s, lying within $\lesssim$ 0.8 eV of the continuum, are also produced by the dissociative recombination process.

*Research supported, in part, by ONR/ARPA (N000-1476-C0098).

NB5 Electron-Ion Recombination Rates in Gas Mixtures, T. W. MEYER, J. D. HINES, and P. D. TANNEN, Air Force Weapons Laboratory--Electron-Ion recombination rates in high pressure gas mixtures cannot be readily calculated from basic theory since neither the ionic species nor the recombination processes are easily identifiable. Knowledge of these rates is extremely important to the design and scaling of electron-beam-sustained gas discharge lasers. Experimental measurement of these rates in a wide range of He-N_2-CO_2 mixes has been performed over the pressure range of 400-600 torr and the E/N range of 1-25 X 10^{-17} v-cm^2. The apparatus consisted of an aluminum honeycomb cathode and a copper anode 10 cm in dia., separated by 2.3 cm. The discharge was powered by a 6.4μf capacitor. It was switched on by an electron beam which uniformly irradiated the discharge region through a 0.025 cm Al. foil stretched across the honeycomb. Recombination rates were determined from the current decay of the anode when the e-beam was switched off. The pure N_2 results are compared to those of Douglas-Hamilton[1].

[1]D. H. Douglas-Hamilton, J. Chem. Phys., 58, 4820 (1973)

NB6 Mutual Neutralization of Simple and Clustered Positive and Negative Ions. D.SMITH and M.J.CHURCH, University of Birmingham, England.--The coefficients for binary mutual neutralization at thermal energies for several reactions of both simple and 'clustered'positive and negative ion reactions will be presented. The measurements were carried out in ion-ion flowing afterglow plasmas using Langmuir probe and mass spectrometric diagnostics[1]. It will be shown that the measured coefficients for simple molecular ions are in reasonable agreement with theory, although the effect of clustering appears to be small, somewhat contrary to theoretical expectations[2]. All of the coefficients will be seen to be significantly smaller than the merged beam values. The temperature dependence of the cross-section for the reaction $NO^+ + NO_2^-$ from 185-530K will be presented and, from an assessment of all the available data, the most appropriate values for ionic recombination coefficients in the various regions of the Earth's atmosphere below 90Km will be tentatively suggested.

[1]D.Smith and M.J.Church, Int.J.Mass Spectrom.Ion Phys. 19, 185 (1976).
[2]D.Smith, N.G.Adams and M.J.Church, Planet.Space Sci. 24, 697 (1976).

NB7 Ionic Recombination and Chemical Reactions in Electron Irradiated Air.* MERLE N. HIRSH, UMM.--Thermal plasmas dominated by NO^+ and four negative ionospheric ions (NO_2^-, $NO_2^- \cdot H_2O$, NO_3^-, $NO_3^- \cdot H_2O$) have been produced by electron irradiation of airlike N_2:O_2 mixtures at 2 and 5 Torr. From analysis of the decays of minority ions, we conclude that the neutral NO density builds up as (irradiation time)$^{\frac{1}{2}}$. The NO_2 density grows directly with time at a rate of 1 molecule/100 electron-ion pairs produced. Computer predictions of the growth of these neutrals and of the positive ion spectra now agree well with observations; however, the negative ion chemistry is still poorly understood. From NO^+ afterglow decays, an effective rate coefficient for mutual neutralization of NO^+ with the negative ion mixture of $(1.8 \pm 0.5) \times 10^{-7}$ cm^3/s is deduced. The unknown chemistry greatly complicates the analysis of the negative ion decays, but preliminary results suggest the following approximate coefficients for recombination of NO^+ with the individual negative ions: NO_2^-:(1-2); NO_3^-:(5-8); $NO_2^- \cdot H_2O$(0.1-0.5); $NO_3^- \cdot H_2O$: (0.1-1), all x 10^{-7} cm^3/s.

*Work supported by BRL through ARO, and SRI through AFGL.

NB8 Uses and Basic Characteristics of a Coaxial Discharge Diffusion Plasma Column, M.Kamitsuma, Sin-Li Chen, Musashi Institute of Technology, Japan, Jen-Shih Chang, York University, Canada -- A quiet homogeneous cylindrical plasma column has been produced by using a coaxial diffusion discharge tube at medium pressure ($p \geq 1$), with a cold cathode D.C. discharge. The homogeneity of the charge density, potential and electron temperature distributions inside the diffusion plasma column has been checked by an electrostatic probe. In order to verify the experimental results, an exact numerical treatment of the charge density and the potential distribution has been done for various discharge conditions. The experimental results show that: (1) A quiet homogeneous plasma exists in the center region of the diffusion plasma. Therefore we may use this type of plasma column as a medium pressure plasma test chamber; (2) The plasma parameters can be controlled easily by varying the gas pressure and input D.C. power to obtain plasma densities from 10^6 to 10^{11} cm^{-3}, and electron temperatures from 10^{-1} to a few eV; (3) The numerical charge density distribution shows strong dependence on the volume recombination at the edge of the plasma column. This suggests the possibility for time-indepent measurements of the volume recombination coefficient using the present apparatus.

Index to Abstracts

Adams, N.G. BB4

Ahouse, D.R. DA1, FA4

Akerman, M.A. CA9, CA10

Albritton, D.L. CB1, HA6

Alroy, S. HB5

Anderson, C.E. CA3

Anderson, R.S. CA3

Ayyaswamy, P.S. FB6

Babcock, R.V. DA2

Bar-Ziv, E. DB10

Bardsley, J.N. HA2

Bastien, F. HB6

Bauder, U.H. FB3

Bearman, G.H. BB6

Benenson, D.M. GB2

Berlande, J. BA6

Bienkowski, G. FA5

Biondi, M.A. BB1, J5, NB4

Birely, J. E2

Bletzinger, P. DA7

Bondybey, V.E. IA7

Boness, M.J.W. L6

Bonham, R.A. NA4

Bonifield, T. D. BA3

Bradford, R.S., Jr. A7

Brau, C. A2

Bricks, B.G. CA3

Brink, J. DA5

Burns, D.J. GA3

Burrow, P.D. GA6, L3

Butterfield, K.B. BB5

Byron, S.R. FA3

Cailleteau, J. FB3

Celotta, R.J. NA6

Chang, J.S. HB3

Chantry, P.J. IB1

Chen, C.H. A4

Chen, H.C. IB5

Chen, S.L. DA6, HB3

Chen, S.T. GA1, NA5

Cherrington, B.E. CA1

Choi, C.W. GA9

Christiansen, W.H. HB5

Christophorou, L.G. IB6

Choi, C.K. GB6

Church, M.J. NB6

Cohen, J.S. DB11

Cohen, I.M. FB6

Collins, C.B. DB1

Collins, G.J. BA7, BA8, BB2, BB5

Colonna-Romano, L.M. HA4

Colton, D.P. DB2, HB4, NB2

Cook, J.D. DB6

Cooper, G.W. CA5

Corbin, R.J. CB2, GA4
Cosby, P.C. IA1
Crane, J.K. CA1
Daiber, J.W. FA2
Das, G.C. FB6
Davidson, J.A. HA6
Dotan, I. CB1, HA6
De Hoog, F.J. BA7
Denes, L.J. DA2
DeTemple, T.A. HB2
Dethlefsen, R. FB2
Devoto, R.S. FB3
DeYoung, R.J. CA6, CA7, CA8
Dunbar, R.C. IA3
Dunning, J.W., Jr. DA4
Durup, J. IA3
Ecker, G.H. K4
Edelstein, S.A. BA4
Fairchild, C.E. DB8, IA5, IA6
Fansler, T.D. HA4
Farrall, G.A. K1
Feeney, R.K. GA5
Fehsenfeld, F.C. CB1, HA6, J2
Ferray, M. BA6
Fisher, E. R. FA11
Fujimoto, T. DB7
Gale, P.J. HA5
Gallagher, A.C. DB7, GA1
Gallagher, T.F. BA4
Gallo, C.F. IB3
Garamoon, A.A. IB2
Garcia, M. FA5
Garrett, W.R. CB3
Garscadden, A. DA8, FA10, GA2
Gatland, I.R. HA1
Gerstenberg, D.C. BB5
Gleason, R.E. BA3
Gousset, G. IB4
Gordon, R.J. DB10
Greene, A.E. DB11, DB12
Grosjean, D.F. DA7
Hagstrom, S.A. GA7
Hall, E.T. DB4
Hammond, T.J. IB3
Hanson, R.K. FA1
Harris, H.H. BB6
Harris, L.P. K3
Harvey, A.B. IB8
Hasson, V. DA5
Hawryluk, A.M. A3
Herzenberg, A. L2
Hill, A.E. FA9
Hill, R.M. A5
Hines, J.D. NB5
Hirsh, M.N. NB7
Hoff, P.W. BA2

Hohl, F. CA6, CA8
Hopper, D.G. BB3
Howser, G.W. GA4
Huang, C.M. BB1, J5
Huber, B.A. CB5
Huestis, D.L. A5, M3
Hughes, W.M. BA1
Hummer, C.R. GA3
Hurst, G.S. A4, GA8
Ikutan, N. NA2
Ingold, J.H. FB5
Ismail, I.A. IB2
Jacob, J.H. A1
Jalufka, R.J. CA6, CA7, CA8
James, D.R. IB6
James, P.B. BB6
Johnsen, R. BB1, J5
Jones, E.G. BB3
Jones, T.J. FA7
Jones, W.P. IB7
Jordan, K.D. L3
Judd, O. CA2
Judish, J.P. A4
Karras, T.W. CA3
Kebarle, P. J1
Kennerly, R.E. NA4
Keto, J.W. BA3
Keyser, J. NB3
Khayrallah, G.A. NA5
Kimblin, C.W. K2
King, J.D. BA1
Kline, L.E. A6, DA2
Klosterman, E.L. FA3
Kocher, C.A. DB8
Kuyatt, C.E. L1
Lacina, W.B. A7
Lake, M.L. GA2
Lam, L. DB7
Lama, W.L. IB3
Lancashire, R.B. DA4
Laudenslager, J.B. BA4
Lawless, J. FA5
Lawrence, G.M. IA5, IA6
Lawton, S.A. M2
Lee, F.W. BB2, DB1
Leichner, P.K. DB4, DB5, DB6
Leycuras, A. FB1
Leventhal, J.J. BB6
Liebermann, R.W. FB7
Lin, S.L. HA2
Ling, J.H. IA1
Lockett, A.M. III, DB12
Long, W.H., Jr. FA10, NA3
Loree, T.R. A2
Lorents, D.C. A5, BA4
Lozingot, J. BA6

Lucas, J. M4, NA1
Ludwig, H.C. GB1
Lum, R.M. IA7
Mangano, J.A. A1
Manista, E.J. DA4
Marode, E. HB6
Mason, E.A. HA1
Maya, J. GB7
McAfee, K.B., Jr. IA7
McCusker, M.V. A5
McGowan, J.W. NB3
McKenzie, R.L. DB9
McNeil, J.R. BA8
Meyer, T.W. NB5
Michejda, J.A. GA6, L3
Miley, G.H. CA9, GB6
Milloy, H.B. M1
Mitchell, B. NB3
Mitchner, M. FA1
Moeny, W.M. FA9
Morgan, W.L. FA11
Moseley, J.T. CB5, IA1, IA3, J4
Moy, J. DB10
Mukherjee, D. M3
Muller, C.H. IA9
Myers, G.D. DB2, HB4, NB2
Nakamura, Y. NA1
Nakano, H.H. A5, BA4
Narcisi, R.S. J3
Nederhand, B.R.P. FB4
Newman, L.A. HB2
Nibler, J.W. IB8
Nighan, W.L. DA3
Nygaard, K.J. CB2, GA4
Olson, R.A. DA8
Ono, S. DA6
Orth, R.G. IA4
Ozenne, J.-B. IA3
Pacala, T.J. BA9
Pace, M.O. IB6
Pai, R.Y. IB6
Palmer, K.F. DB4
Paulson, J.F. HA5
Payne, M.G. A4, GA9
Pernot, C. IA3
Peterson, J.R. CB5, IA1
Phelps, A.V. DB7, IA9, IB5, M2
Poon, C.C. NB1
Rackov, P.M. CB4
Reiser, P.A. GB2
Rhymes, T. DB3
Rice, J.K. BA5
Robben, F.A. NB1
Rockwood, S.D. A2
Roman, W.C. GB5
Rumble, J.R. GA7

Sahni, O. IB7
Salesky, E.T. A1
Sayer, B. BA6, IB4
Sayle, W.E. II GA5
Schubert, M.R. HB2
Schulz, G.J. CB4
Shaub, W.M. IB8
Shay, T. BB5
Shepherd, W.B. FA7
Shinohara, Y. NA2
Shires, E. FB3
Shiu,Y.J. NB4
Sierra, R.A. DB2, HB4, NB2
Sipler, D.P. NB4
Smith, D. BB4, NB6
Smith, F.T. M3
Smith, J.A. FA6
Snow, W.R. CB2, GA4
Solarz, R. E1
Spreadbury, R.J. DA2
Spence, D. L5, NA7
Srinivasan, G. FA6
Stanton, A.C. FA1
Stehman, R.M. CB6, HA3
Stone, E.J. IA5, IA6
Streit, G.E. HA6
Swanson, N. NA6
Sze, R.C. A2
Tabche-Fouhaille, A. IA3
Tadjeddine, M. IA3
Tam, W.C. CB4
Tannen, P.D. NB5
Taylor, L.H. DA2
Thieneman, M.D. DB5
Thompson, H.M. FA2
Tiernan, T.O. BB3
Turner, C.E., Jr. BA2
Vanderhof, J.A. IA2
van Vliet, J.A.J.M. FB4
Varney, R.N. HA4
Verdeyen, J.T. CA1, CA5
Viehland, L.A. HA1
Von Bergmann, H.M. DA5
Vriens, L. HB1
Wahl, A.C. BB3
Waller, R.A. BB2
Walsh, P.J. CA4, IB3
Walters, G.K. BA3
Weisbach, M.F. FA8
Wells, W.E. CA10
Winters, H.F. IA8
Winters, P.A. CA7
Whealton, J.H. JA3
Whitman, A.M. FB6
Witting, H.L. GB3
Wong, S.F. CB4, L4

Woo, S.B. CB6, HA3

Woodworth, J.R. BA5

Wyner, E.F. GB7

Yuasa, S. NA2

Yoder, M.J. DA1, FA4

Young, J.P. GA8

Zollweg, R.J. FB7, GB4